REPORT NO.
UCB/EERC-92/03
MARCH 1992

EARTHQUAKE ENGINEERING RESEARCH CENTER

MODELS FOR NONLINEAR EARTHQUAKE ANALYSIS OF BRICK MASONRY BUILDINGS

by

YALCIN MENGI
HUGH D. McNIVEN
A. KAMIL TANRIKULU

Report to NATO, Scientific Affairs Division

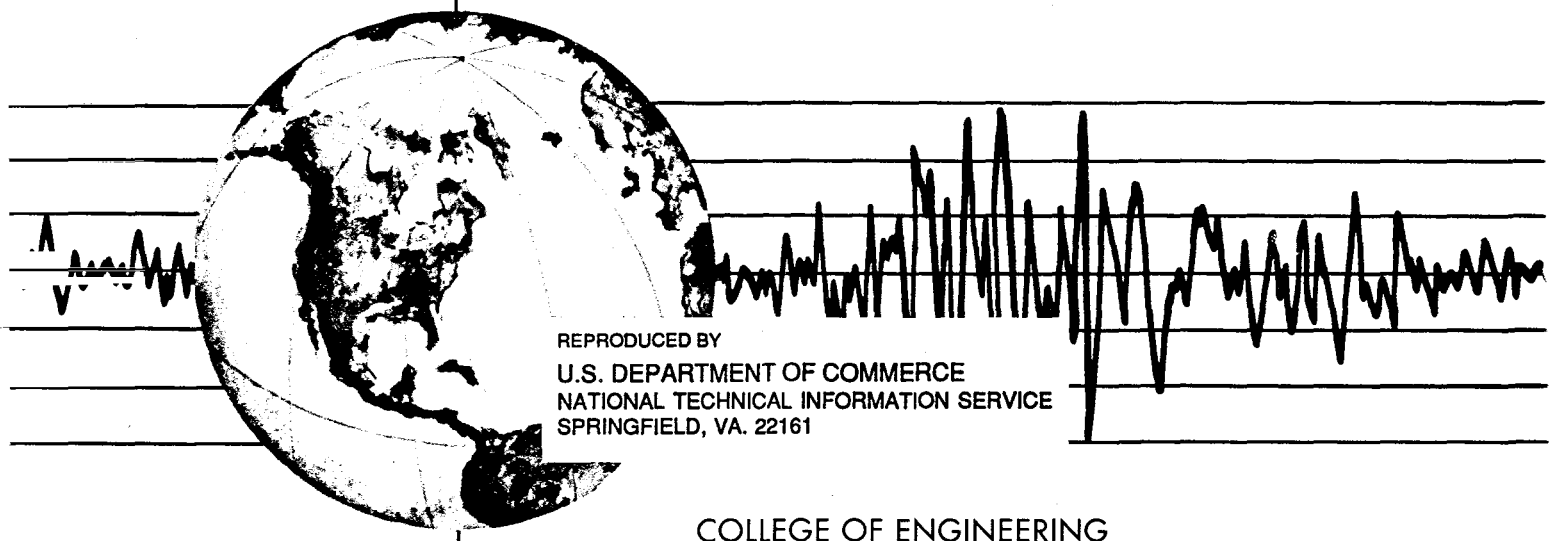

COLLEGE OF ENGINEERING

UNIVERSITY OF CALIFORNIA AT BERKELEY

For sale by the National Technical Information Service, U.S. Department of Commerce, Springfield, Virginia 22161

See back of report for up to date listing of EERC reports.

50272-101

REPORT DOCUMENTATION PAGE	1. REPORT NO. UCB/EERC-92/03	2.	3 PB93-120293

4. Title and Subtitle
Models for Nonlinear Earthquake Analysis of Brick Masonry Buildings

5. Report Date
March 1992

6.

7. Author(s)
Yalcin Mengi, Hugh D. McNiven and A. Kamil Tanrikulu

8. Performing Organization Rept. No.
92/03

9. Performing Organization Name and Address
Earthquake Engineering Research Center
University of California, Berkeley
1301 So. 46th Street
Richmond, Calif. 94804

10. Project/Task/Work Unit No.

11. Contract(C) or Grant(G) No.
(C)
(G) 0364/086

12. Sponsoring Organization Name and Address
NATO,
Scientific Affairs Division

13. Type of Report & Period Covered

14.

15. Supplementary Notes

16. Abstract (Limit: 200 words)

Mathematical models are proposed for the three-dimensional, nonlinear earthquake analysis of unreinforced and reinforced brick masonry buildings. In the development of the models, the floors are modeled as rigid diaphragms. For the unreinforced case it is assumed that the wall elements possess only shear resistance and only in their own planes; for the reinforced case the stiffness of wall elements in out-of-plane directions is taken into account. In view of the data obtained from shaking table experiments, a bilinear form for the shear modulus of the masonry wall materials and trilinear form for its viscous counterpart are assumed in the analysis for their variations with the shear strain. For the nonlinear earthquake analysis of masonry buildings, two different approaches are used. The first one involves the use of the "equivalent linear method" (ELM), which was used successfully by some researchers in nonlinear soil-structure interaction analyses. ELM finds the nonlinear earthquake response of a masonry building approximately through iterations. The second approach employs "the actual nonlinear model" (ANM) which takes into account hysteretic behavior of wall elements established experimentally in shaking table experiments. To assess the models five example problems are presented. The results indicate that the proposed models can be used reliably in the earthquake analysis of masonry buildings.

17. Document Analysis a. Descriptors

b. Identifiers/Open-Ended Terms

c. COSATI Field/Group

18. Availability Statement
Release Unlimited

19. Security Class (This Report) unclassified

21. No. of Pages 159

20. Security Class (This Page) unclassified

22. Price

(See ANSI-Z39.18) *See Instructions on Reverse* OPTIONAL FORM 272 (4-77)
(Formerly NTIS-35)
Department of Commerce

MODELS FOR NONLINEAR EARTHQUAKE ANALYSIS OF BRICK MASONRY BUILDINGS

by

Yalcin Mengi
Professor of Engineering
Cukurova University
Adana, Turkey

and
Hugh D. McNiven
Professor of Engineering Science
University of California at Berkeley
California, U.S.A.

and
A. Kamil Tanrikulu
Instructor
Cukurova University
Adana, Turkey

Report to Nato, Scientific Affairs Division

Report No. UCB/EERC-92/03
Earthquake Engineering Research Center
College of Engineering
University of California at Berkeley

March 1992

ABSTRACT

Mathematical models are proposed for the three-dimensional, nonlinear earthquake analysis of unreinforced and reinforced brick masonry buildings. In the development of the models, the floors are modeled as rigid diaphragms. For the unreinforced case it is assumed that the wall elements possess only shear resistance and only in their own planes; for the reinforced case the stiffness of wall elements in out-of-plane directions is taken into account. In view of the data obtained from shaking table experiments, a bilinear form for the shear modulus of the masonry wall materials and a trilinear form for its viscous counterpart are assumed in the analysis for their variations with the shear strain. For the nonlinear earthquake analysis of masonry buildings, two different approaches are used. The first one involves the use of the "equivalent linear method" (ELM), which was used successfully by some researchers in nonlinear soil-structure interaction analyses. ELM finds the nonlinear earthquake response of a masonry building approximately through iterations. The second approach employs "the actual nonlinear model" (ANM) which takes into account hysteretic behavior of wall elements established experimentally in shaking table experiments. To assess the models five example problems are presented. The results indicate that the proposed models can be used reliably in the earthquake analysis of masonry buildings.

ACKNOWLEDGEMENT

The authors wish to acknowledge the support provided by the Scientific Affairs Division of NATO (Research Grant No. 0364/086).

CONTENTS

LIST OF TABLES

LIST OF FIGURES

1. INTRODUCTION

To our best knowledge, there is no work available in the literature aimed at developing a mathematical model which can be used for the three-dimensional earthquake analysis of brick masonry buildings. The construction of such a model is important for the following reasons. A great portion of world's population live in low strength masonry houses. The existence of the model mentioned above will make it possible not only to predict the earthquake behavior of these houses and to design new ones against earthquake forces, but also to assist in establishing the retrofit techniques for houses damaged after an earthquake.

In the present work, some mathematical models are proposed for the three-dimensional, linear and nonlinear earthquake analyses of masonry buildings, and, based on these models, some general purpose computer programs are prepared. The development of the models involves two main assumptions. (i) The floors of the masonry building are reinforced concrete slabs which are infinitely rigid in their own planes. The use of this assumption makes it possible to employ rigid diaphragm modeling [1] in the analysis. (ii) For unreinforced masonry buildings, the bending rigidity of the wall elements in their planes is very large compared to their shear rigidity and in out-of-plane directions the wall elements have negligible rigidities. For the reinforced case, the assumption regarding the inplane rigidity of the wall elements is the

same as that for unreinforced case, but, in the reinforced case the rigidity in the out-of-plane direction is also taken into account.

To account for the nonlinear effects in masonry buildings, two different methods are used. The first one is an iterative approximate method, called the "equivalent linear method" (ELM). ELM, first used by Seed and Idriss [2] in nonlinear soil-structure interaction analysis, performs the nonlinear analysis in terms of linear analyses. In this method, the system is first assumed to be linear, and, by using the linear values of its elastic and viscous properties, the system is analyzed and its deformation state is determined. Then, the secant values of elastic and viscous properties compatible with that deformation state are computed, and by using these values the system is analyzed again linearly. We continue the iterations until no significant changes occur in the values of the elastic and viscous properties of the system. The second method employes the actual model established in [3,4] experimentally in conjunction with the nonlinear earthquake behavior of brick masonry wall elements.

The use of ELM and the actual model in the nonlinear earthquake analysis of masonry buildings requires knowledge of the changes of the dynamic elastic and viscous properties of masonry wall material as it deforms. The elastic and viscous properties of the wall material pertinent to the nonlinear response can be described, in view of the

assumption (ii) stated above, by the shear modulus G and its viscous counterpart G'. The variations of the dynamic values of G and G' with the shear strain were established using a clay brick wall element in [3,4] in shaking table experiments. In view of the findings established in these works, it may be assumed that the variations of G and G' with the shear strain can be described respectively by bilinear and trilinear functions. These functions and the parameters defining them will be discussed in the main text of the study.

The study is organized as follows. In Chapter 2, the functions assumed in the analysis for the variations of the dynamic values of G and G' with the shear strain are presented and discussed. In Chapter 3, the formulation for the linear and nonlinear earthquake analysis of an arbitrary masonry building is carried out using the assumptions (i) and (ii) stated above. In the formulation it is assumed that the propagation direction of earthquake disturbances is arbitrary. The disturbances involve two horizontal displacement components, one parallel to the propagation direction and the other perpendicular. In Chapter 4, the methods used in the integration of the equations of linear and nonlinear models are discussed. In that chapter, the numerical methods employed in free vibration and earthquake spectrum analyses for the linear behavior of masonry buildings are also presented. Chapter 5 contains two general purpose computer programs prepared for linear and nonlinear earthquake analyses of masonry buildings. The

first program performs free vibration, earthquake spectrum and time history analyses for linear behavior, and time history analysis for nonlinear behavior by ELM. The second program carries out a time history analysis for the nonlinear earthquake behavior by using the actual nonlinear model. The programs perform the analyses for both unreinforced and reinforced masonry buildings. In this chapter, the manuals for both of the programs are also presented. In Chapter 6, some numerical examples are given. The first example is given with the object of comparing the experimental data available for a single story adobe house with those predicted by the models proposed in this study. The other examples involve a three-story masonry building having a complicated geometry. Finally in Chapter 7, the models proposed in this study are assessed in view of the results obtained from example problems and some conclusions are drawn.

2. NONLINEAR DYNAMIC PROPERTIES OF MASONRY WALL ELEMENTS

In the analysis it is assumed that the nonlinear wall behavior arises from the shear deformation of the wall elements in their own planes. This assumption dictates that only the inplane shear modulus G of a masonry wall element and its viscous counterpart G' will enter the nonlinear formulation. For this reason, the discussions in this section are restricted to the properties of G and G'.

The dependence of the dynamic values of G and G' on the deformation state of a masonry wall were investigated experimentally in [3] and [4] by subjecting clay-brick masonry wall specimens to inplane earthquake excitations using the shaking table available at the laboratories of the Earthquake Engineering Research Center, University of California, Berkeley. In [4], the curves describing the variation of G with the shear strain γ and that of G' with the shear strain rate $\dot{\gamma}$ (dot designates the time derivative) are presented. However, the use of "the equivalent linear method" (ELM) in nonlinear formulation requires that we relate both G and G' to the shear strain γ. For this reason, in this study we reexamined the experimental data in [3] and [4], and related G' to γ instead of to $\dot{\gamma}$. The resulting curves are shown in Fig.1, where the variations of G and G' with γ are represented by bilinear and trilinear functions, respectively.

As seen from Fig.1, the wall behaves linearly up to a

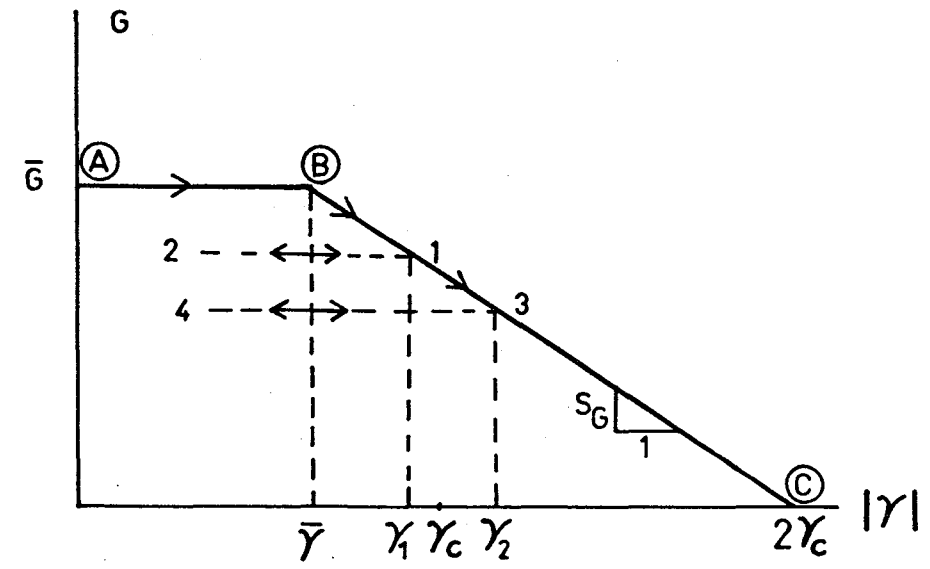

(a)

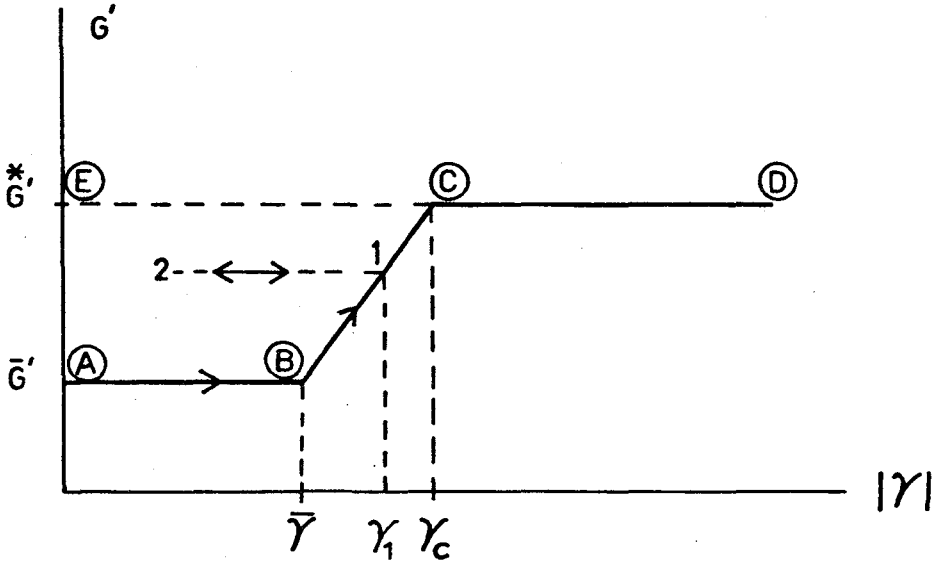

(b)

Figure 1 The variations of the shear modulus and its viscous counterpart with the shear strain (a) for the shear modulus (b) for the viscous coefficient

shear strain value $\bar{\gamma}$ with the shear modulus $\bar{G}$ and viscous coefficient $\bar{G}'$. After $\bar{\gamma}$, the degradation starts and the shear modulus, G, decreases linearly with increasing strain values having the slope S_G; the viscous coefficient, G', increases linearly up to the strain γ_c after which it remains constant. This constant value is denoted by $\overset{*}{G}'$ in the figure. It should be noted the G and G' in Fig.1 describe the secant values. γ_c in Fig.1 represents the shear strain corresponding to the peak of the elastic shear stress-shear strain (τ-γ) curve as indicated in Fig.2. As seen from Fig.1, the variation of G with $|\gamma|$ is described by the three parameters $\bar{\gamma}$, γ_c and $\bar{G}$ while that of G' is governed by four parameters γ, γ_c, $\bar{G}'$ and $\overset{*}{G}'$. Since the parameters $\bar{\gamma}$ and γ_c are common to G and G', the total number of parameters needed for the description of G and G' is five. The values of these parameters were determined experimentally in [4] for a masonry wall which is made of fired clay bricks. They are

$$\begin{aligned}
\bar{G} &= 0.1680 \text{ kN/mm}^2 \\
&\quad (24.3899 \text{ ksi}) \\
\bar{G}' &= 0.8969 \times 10^{-3} \text{ kN-s/mm}^2 \\
&\quad (0.1302 \text{ ksi-s}) \\
\overset{*}{G}' &= 1.8557 \times 10^{-3} \text{ kN-s/mm}^2 \\
&\quad (0.2694 \text{ ksi-s}) \\
\bar{\gamma} &= 5.1329 \times 10^{-4} \text{ rad} \\
\gamma_c &= 1.58 \times 10^{-3} \text{ rad}
\end{aligned} \qquad (1)$$

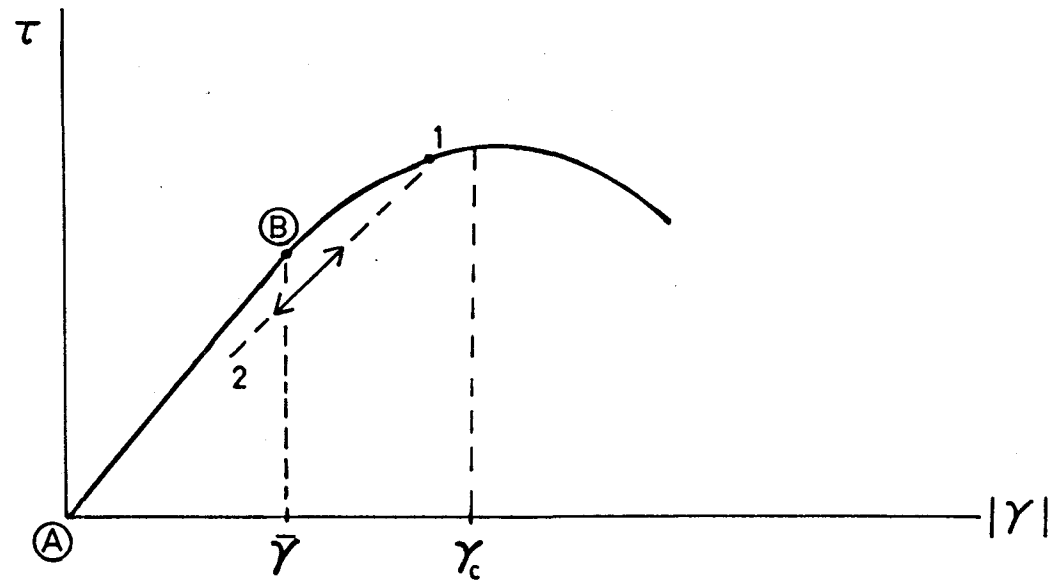

Figure 2 Elastic shear stress - shear strain curve

It may be noted that these values give one a feeling about the order of the values of the parameters for the masonry wall elements which are made of different bricks and constructed by using different workmanship than the ones tested on the shaking table in [4].

The solid lines in Fig.1 represent the envelope (skeleton) lines for the variations of G and G' with $|\gamma|$ which are discussed above. We now explain loading and unloading characteristics of G and G'. We do this first for G by using a specified earthquake loading. Let us consider a virgin masonry wall which is excited in its plane by an earthquake causing shear strain in the wall with a certain time history. Suppose that the shear strain first increases monotically and reaches a peak value, say γ_1 (absolutely), at the time $t=t_1$. Further, suppose that the peak values after $t=t_1$ remain smaller than γ_1 and that γ_1 is larger than the initial yield strain $\bar{\gamma}$. The path describing the variation of G during this excitation would be as follows (see.Fig.1a). Until $|\gamma|$ reaches the value $\bar{\gamma}$, G remains constant along the horizontal line AB in the linear range, with the value $\bar{G}$. At B, the degradation in the value of G starts and it continues along the line B1 as the crack accumulation in the wall increases. At the point 1, the peak value γ_1 is reached; after this point no further cracking takes place since remaining peak values are smaller than γ_1. Accordingly, during loading and unloading occuring after the point 1, G remains constant along the horizontal

line 12. This loading and unloading line 12 is also shown in the shear strain-shear stress plane in Fig.2.

We consider now a second loading in which we assume the wall has a damaged state which is caused by the excitation considered in the first loading. We assume now that this nonvirgin wall is subjected to an earthquake excitation having the same characteristics as those of the excitation which was used in the previous example, except that the maximum shear strain is now γ_2 where $\gamma_2 > \gamma_1$. For this loading, G first remains constant along the horizontal line 12 with the value representing the shear modulus of the non-virgin state (see Fig.1a). Degradation starts at the point 1 and continues to the point 3, where the maximum value γ_2 is reached. After the point 3, no further cracking takes place in the wall, and G has a constant value along the horizontal line 34.

The loading and unloading characteristics of G′ are similar to those of G. The solid line ABCD in Fig.1b represents the envelope curve for G′. The path AB12 in this figure describes the variation of G′ for a virgin wall subjected to the first earthquake loading considered in the discussions pertaining to G. As the interpretation of this path AB12 is similar to that given for G, it will not be presented here. The loading and unloading rules for G′ for a nonvirgin (damaged) wall are the same as those discussed for G, and not to complicate the figure the paths associated with these rules are not indicated in Fig.1b. From the

examination of the figure it is evident that when $|\gamma|$ during an earthquake loading reaches a peak value (say at $t=\overset{*}{t}$) which is equal to or larger than γ_c , after $t=\overset{*}{t}$ G′ will remain constant, with the value $\overset{*}{G}'$, during loadings and unloadings occurring along the horizontal line ED.

In reference 4, a criterion measuring the amount of damage in a masonry wall element caused by an earthquake excitation was also proposed. This criterion is modified slightly in this study and described by the equations

$$D = \frac{|\gamma_{eff} - \bar{\gamma}|}{|2\gamma_c - \bar{\gamma}|} \quad \text{for } \gamma_{eff} > \bar{\gamma}$$
$$D = 0 \quad \text{for } \gamma_{eff} < \bar{\gamma} \,, \tag{2}$$

where D designates the amount of damage and γ_{eff} denotes the effective shear strain which is, through a constant, related to the maximum value of $|\gamma|$ that occurs in the wall element during an earthquake excitation.

3. THE MODEL USED FOR THE EARTHQUAKE ANALYSIS OF MASONRY BUILDINGS

In this section we formulate a model which governs the nonlinear response of a masonry building to an earthquake excitation. The building has "n" stories where floors are reinforced concrete slabs (see Fig.3). The floors are numbered in increasing order in the upward direction. The story heights are assumed to be different and the height of the i th story is designated by "h_i". The building, which is composed of wall assemblies as shown in Fig.3, is referred to a right handed global cartesian coordinate system xyz in which the xy`plane is parallel to the floor, the z axis is directed upwards and the origin is at the base. A wall assembly extends the full height of the building. The part of the assembly that is between two adjacent floors will be called a "wall element" in our study. Each wall assembly is referred to a right handed local cartesian coordinate system uvw in which the axis w is parallel to the z axis and passes through the centroid of the wall section, and the u axis is in the inplane horizontal direction of the assembly. The orientation of the local coordinate system with respect to the global coordinate system is described by the angle θ which measures the angle between the u axis and the x axis in a counterclockwise direction. We designate the width and thickness of a wall assembly by "H" and "B", respectively, as shown in Fig.3. In the formulation we assume that for a

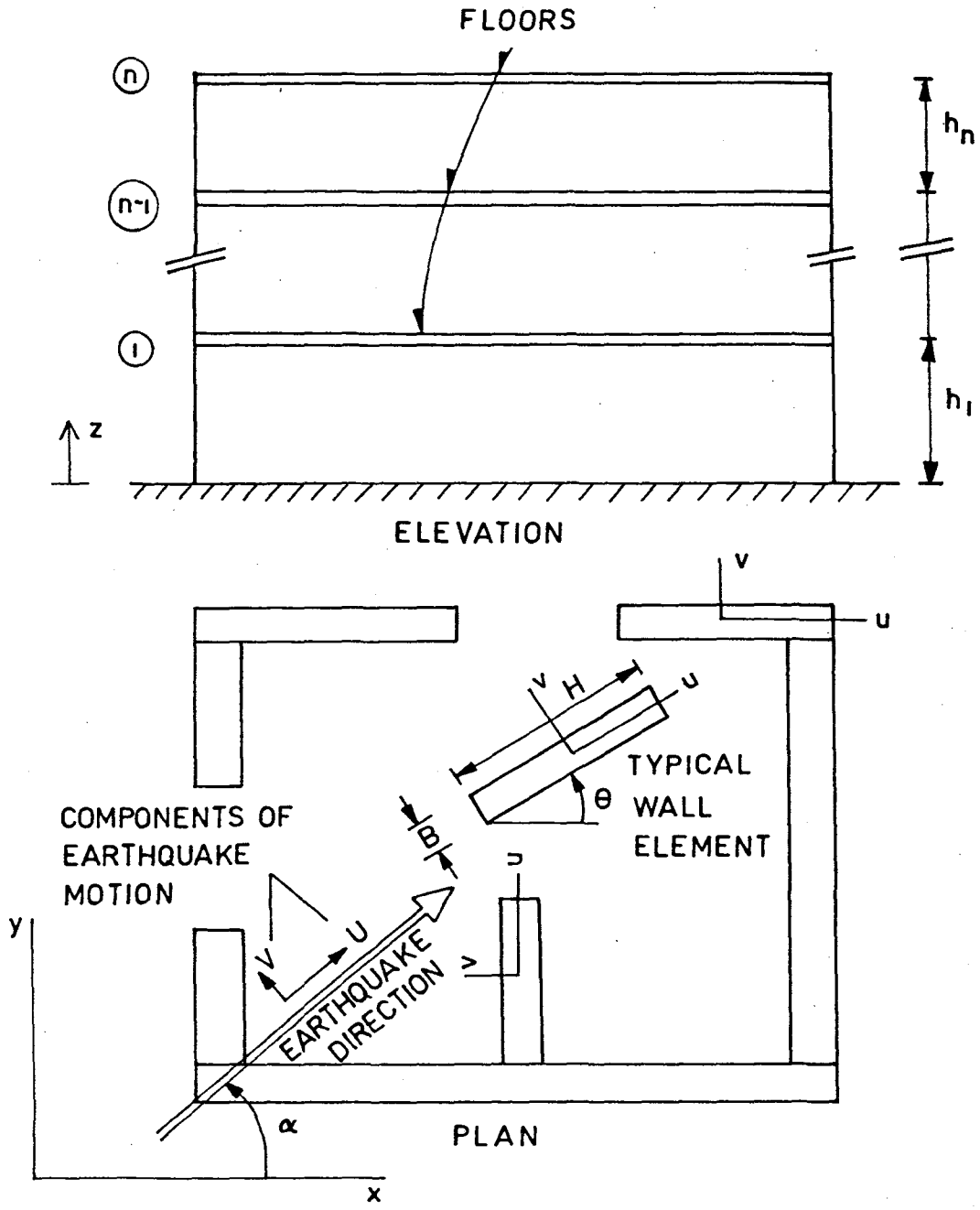

Figure 3 Masonry building

wall assembly H and B values may change from one story to another, but the location of the centroid of the wall sections remains the same for all the stories.

The masonry building is subjected to an earthquake excitation which propagates horizontally and has a propagation direction that makes an angle α with the x axis in a counterclockwise direction (see Fig.3). The earthquake motion involves two ground displacement components, namely U and V, which are respectively parallel and perpendicular to the earthquake propagation direction.

To formulate the model for the nonlinear response of the masonry building to the earthquake input described above, we will use the following simplifying assumptions:

a) In the formulation the axial deformations will be neglected, but the torsional rigidity of wall elements will be taken into account.

b) For unreinforced masonry buildings the behavior of wall elements in their planes is governed by their inplane shear deformations and the rigidities of wall elements in out-of-plane directions are neglected.

c) For reinforced masonry buildings the assumption regarding the inplane behavior of wall elements is the same as that stated in part (b); but, in this case the rigidities of wall elements in out-of-plane directions are not neglected.

d) The nonlinear behavior of masonry buildings arises from the nonlinear properties of wall elements associated with

their inplane shear deformations, which were discussed in the previous chapter. The wall behavior in the out-of-plane direction remains linear. The validity of the last assumption will be discussed later in view of the results obtained from example problems which will be presented in Chapter 6. In the study, the elasticity modulus E and its viscous counterpart E′ associated with the out-of-plane deformations will be assumed to be given by

$$E = 2\,\bar{G}$$
$$E' = 2\,\bar{G}' \quad , \tag{3}$$

where $\bar{G}$ and $\bar{G}'$ are the linear values of the inplane shear modulus and its viscous counterpart (see Fig.1).

e) The parameters defining G and G′ are the same for all of the wall elements of the masonry building.

f) The masses of the building are lumped at floor levels.

g) The floors are infinitely rigid in their own planes. The use of this assumption makes it possible to employ rigid diaphragm modelling [1] in the formulation which decreases the number of unknowns in the analysis.

In what follows, we first discuss very briefly the rigid diaphragm model. Then, we present the formulation for the linear earthquake responses of unreinforced and reinforced masonry buildings. Finally we formulate the nonlinear earthquake response by using two approaches. The first one involves the use of "equivalent linear method" (ELM), which determines the nonlinear response approximately through

iterations in each of which the building behavior is linear. The second approach used in the nonlinear analysis employs the actual nonlinear model for wall behavior discussed in Chapter 2.

3.1 Rigid Diaphragm Model

In the formulation we model the floors as diaphragms which are infinitely rigid in their own planes. In view of this assumption, we can relate the horizontal displacements (d_x, d_y) and the rotation about the z axis, d_θ, of an arbitrary point P on the floor to the horizontal displacements (D_x, D_y) and the rotation D_θ of a master point M (chosen on the same floor) by (see Fig.4)

$$\begin{aligned} d_x &= D_x - (y - y_m) D_\theta \\ d_y &= D_y + (x - x_m) D_\theta \\ d_\theta &= D_\theta \end{aligned} \tag{4}$$

where (x_m, y_m) and (x,y) denote respectively the coordinates of the master point M and the arbitrary point P. It may be noted that the use of this model makes it possible to express the displacements of all of the wall assemblies at a certain floor level in terms of the displacements of the master point of the same floor level, which decreases the number of unknowns considerably. The location of the master point may be arbitrary for a static problem; but, since we are dealing with a dynamic problem its formulation dictates that the master point in our case should be chosen to coincide with the mass center of the floor.

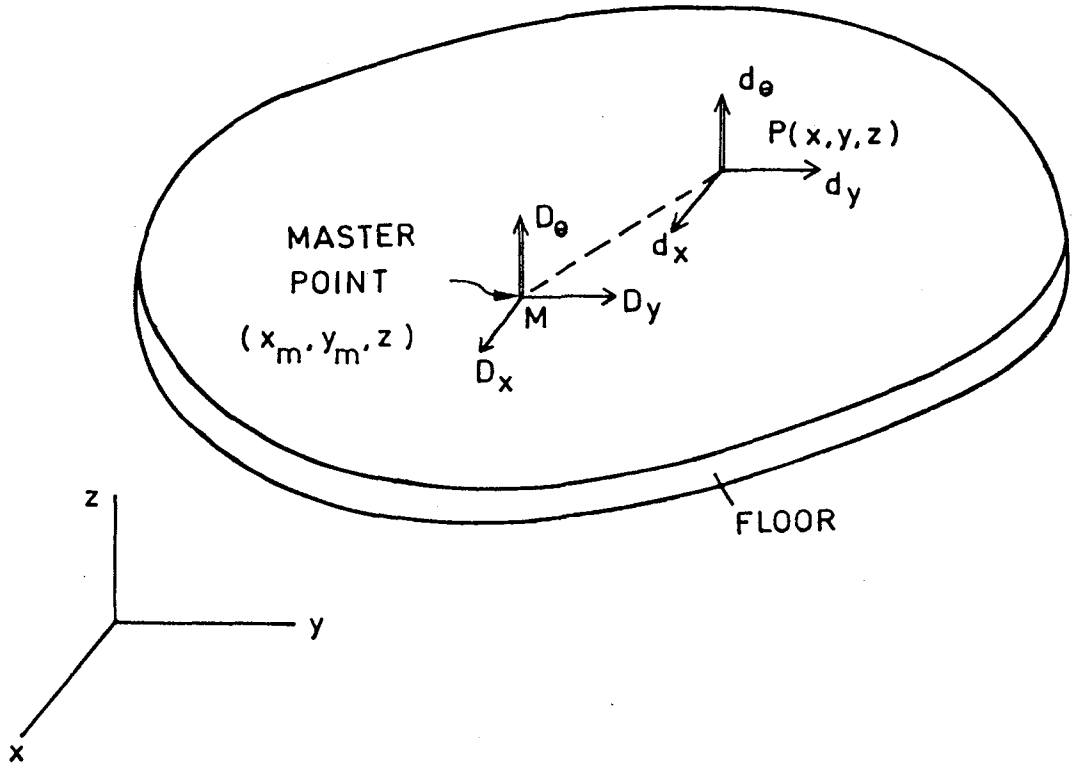

Figure 4 Rigid diaphragm model

3.2 Formulation for Linear Response

In this section, the formulations will be presented for the linear response of unreinforced and reinforced masonry buildings.

3.2.1 Unreinforced Case

We will formulate the model for the linear response of unreinforced masonry buildings using the stiffness (displacement) method. We start the formulation by referring to Fig.5 which shows the free body diagram of a typical wall assembly. The wall assembly is referred to the local coordinate system uvw defined in Fig.3. As stated previously, the wall assembly may have a different width and thickness for each story, but it has a common w axis. In view of the assumptions (a) and (b), it can be shown that the assembly forces are related to the assembly displacements by

$$\underbrace{\begin{bmatrix} \underset{\sim}{p}_u \\ \cdots \\ \underset{\sim}{p}_\theta \end{bmatrix}}_{\underset{\sim}{p}} = \underbrace{\begin{bmatrix} \tilde{\underset{\sim}{k}}_u & \vdots & \underset{\sim}{0} \\ \cdots & \cdots & \cdots \\ \underset{\sim}{0} & \vdots & \underset{\sim}{k}_\theta \end{bmatrix}}_{\tilde{\underset{\sim}{k}}} \underbrace{\begin{bmatrix} \underset{\sim}{d}_u \\ \cdots \\ \underset{\sim}{d}_\theta \end{bmatrix}}_{\underset{\sim}{d}} \tag{5}$$

or, in compact form, by

$$\underset{\sim}{p} = \tilde{\underset{\sim}{k}} \; \underset{\sim}{d} \quad . \tag{6}$$

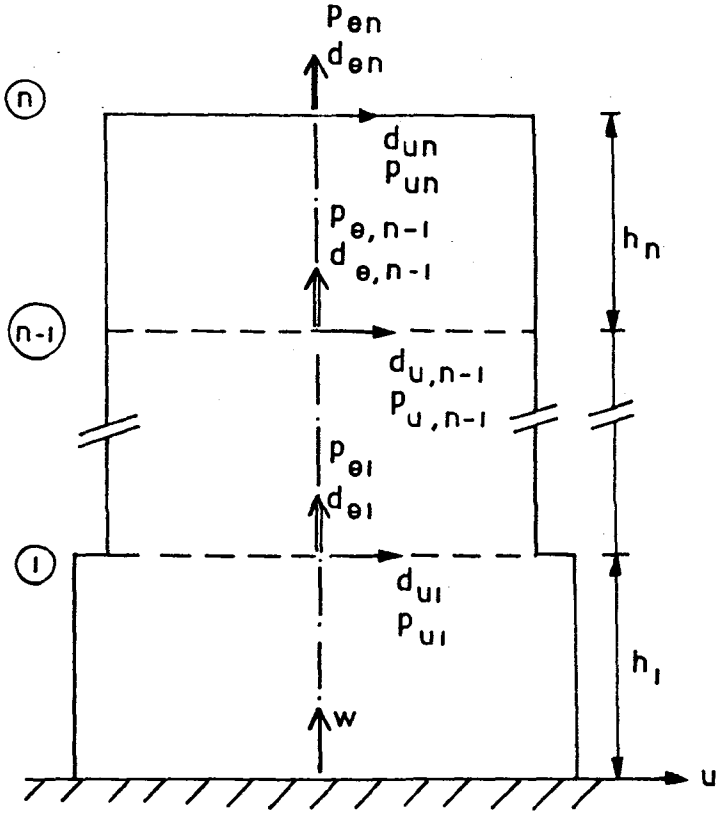

Figure 5 A typical wall assembly

In Eq.(5)

$$\underset{\sim}{p}_{\beta} = (\; p_{\beta 1} \quad p_{\beta 2} \quad \cdots \quad p_{\beta n} \;)^{T}$$

$$\underset{\sim}{d}_{\beta} = (\; d_{\beta 1} \quad d_{\beta 2} \quad \cdots \quad d_{\beta n} \;)^{T} \quad , (\beta = u, \theta) \tag{7}$$

where the undertilde is used to designate a matrix or vector and the superscript T denotes the transpose. p_{ui} and $p_{\theta i}$ describe, respectively, the horizontal force in the u direction and the torque about the w axis acting on the i th floor of the assembly (see Fig.5), which will be called assembly forces. On the other hand, d_{ui} and $d_{\theta i}$ are the assembly displacements which represent, respectively, the horizontal displacement in the u direction and the rotation about the w axis of the i th floor of the assembly. The matrices $\underset{\sim}{\tilde{k}}_{u}$ and $\underset{\sim}{\tilde{k}}_{\theta}$ are defined by

$$\underset{\sim}{\tilde{k}}_{u} = \begin{bmatrix} (k_1+k_2) & -k_2 & & & & \\ -k_2 & (k_2+k_3) & -k_3 & & \underset{\sim}{0} & \\ & \ddots & \ddots & \ddots & & \\ & & \ddots & \ddots & \ddots & \\ & \underset{\sim}{0} & & -k_{n-1} & (k_{n-1}+k_n) & -k_n \\ & & & & -k_n & k_n \end{bmatrix}$$

$$\underset{\sim}{\tilde{k}}_{\theta} = \begin{bmatrix} (\alpha_1+\alpha_2) & -\alpha_2 & & & & \\ -\alpha_2 & (\alpha_2+\alpha_3) & -\alpha_3 & & \underset{\sim}{0} & \\ & \ddots & \ddots & \ddots & & \\ & & \ddots & \ddots & \ddots & \\ & \underset{\sim}{0} & & -\alpha_{n-1} & (\alpha_{n-1}+\alpha_n) & -\alpha_n \\ & & & & -\alpha_n & \alpha_n \end{bmatrix} \tag{8}$$

In Eqs.(8) k_i and α_i are given by

$$k_i = \left[\frac{\tilde{G} \; A}{h} \right]_i$$

$$\alpha_i = \left[\frac{\tilde{G} \; J}{h} \right]_i \qquad (9)$$

in which $\tilde{G}$ is the operator defined by

$$\tilde{G} = G + G' \frac{d}{dt} \qquad (10)$$

where t denotes the time. In Eqs.(9), the index i corresponds to the story number, and A and J designate respectively the shear area and torsional inertial moment of the wall section. We note that, in view of Fig.3, for A we can write

$$A = B \; H * k \qquad (11)$$

where k is the coefficient of the shear area.

In Eq.(10), G and G' represent, respectively, the linear values of the shear modulus and its viscous counterpart. In view of the definition of $\tilde{G}$ in Eq.(10), from Eqs.(5), (8) and (9) it follows that $\underset{\sim}{\tilde{k}}$ appearing in Eq.(6) is an operator

defined by

$$\tilde{\underset{\sim}{k}} = \underset{\sim}{k} + \underset{\sim}{c}\ \frac{d}{dt} \quad , \tag{12}$$

where $\underset{\sim}{k}$ and $\underset{\sim}{c}$ represent, respectively, the stiffness and damping matrices of the wall assembly. The expressions defining the matrices $\underset{\sim}{k}$ and $\underset{\sim}{c}$ remain the same as those of $\tilde{\underset{\sim}{k}}$ given by Eqs.(5) and (8) provided that $\tilde{G}$ in Eqs.(9) is replaced by G and G', respectively.

It may be noted that Eq.(6) is written for a typical assembly and it should contain an index identifying different assemblies of the masonry building; but, that index is ignored in Eq.(6) to prevent complicating the notation.

We now relate the assembly displacements $\underset{\sim}{d}$, which are written in local coordinates in Eqs.(7), to the displacements of the master points of the floors. To this end we first express $\underset{\sim}{d}$ in global coordinates, and then use the equations of the rigid diaphragm model, Eqs.(4). After some manipulation, we get

$$\underset{\sim}{d} = \underset{\sim}{B}\ \underset{\sim}{D} \quad , \tag{13}$$

where $\underset{\sim}{D}$ represents the master point displacements in the global coordinate system xyz and is defined by

$$\underset{\sim}{D} = (\underset{\sim}{D}_x \quad \underset{\sim}{D}_y \quad \underset{\sim}{D}_\theta)^T \tag{14}$$

in which

$$\underset{\sim}{D}_\beta = (D_{\beta 1} \quad D_{\beta 2} \quad \ldots \quad D_{\beta n})^T \quad , (\beta = x, y, \theta) \tag{15}$$

Here, D_{xi}, D_{yi} and $D_{\theta i}$ designate, respectively, the displacements of the master point in the x and y directions, and its rotation about the z axis for the i th floor. The matrix $\underset{\sim}{B}$ in Eq.(13) is given by

$$\underset{\sim}{B} = \begin{bmatrix} \underset{\sim}{I}\cos\theta & \underset{\sim}{I}\sin\theta & -[y-y_{mi}]\cos\theta \\ & & +[x-x_{mi}]\sin\theta \\ \underset{\sim}{0} & \underset{\sim}{0} & \underset{\sim}{I} \end{bmatrix} \tag{16}$$

where (x,y) are the x and y coordinates of the axis of the wall assembly under consideration, and (x_{mi}, y_{mi}) denote the x and y coordinates of the master point of the i th floor. $\underset{\sim}{I}$ in Eq.(16) is the n - dimensional identity matrix, and $[x-x_{mi}]$ and $[y-y_{mi}]$ designate n - dimensional diagonal matrices with the elements $(x-x_{mi})$ and $(y-y_{mi})$ respectively. We note that the angle θ for an assembly was already defined in Fig.3.

It can be shown that the assembly forces $\underset{\sim}{p}$ and their static equivalences at master points are related by

$$\underset{\sim}{f} = \underset{\sim}{B}^T \underset{\sim}{p} \tag{17}$$

Here

$$\underset{\sim}{f} = (\underset{\sim}{f}_x \quad \underset{\sim}{f}_y \quad \underset{\sim}{f}_\theta)^T \tag{18}$$

where

$$\underset{\sim}{f}_\beta = (f_{\beta 1} \quad f_{\beta 2} \quad \ldots \quad f_{\beta n})^T \quad ,(\beta=x,y,\theta) \tag{19}$$

defines the assembly forces at master points which are expressed in the global coordinate system. In Eq.(19), f_{xi}, f_{yi}, and $f_{\theta i}$ designate the components of these forces for the i th floor.

When Eq.(13) is substituted in Eq.(6), and the resulting expression is used in Eq.(17), one finds

$$\underset{\sim}{f} = (\underset{\sim}{B}^T \tilde{\underset{\sim}{k}} \underset{\sim}{B}) \underset{\sim}{D} \tag{20}$$

which relates the static equivalences of the assembly forces at master points to the master point displacements.

Eq.(20) is written for a typical assembly. When we write this equation for all of the assemblies and combine them by considering the equilibrium of each floor (in the sense of D'Alembert's principle), we obtain

$$\tilde{\underset{\sim}{K}} \underset{\sim}{D} = \underset{\sim}{F} \tag{21}$$

where

$$\tilde{\underset{\sim}{K}} = \Sigma\ \underset{\sim}{B}^T\ \tilde{\underset{\sim}{k}}\ \underset{\sim}{B} \tag{22}$$

and $\underset{\sim}{F}$ designates the inertia forces acting at master points and is defined by

$$\underset{\sim}{F} = (\ \underset{\sim}{F}_x \quad \underset{\sim}{F}_y \quad \underset{\sim}{F}_\theta\ )^T \tag{23}$$

where

$$\underset{\sim}{F}_\beta = (\ F_{\beta 1} \quad F_{\beta 2} \quad \ldots \quad F_{\beta n}\ ) \quad ,(\beta = x,y,\theta) \quad . \tag{24}$$

In Eq.(24), F_{xi}, F_{yi} and $F_{\theta i}$ designate respectively the inertia forces in the x and y directions and the inertial moment about the z axis acting at the master point of the i th floor.

In Eq.(22), the summation is to be understood as taken over wall assemblies. In view of the definition of $\tilde{\underset{\sim}{k}}$ in Eq.(12), one can write for $\tilde{\underset{\sim}{K}}$

$$\tilde{\underset{\sim}{K}} = \underset{\sim}{K} + \underset{\sim}{C}\ \frac{d}{dt} \tag{25}$$

where

$$\begin{aligned} \underset{\sim}{K} &= \Sigma\ \underset{\sim}{B}^T\ \underset{\sim}{k}\ \underset{\sim}{B} \\ \underset{\sim}{C} &= \Sigma\ \underset{\sim}{B}^T\ \underset{\sim}{c}\ \underset{\sim}{B} \end{aligned} \tag{26}$$

are respectively system stiffness and damping matrices.

We now establish the equation governing the linear response of the masonry building to the earthquake

excitation defined in Fig.3. First we note that $\underset{\sim}{D}$ in Eq.(21) designates the master point displacements relative to the ground. In view of the assumed earthquake excitation, one can now write for the inertia forces

$$\underset{\sim}{F}_x = -\underset{\sim}{\bar{M}} \left(\ddot{\underset{\sim}{D}}_x + \underset{\sim}{1} \cos\alpha\, \ddot{U} - \underset{\sim}{1} \sin\alpha\, \ddot{V}\right)$$

$$\underset{\sim}{F}_y = -\underset{\sim}{\bar{M}} \left(\ddot{\underset{\sim}{D}}_y + \underset{\sim}{1} \sin\alpha\, \ddot{U} + \underset{\sim}{1} \cos\alpha\, \ddot{V}\right) \qquad (27)$$

$$\underset{\sim}{F}_\theta = -\underset{\sim}{I}_m \ddot{\underset{\sim}{D}}_\theta \quad ,$$

where the dot denotes differentiation with respect to time, $\underset{\sim}{1}$ is an n - dimensional vector defined by

$$\underset{\sim}{1} = (\, 1 \quad 1 \quad \ldots \quad 1\,)^T \quad ,$$

and $\underset{\sim}{\bar{M}}$ and $\underset{\sim}{I}_m$ are n - dimensional diagonal matrices with the elements $\bar{M}_i$ and I_{mi} respectively. Here, $\bar{M}_i$ and I_{mi} designate respectively the mass and the mass inertia moment about the mass center for the i th floor.

When we substitute Eqs.(27) into Eq.(21) by using Eqs.(14) and (23), and take into account Eq.(25), we get

$$\underset{\sim}{M}\ \ddot{\underset{\sim}{D}} + \underset{\sim}{C}\ \dot{\underset{\sim}{D}} + \underset{\sim}{K}\ \underset{\sim}{D} = -\underset{\sim}{M}\ \underset{\sim}{r}_u\, \ddot{U} - \underset{\sim}{M}\ \underset{\sim}{r}_v\, \ddot{V} \quad , \qquad (28)$$

where

$$\underset{\sim}{M} = \begin{bmatrix} \bar{\underset{\sim}{M}} & & \underset{\sim}{0} \\ & \bar{\underset{\sim}{M}} & \\ \underset{\sim}{0} & & \underset{\sim}{I}_m \end{bmatrix}$$

$$\underset{\sim}{r}_u = (\underset{\sim}{1} \cos\alpha \quad \underset{\sim}{1} \sin\alpha \quad \underset{\sim}{0})^T \tag{29}$$

$$\underset{\sim}{r}_v = (-\underset{\sim}{1} \sin\alpha \quad \underset{\sim}{1} \cos\alpha \quad \underset{\sim}{0})^T$$

For a given earthquake input, the solution of Eq.(28) determines the master point displacements $\underset{\sim}{D}$. Having $\underset{\sim}{D}$, one can compute the displacements of the wall elements in local coordinates by using Eq.(13). Finally, the forces and the inplane shear strain of the wall element e in local coordinates can be found from

$$V_e = k_e \left(d_u^2 - d_u^1 \right)_e$$

$$T_e = \alpha_e \left(d_\theta^2 - d_\theta^1 \right)_e \tag{30}$$

$$\gamma_e = \frac{\left(d_u^2 - d_u^1 \right)_e}{h_e}$$

where V_e, T_e and γ_e designate respectively the inplane shear force, the torque and the inplane shear strain in the element e; k_e and α_e are defined by Eqs.(9) when the index i in these equations is replaced by e; h_e is the height of the wall element e and the superscripts 1 and 2 designate respectively the lower and upper ends of the wall element.

3.2.2 Reinforced Case

In this case the rigidities of the wall elements in the out-of-plane direction v (see Fig.3) will be taken into account. These rigidities will accommodate both the bending and shear deformations of the wall element in the v-w plane. The element equation for a typical wall element describing the wall behavior in this plane can be written as

$$\underset{\sim}{p}_e = \tilde{\underset{\sim}{k}}_e \; \underset{\sim}{d}_e \quad , \tag{31}$$

where $\underset{\sim}{p}_e = (p_1, \ldots, p_4)$ and $\underset{\sim}{d}_e = (d_1, \ldots, d_4)$ designate the element forces and displacements associated with the directions shown in Fig.6, and the generalized stiffness matrix $\tilde{\underset{\sim}{k}}_e$ is given by

$$\tilde{\underset{\sim}{k}}_e = \frac{\tilde{E}\, I}{h^3(1+a)} \begin{bmatrix} 12 & -12 & 6\,h & 6\,h \\ -12 & 12 & -6\,h & -6\,h \\ 6\,h & -6\,h & (4+a)h^2 & (2-a)h^2 \\ 6\,h & -6\,h & (2-a)h^2 & (4+a)h^2 \end{bmatrix} \tag{32}$$

In Eq.(32)

$$\tilde{E} = E + E' \frac{d}{dt} \quad , \tag{33}$$

where the elasticity modulus E and its viscous counterpart E' are assumed to be related to the linear values of G and G' by Eqs.(3). $I = H\,B^3/12$ is the inertial moment of the wall section about the u axis (see Fig.3); h is the height of the wall element; and a is defined by

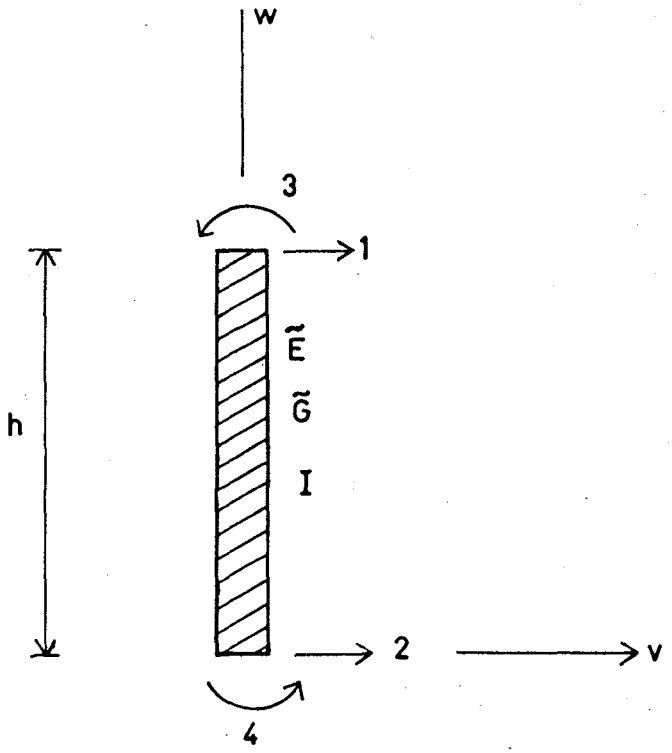

Figure 6 The view of a typical element in vw plane

$$a = \frac{12\ E\ I}{h^2\ G\ A} = \frac{12\ E'\ I}{h^2\ G'\ A} \quad ,$$

where A is the shear area of the wall section and G and G' stand for the linear values of the shear modulus and its viscous counterpart. In view of Eqs.(3), the last expression defining "a" reduces to

$$a = \frac{24\ I}{h^2\ A} \quad . \tag{34}$$

After this preparation, we now turn our attention to how the formulation changes when the rigidities in the out-of-plane directions are included in the analysis. The form of Eq.(6) relating the assembly forces to the assembly displacements remains the same for the reinforced case provided that the definitions of $\underset{\sim}{p}$, $\underset{\sim}{d}$ and $\underset{\sim}{\tilde{k}}$ are modified as

$$\begin{aligned} \underset{\sim}{p} &= (\underset{\sim}{p}_u \quad \underset{\sim}{p}_v \quad \underset{\sim}{p}_\theta)^T \\ \underset{\sim}{d} &= (\underset{\sim}{d}_u \quad \underset{\sim}{d}_v \quad \underset{\sim}{d}_\theta)^T \quad , \end{aligned} \tag{35}$$

and

$$\underset{\sim}{\tilde{k}} = \begin{bmatrix} \underset{\sim}{\tilde{k}}_u & \vdots & \underset{\sim}{0} & \vdots & \underset{\sim}{0} \\ \cdots & \cdots & \cdots & \cdots & \cdots \\ \underset{\sim}{0} & \vdots & \underset{\sim}{\tilde{k}}_v & \vdots & \underset{\sim}{0} \\ \cdots & \cdots & \cdots & \cdots & \cdots \\ \underset{\sim}{0} & \vdots & \underset{\sim}{0} & \vdots & \underset{\sim}{\tilde{k}}_\theta \end{bmatrix} \quad . \tag{36}$$

In Eqs.(35)

$$\underset{\sim}{p}_v = (\; p_{v1} \quad p_{v2} \quad \cdots \quad p_{vn} \;)^T$$

$$\underset{\sim}{d}_v = (\; d_{v1} \quad d_{v2} \quad \cdots \quad d_{vn} \;)^T \tag{37}$$

are, respectively, assembly forces and displacements associated with the v (out-of-plane) direction. $\tilde{\underset{\sim}{k}}_v$ in Eq.(36) describes the generalized stiffness matrix of the wall assembly in the v-w plane. The other variables appearing in Eqs.(35) and (36) were defined in the previous section.

To determine $\tilde{\underset{\sim}{k}}_v$ we make a simplifying assumption. This assumption involves restraining the rotations of the wall assembly about the u axis at the floor levels (see Fig.3). When the element stiffness matrices Eq.(32), are combined for a wall assembly by using coding technique and when the above mentioned assumption is taking into account, one gets

$$\tilde{\underset{\sim}{k}}_v = \begin{bmatrix} (s_1+s_2) & -s_2 & & & & \\ -s_2 & (s_2+s_3) & -s_3 & & \underset{\sim}{0} & \\ & \ddots & \ddots & \ddots & & \\ & & \ddots & \ddots & \ddots & \\ & \underset{\sim}{0} & & -s_{n-1} & (s_{n-1}+s_n) & -s_n \\ & & & & -s_n & s_n \end{bmatrix} \tag{38}$$

where s_i is defined by

$$s_i = \left[\frac{12 \; \tilde{E} \; I}{h^3(1+a)} \right]_i \quad . \tag{39}$$

The other equations presented for the unreinforced case remain the same as the reinforced case except that the transformation matrix $\underset{\sim}{B}$ should also involve the v direction, which implies that $\underset{\sim}{B}$ is given by

$$\underset{\sim}{B} = \begin{bmatrix} \underset{\sim}{I}\cos\theta & \underset{\sim}{I}\sin\theta & -[\,y-y_{mi}\,]\cos\theta \\ & & +[\,x-x_{mi}\,]\sin\theta \\ -\underset{\sim}{I}\sin\theta & \underset{\sim}{I}\cos\theta & [\,y-y_{mi}\,]\sin\theta \\ & & +[\,x-x_{mi}\,]\cos\theta \\ \underset{\sim}{0} & \underset{\sim}{0} & \underset{\sim}{I} \end{bmatrix} . \qquad (40)$$

It should be noted that $\underset{\sim}{k}$ and $\underset{\sim}{c}$ matrices appearing in Eq.(12) for the reinforced case are to be computed by replacing $\tilde{G}$ and $\tilde{E}$ by G and E in Eqs.(9) and (39) for the matrix $\underset{\sim}{k}$, and by G′ and E′ in the same equations for the matrix $\underset{\sim}{c}$.

If we summarize, the equations for the reinforced case are given by the equations presented in the previous section for the unreinforced case provided that the generalized assembly stiffness matrix $\underset{\sim}{\tilde{k}}$ and the transformation matrix $\underset{\sim}{B}$ are given respectively by Eqs.(36) and (40). After we determine the master point displacements from Eq.(28) and the assembly displacements from Eq.(13), the inplane element forces can be computed by using Eqs.(30) and out-of-plane element forces, by using Eq.(31).

3.3 Formulation for Nonlinear Response

As stated in the basic assumptions listed in Chapter 3, we assume that the nonlinear response of both reinforced and unreinforced masonry buildings originates in the inplane shear deformations of wall elements. In the out-of-plane direction, the wall rigidity is neglected for the unreinforced case and it is taken into account for the reinforced case by assuming that its behavior in that direction remains linear. These assumptions imply that the nonlinear effects in the response of masonry buildings will enter the formulation through the nonlinear properties of G and G' which were discussed in Chapter 2.

For the nonlinear earthquake analysis of masonry buildings we will use two methods. The first is an approximate method called "equivalent linear method" (ELM) proposed by Seed and Idriss in [2] in conjunction with nonlinear soil-structure interaction problems. The second one involves the exact model, which will be called the actual nonlinear model (ANM) in this study. The latter method performs the nonlinear analysis by using the loading and unloading characteristics of G and G' discussed in Chapter 2, which were established in [3,4] experimentally. Both of these methods are valid for both reinforced and unreinforced masonry buildings. In what follows we discuss the two methods separately.

3.3.1 Equivalent Linear Method (ELM)

ELM performs the nonlinear analysis in terms of linear analyses by using iterations. Each iteration of ELM involves the use of the secant values of the elastic moduli and viscous coefficients which are compatible with the deformation state of the previous iteration. The iterations of ELM can be carried out by solving the equations of the linear model presented in Section 3.2.1 for the unreinforced case and in Section 3.2.2 for the reinforced case.

In employing ELM in nonlinear analysis, we first define the effective shear strain γ_{eff} by

$$\gamma_{eff} = c \ \gamma_{max} , \tag{41}$$

where c is a constant smaller than 1 and γ_{max} designates the absolute maximum value of the shear strain (with respect to time) which a wall element experiences during earthquake loading. In [5], the use of the value 0.65 for the constant c is suggested in soil-structure interaction analysis.

We now state, in algorithm form, the steps of ELM which is used in our analysis.

i) Start the iterations by assuming that the values of the shear modulus and its viscous counterpart are equal to the their linear values, i.e., $G=\bar{G}$ and $G'=\bar{G}'$ (see Fig.1).

ii) Using these values of G and G′ carry out the linear analysis described in the previous section and determine, for each wall element, the time

variation of γ and compute γ_{eff} from Eq.(41).

iii) Corresponding to γ_{eff} values found in (ii), compute the new secant values of G and G′ for each wall element by using the envelope lines given in Fig.1, and check the convergence by employing the criteria

$$T = \frac{1}{N} \sum \frac{\left| G_{new} - G_{old} \right|}{G_{new}} \leq \varepsilon$$

$$T' = \frac{1}{N} \sum \frac{\left| G'_{new} - G'_{old} \right|}{G'_{new}} \leq \varepsilon \qquad (42)$$

where ε is a small prescribed convergence factor and N is the total number of wall elements. The summation in Eq.(42) is to be taken over all of the wall elements of the masonry building. (G_{old}, G'_{old}) and (G_{new}, G'_{new}) denote the values of (G, G′) before and after the iteration respectively. If the convergence criteria in Eqs.(42) are satisfied stop the iterations; if not, with the new values of G and G′ go to the step (ii).

iv) With the converged values of G and G′, compute the time variations for the desired displacements and element forces. Also, for each wall element determine the damage ratio D by using Eq.(2), and the maximum values of element forces.

As mentioned previously, the use of ELM in nonlinear analysis requires the solution of the equations of the linear model in each iteration of the algorithm stated above. The numerical methods used in solving these equations will be discussed in later sections.

3.3.2 Actual Nonlinear Model (ANM)

In this section, we establish a model for the nonlinear earthquake behavior of masonry buildings by taking into account the hysteretic characteristics of the shear modulus G and its viscous counterpart G'. To this end, we first note that in the linear models established in Sections 3.2.1 and 3.2.2, G and G' are constant and have respectively the values $\bar{G}$ and $\bar{G}'$ which represent the values of G and G' in linear range (see Fig.1). Examination of the derivation of the linear models indicates that the form of these models will also be valid for the nonlinear behavior of masonry buildings provided that G and G' appearing in the definitions of $\underset{\sim}{\tilde{k}}_u$ and $\underset{\sim}{\tilde{k}}_\theta$ in Eqs.(5) and (36) are treated as parameter functions whose values depend on the time history of the inplane shear strain γ of a wall element. These parameters will be designated symbolically as $G(\gamma)$ and $G'(\gamma)$. We say "symbolically" because these parameter functions are not simple functions of γ ; instead, they describe hysteretic, i.e., loading and unloading, characteristics of a wall element associated with its inplane deformation. The envelope lines and hysteretic

(loading and unloading) characteristics of $G(\gamma)$ and $G'(\gamma)$ were already discussed in Chapter 2 and described in Fig.1.

We now summarize the actual nonlinear model. The equations of ANM will be given by those in Section 3.2.1 for the unreinforced case and in Section 3.2.2 for the reinforced case provided that G and G' appearing in Eq.(10) are replaced by $G(\gamma)$ and $G'(\gamma)$ respectively. The envelope lines and loading and unloading characteristics of the parameter functions $G(\gamma)$ and $G'(\gamma)$ are to be taken from Chapter 2.

The numerical integration of the equations of ANM will be discussed in a later section.

4. THE METHODS OF ANALYSIS USED IN THE STUDY

In this chapter we discuss the computational methods used in linear and nonlinear analysis of masonry buildings. The linear analysis involves the free vibration, earthquake spectrum and earthquake time history analyses whereas the nonlinear analysis involves only the earthquake time history analysis.

4.1 The Methods Used in Linear Analysis and in the Nonlinear Analysis by ELM

In what follows we present the methods used in this study in free vibration, earthquake spectrum and earthquake time history analyses for the linear response of masonry buildings. It may be noted that the method presented in this section for the linear time history analysis can be used also to determine the nonlinear response by ELM since each iteration of ELM involves linear analysis.

4.1.1 Free Vibration Analysis

In the free vibration analysis of masonry buildings we ignore damping. It should be noted that since the damping matrix $\underset{\sim}{C}$ in Eq.(28) is proportional to the stiffness matrix $\underset{\sim}{K}$ in linear analysis, the mode shape vectors found for the undamped case will be orthogonal not only with respect to the mass matrix $\underset{\sim}{M}$ and the stiffness matrix $\underset{\sim}{K}$ but also with respect to the damping matrix $\underset{\sim}{C}$; thus, the mode shape vectors which will be found for the undamped case can be

used to transform the coupled system, Eq.(28), into an uncoupled system.

When the damping matrix $\underset{\sim}{C}$ in Eq.(28) is neglected, external loading is ignored and harmonic time variation for displacement vector $\underset{\sim}{D}$ (representing the master point displacements) is assumed, the equation governing free vibrations of a masonry building can be found as

$$\underset{\sim}{K}\ \underset{\sim}{a} = \lambda\ \underset{\sim}{M}\ \underset{\sim}{a}\ . \qquad (43)$$

with $\lambda = \omega^2$. Here is angular free vibration frequency and $\underset{\sim}{a}$ is mode shape vector.

In this study, the eigenvalue problem in Eq.(43) governing free vibration characteristics of masonry buildings is solved by using an inverse iteration method [6,7] and by normalizing the mode shape vectors with respect to the mass matrix $\underset{\sim}{M}$. A brief description of this method is presented below.

First, without loss of generality, we assume that the eigenvalues of the eigenvalue problem in Eq.(43) are ordered as

$$\lambda_m > \lambda_{m-1} > \ldots\ldots > \lambda_2 > \lambda_1\ , \qquad (44)$$

where m=3n (n:number of stories) represents the degree of freedom of the masonry building. Let $\underset{\sim}{a}_k$ (k=1-m) be the eigenvector (mode shape vector) corresponding to the k th eigenvalue λ_k . In the inverse iteration method we first determine (λ_1, $\underset{\sim}{a}_1$); then, using $\underset{\sim}{a}_1$ we compute (λ_2, $\underset{\sim}{a}_2$);

then, with the aid of $\underset{\sim}{a}_1, \underset{\sim}{a}_2$ we compute $(\lambda_3, \underset{\sim}{a}_3)$, and so on.

Computation of λ_1 and $\underset{\sim}{a}_1$

First choose

$$\underset{\sim}{a}^{o} = [\ 1\ \ .\ .\ .\ .\ \ 1\ ]^{T} \tag{45}$$

as the initial approximation for $\underset{\sim}{a}_1$. Then using the formulas

$$\underset{\sim}{K}\ \underset{\sim}{z}^{i+1} = \underset{\sim}{M}\ \underset{\sim}{a}^{i} \quad ====> \quad \underset{\sim}{z}^{i+1}$$

$$R_{i+1} = [(\underset{\sim}{z}^{i+1})^{T}\ \underset{\sim}{M}\ \underset{\sim}{z}^{i+1}]^{1/2} \tag{46}$$

$$\underset{\sim}{a}^{i+1} = \frac{\underset{\sim}{z}^{i+1}}{R_{i+1}} \qquad (\ i = 0,1,\ ....)$$

generate the sequences $\{R_1, R_2, ...\}$ and $\{\underset{\sim}{a}^1, \underset{\sim}{a}^2, ...\}$. The sequences $\{R_i\}$ and $\{\underset{\sim}{a}^i\}$ thus computed would converge respectively to $1/\lambda_1$ and $\underset{\sim}{a}_1$. In this study, as the convergence criterion,

$$\left| \frac{R_{i+1} - R_i}{R_i} \right| < \varepsilon \quad (i = 0,1,\ ...) \tag{47}$$

is used. Here, ε is a convergence factor whose value depends on the desired accuracy.

Computation of λ_2 and $\underset{\sim}{a}_2$

For the determination of $(\lambda_2, \underset{\sim}{a}_2)$, a procedure similar to that used for $(\lambda_1, \underset{\sim}{a}_1)$ will be followed; but, in this case the vector in each iteration is modified so that it will be orthogonal to $\underset{\sim}{a}_1$ with respect to the mass matrix $\underset{\sim}{M}$.

Again, choose $\underset{\sim}{a}^o$ in Eq.(45) as initial approximation for $\underset{\sim}{a}_2$. Now, generate the sequences $\{R_i\}$ and $\{\underset{\sim}{a}^i\}$ by

$$
\begin{aligned}
b_1^i &= \underset{\sim}{a}_1^T \ \underset{\sim}{M} \ \underset{\sim}{a}^i \\
\underset{\sim}{Y}^i &= \underset{\sim}{a}^i - b_1^i \ \underset{\sim}{a}_1 \\
\underset{\sim}{K} \ \underset{\sim}{z}^{i+1} &= \underset{\sim}{M} \ \underset{\sim}{Y}^i \quad \Longrightarrow \quad \underset{\sim}{z}^{i+1} \\
R_{i+1} &= \left[(\underset{\sim}{z}^{i+1})^T \ \underset{\sim}{M} \ \underset{\sim}{z}^{i+1} \right]^{1/2} \\
\underset{\sim}{a}^{i+1} &= \frac{\underset{\sim}{z}^{i+1}}{R_{i+1}} \qquad (i = 0,1, \ldots .) .
\end{aligned}
\tag{48}
$$

Continue the iterations until the convergence criterion, Eq.(47), is satisfied. The converged values of $\{R_i\}$ and $\{\underset{\sim}{a}^i\}$ will give respectively $1/\lambda_2$ and $\underset{\sim}{a}_2$.

Computation of λ_3 and $\underset{\sim}{a}_3$

To compute $(\lambda_3, \underset{\sim}{a}_3)$, the iteration vector in each iteration should be modified so that it will be orthogonal to both $\underset{\sim}{a}_1$ and $\underset{\sim}{a}_2$ with respect to the mass matrix $\underset{\sim}{M}$.

After choosing $\underset{\sim}{a}^o$in Eq.(45) as initial approximation for

$\underset{\sim}{a}_3$, generate the sequences $\{R_i\}$ and $\{\underset{\sim}{a}^i\}$ by using

$$
\begin{aligned}
b_1^i &= \underset{\sim}{a}_1^T \ \underset{\sim}{M} \ \underset{\sim}{a}^i \\
b_2^i &= \underset{\sim}{a}_2^T \ \underset{\sim}{M} \ \underset{\sim}{a}^i \\
\underset{\sim}{Y}^i &= \underset{\sim}{a}^i - b_1^i \ \underset{\sim}{a}_1 - b_2^i \ \underset{\sim}{a}_2 \\
\underset{\sim}{K} \ \underset{\sim}{z}^{i+1} &= \underset{\sim}{M} \ \underset{\sim}{Y}^i \quad \Longrightarrow \quad \underset{\sim}{z}^{i+1} \\
R_{i+1} &= [(\underset{\sim}{z}^{i+1})^T \ \underset{\sim}{M} \ \underset{\sim}{z}^{i+1}]^{1/2} \\
\underset{\sim}{a}^{i+1} &= \frac{\underset{\sim}{z}^{i+1}}{R_{i+1}} \qquad (i = 0,1, \ldots) \quad .
\end{aligned}
\tag{49}
$$

The converged values of $\{R_i\}$ and $\{\underset{\sim}{a}^i\}$ will determine $1/\lambda_3$ and $\underset{\sim}{a}_3$ respectively.

Using the inverse iteration method discussed above, as many eigenvalues and eigenvectors as desired can be computed. The numerical examples which will be presented in Chapter 6 indicate that the inverse iteration method can be used reliably in the free vibration analysis of masonry buildings and is capable of computing all the frequencies without skipping any of them regardless of how close they are to each other.

4.1.2 Earthquake Spectrum Analysis

As is known, earthquake spectrum analysis (ESA) is valid for linear responses of structural systems [8]; so, the

analysis which will be presented in this section can be used only for linear behavior of masonry buildings. It is also known that ESA is based on mode superposition technique [8,9] whose use requires the assumption that mode shape vectors are orthogonal not only with respect to mass and stiffness matrices but also with respect to the damping matrix. As mentioned previously, it may be noted that this assumption holds in our case since the damping matrix $\underset{\sim}{C}$ appearing in the governing equation, Eq.(28), is proportional to the stiffness matrix $\underset{\sim}{K}$ for the linear response of masonry buildings.

In what follows we apply, without going into details, the general formulation used in ESA [8] to our problem, i.e., to the linear earthquake response of masonry buildings whose governing equation is given by Eq.(28). To this end, we expand the master point displacement vector $\underset{\sim}{D}$ as

$$\underset{\sim}{D} = \underset{\sim}{a}_1 Y_1 + \underset{\sim}{a}_2 Y_2 + ... + \underset{\sim}{a}_m Y_m \quad , \tag{50}$$

where m=3n (n:number of stories), Y_k's are time dependent modal displacements and $\underset{\sim}{a}_k$'s are mode shape vectors.

The object of the ESA is to determine absolute maximum values of displacements, element forces, etc. To determine these maximum values we first note that the earthquake excitation considered in this study involves two ground displacement components U and V which are respectively parallel and perpendicular to the earthquake propagation direction (see Fig.3). Since our problem is linear,

in what follows we first determine the responses caused by the earthquake ground displacements U and V separately and then we superpose these two responses to obtain the total response. In the presentation of the equations, we use a terminology in which the two responses produced by the ground displacement components U and V are differentiated by the superscripts u and v respectively.

When one applies the procedure followed in general formulation [8] to our case, i.e., to Eq.(28), and takes into account the discussions and terminology stated above, one finds the maximum values of modal displacements as

$$(Y_k^u)_{max} = \max_t |Y_k^u| = \frac{a_k^u}{\omega_k^2} S_{ak}^u$$
$$(Y_k^v)_{max} = \max_t |Y_k^v| = \frac{a_k^v}{\omega_k^2} S_{ak}^v \quad , \tag{51}$$

where

$$a_k^u = \frac{\underset{\sim}{a}_k^T \underset{\sim}{M} \underset{\sim}{r}_u}{m_k} \quad , \quad a_k^v = \frac{\underset{\sim}{a}_k^T \underset{\sim}{M} \underset{\sim}{r}_v}{m_k} \quad . \tag{52}$$

In Eqs.(51), Y_k^u and Y_k^v designate the modal displacements produced by the earthquake displacement components U and V respectively (see.Fig.3); $m_k = \underset{\sim}{a}_k^T \underset{\sim}{M} \underset{\sim}{a}_k$ is the k th modal mass which is equal to one in our case since we are using normalization with respect to mass matrix; S_{ak}^u and S_{ak}^v represent the earthquake acceleration spectrum values for the k th mode associated with the earthquake components U

and V respectively; $\max_t$ () designates the maximum value of () with respect to time. α_k^u and α_k^v in Eqs.(52) are modal participation factors. $\underset{\sim}{r}_u$ and $\underset{\sim}{r}_v$ appearing in Eqs.(52) were defined previously in Eqs.(29).

The maximum contributions coming from the k th mode to the master point displacements are, in view of Eq.(50),

$$\underset{\sim}{D}^{ku} = \underset{\sim}{a}_k \, (Y_k^u)_{max}$$

$$\underset{\sim}{D}^{kv} = \underset{\sim}{a}_k \, (Y_k^v)_{max} \quad , \tag{53}$$

which are respectively associated with the ground displacements U and V. Having determined the master point displacements from Eqs.(53), one can evaluate,for the k th mode, the assembly displacements $\underset{\sim}{d}$ and element forces $\underset{\sim}{p}_e$ using Eqs.(13) and elastic parts of Eqs.(30) and (31). Let them be designated by

$$(\underset{\sim}{d}^{ku}, \underset{\sim}{p}_e^{ku})$$

$$(\underset{\sim}{d}^{kv}, \underset{\sim}{p}_e^{kv}) \tag{54}$$

which respectively pertain to the ground displacements U and V.

Eqs.(53) and (54) define the contributions coming from the k th mode to the response quantities. To combine the contributions of the first K modes to the response, in this study "complete quadratic combination" (CQC) technique [10] is employed. The CQC formula is given by

$$A_{max} \cong \left[\sum_{k=1}^{K} A_k^2 + \sum_{k=1}^{K} \sum_{\substack{m=1 \\ k \neq m}}^{K} \frac{A_k \, A_m}{1 + \varepsilon_{km}^2} \right]^{1/2} \tag{55}$$

$$\varepsilon_{km} = \frac{\sqrt{1 - \xi^2}}{\xi} \, \frac{\omega_k - \omega_m}{\omega_k + \omega_m} \quad ,$$

where

$A_{max} = \max_t | A |$

A : a response quantity

A_k: the contribution of the k th mode to A

K : the number of modes considered

ξ : damping ratio .

In this study, ξ is taken to be the damping ratio of the first mode. It may be noted that the damping ratio ξ_k of the masonry building for the k th mode can be computed by

$$\xi_k = \frac{c_k}{2 \, m_k \, \omega_k} \tag{56}$$

with

$$c_k = \underset{\sim}{a}_k^T \, \underset{\sim}{C} \, \underset{\sim}{a}_k \quad . \tag{57}$$

It can be shown after some simple manipulations that in our linear analysis in which $\underset{\sim}{C}$ is proportional to $\underset{\sim}{K}$, Eq.(56) reduces to

$$\xi_k = \frac{\beta \, \omega_k}{2} \quad , \tag{58}$$

where $\beta = \bar{G}'/\bar{G}$.

Let the response quantities found after the application

of the CQC formula in Eqs.(55) to Eqs.(53) and (54) be designated by

$$\begin{matrix} (\underset{\sim}{D}^{u},\ \underset{\sim}{d}^{u}\ ,\underset{\sim}{p}_{e}^{u}\ ) \\ \\ (\underset{\sim}{D}^{v},\ \underset{\sim}{d}^{v}\ ,\underset{\sim}{p}_{e}^{v}\ ) \end{matrix} \qquad (59)$$

where the contributions of the first K modes are included.

The variables appearing in the first and second lines of Eqs.(59) represent the response quantities corresponding to the earthquake ground displacement components U and V respectively. Now it remains to combine these two types of response quantities to obtain the total response. In our study, this combination is made by using "square root of sum of the squares" (SRSS) technique, i.e., by the formula

$$A_{max} \cong \sqrt{(A^{u})^{2} + (A^{v})^{2}} \qquad (60)$$

where

$A_{max} = \max_{t} \mid A \mid$

A : a response quantity

A^{u}, A^{v} : the values of A associated with the ground displacement components U and V.

We now summarize the steps of ESA in an algorithm form.

a) Choose number of modes K which will be considered in ESA and compute (ω_{k}, $\underset{\sim}{a}_{k}$), (k=1-K).

b) Compute earthquake acceleration spectrum values (S^{u}_{ak}, S^{v}_{ak}) for the frequency values ω_{k}(k=1-K)

from the spectrum values given in tabular form associated with the earthquake displacement components U and V.

c) Determine the master point displacements ($\underset{\sim}{D}^{ku}$, $\underset{\sim}{D}^{kv}$) (k=1-K) from Eqs.(51) and (53); then, evaluate the assembly displacements ($\underset{\sim}{d}^{ku}$, $\underset{\sim}{d}^{kv}$), (k=1-K) by using Eq.(13) and the element forces ($\underset{\sim}{p}_e^{ku}$, $\underset{\sim}{p}_e^{kv}$), (k=1-K) by Eqs.(30), (31).

d) Combining the contributions of the first K modes with the aid of CQC technique, Eqs.(55), compute the element forces, the master point and assembly displacements appearing in Eqs.(59).

e) Finally, by SRSS technique, Eq.(60), combine the response quantities in Eqs.(59) (which are associated with the ground displacements U and V), and thus determine the total response.

4.1.3 Time History Analysis

As mentioned previously, each iteration of ELM involves linear analysis; so, both the linear analysis (LA) and the nonlinear analysis based on ELM (which will be named in this study as "equivalent linear analysis" (ELA)) can be carried out using the integration methods valid for the linear model. In view of the internal organization of the computer programs presented in the next chapter, we found in our study that it would be more convenient if we choose the same numerical integration method for both LA and ELA. As the use of mode superposition technique dictates the

condition that the damping matrix $\underset{\sim}{C}$ be proportional to the stiffness matrix $\underset{\sim}{K}$, it is not possible to choose this technique as integration method for both LA and ELA since the aforementioned condition is satisfied only in LA, but not in ELA (this is because G and G' in each iteration of ELA might have different values for each wall element, which makes the damping matrix to be nonproportional to $\underset{\sim}{K}$). Accordingly, a step-by-step method, namely Runge-Kutta's method of order 4 (RK4) [6], which is applicable to both proportional and nonproportional damping cases is chosen as integration method in both LA and ELA.

In using RK4 in LA and ELA, we first express the governing equation, Eq.(28), as a system of first order ordinary differential equations, which yields

$$\dot{D}_i = V_i$$

$$\dot{V}_i = -\frac{1}{M_i}\left(\sum_{j=1}^{m} K_{ij} D_j + \sum_{j=1}^{m} C_{ij} V_j\right) \qquad (61)$$

$$- r_u^i a_u - r_v^i a_v \equiv f_{Vi} \quad ; \quad (i=1\text{-}m) \ ,$$

where

$m = 3n$: number of degrees of freedom of the masonry building

M_i : the diagonal elements of the system mass matrix $\underset{\sim}{M}$ in Eqs.(29)

K_{ij}, C_{ij}: elements of the system stiffness matrix $\underset{\sim}{K}$ and damping matrix $\underset{\sim}{C}$

r_u^i , r_v^i : components of the vectors $\underset{\sim}{r}_u$ and $\underset{\sim}{r}_v$ appearing in Eqs.(29)

a_u , a_v : ground accelerations in U and V directions (see Fig.3), which are defined by U and V respectively

We note that K_{ij} and C_{ij} values depend, in addition to geometric properties of wall elements, on G, G', E and E'. The values of these moduli are constant both in LA and in each iteration of ELA. From Eqs.(3) and the assumption (e) in Chapter 3, it may be observed that these constant values are the same for all of the elements in LA whereas they may vary from one wall element to another in ELA. In view of discussions stated above, one may see that the K_{ij} and C_{ij}'s are constants in both LA and in each iteration of ELA. Thus, the time dependent variables on which f_{Vi} (in Eqs.(61)) depends are D_s, V_s (s=1-m), a_u and a_v. We show this dependence symbolically as

$$f_{Vi} = f_{Vi}(D_s , V_s , a_u , a_v) \quad . \tag{62}$$

RK4 formulas for the integration of the governing equations, Eqs.(61), over one time step ..t from the time point t_k to t_{k+1} are

$$D_i^{k+1} = D_i^k + \frac{1}{6} (a_{Di} + 2\, b_{Di} + 2\, c_{Di} + d_{Di})$$

$$V_i^{k+1} = V_i^k + \frac{1}{6} (a_{Vi} + 2\, b_{Vi} + 2\, c_{Vi} + d_{Vi}); \ (i=1-m), \tag{63}$$

where

$$a_{Di} = \Delta t * V_i^k$$

$$a_{Vi} = \Delta t * f_{Vi}(D_s^k, V_s^k, a_u(t_k) , a_v(t_k))$$

$$b_{Di} = \Delta t * (V_i^k + \frac{a_{Vi}}{2})$$

$$b_{Vi} = \Delta t * f_{Vi}(D_s^k + \frac{a_{Ds}}{2}, V_s^k + \frac{a_{Vs}}{2}, a_u(t_k + \frac{\Delta t}{2}), a_v(t_k + \frac{\Delta t}{2}))$$

$$c_{Di} = \Delta t * (V_i^k + \frac{b_{Vi}}{2}) \qquad (64)$$

$$c_{Vi} = \Delta t * f_{Vi}(D_s^k + \frac{b_{Ds}}{2}, V_s^k + \frac{b_{Vs}}{2}, a_u(t_k + \frac{\Delta t}{2}), a_v(t_k + \frac{\Delta t}{2}))$$

$$d_{Di} = \Delta t * (V_i^k + c_{Vi})$$

$$d_{Vi} = \Delta t * f_{Vi}(D_s^k + c_{Ds}, V_s^k + c_{Vs}, a_u(t_k + \Delta t), a_v(t_k + \Delta t)) .$$

In Eqs.(63) and (64), the superscript k designates the values at the time point $t=t_k$.

Writing the recursion of RK4 in each time step and starting from the initial time $t=t_0=0$ where the unknown variables D_i, V_i are known (which are zero in our case since we assume that the masonry building is at rest prior to the application of earthquake excitation), we can progress along the time axis and determine the unknowns at the time points $t=t_1, t_2, \ldots$. In the numerical analysis the time increment $\Delta t = t_{k+1} - t_k$ $(k=0,1,\ldots)$ is taken to be constant and chosen to be equal to that by which the earthquake excitation is recorded.

Having known the master point displacements D_i and velocities V_i, one can compute the assembly displacements and velocities from Eq.(13), and then the element forces and inplane shear strains from Eqs.(30) and (31). It may further be noted that with the aid of D_i and V_i, one can also determine the master point accelerations using Eq.(28).

4.2 The Methods Used in Actual Nonlinear Analysis

The time history analysis based on ANM is carried out by integrating the equations of ANM described in Section 3.3.2 with the aid of RK4.

The equations of ANM expressed as a system of first order differential equations are again given, in form, by Eqs.(61); but in this case, K_{ij} and C_{ij} appearing in Eqs.(61) are no longer constants, instead, they become history dependent parameters whose values change with time and are governed by the hysteretic behavior of wall elements, more explicitely, by the loading and unloading characteristics of G and G' of wall elements discussed in Chapter 2.

From the discussions presented above, it follows that f_{Vi} appearing in Eqs.(61), in the actual nonlinear analysis (ANA), depends on the time dependent variables D_s, V_s, K_{rs}, C_{rs} (r,s=1-m), a_u and a_v, i.e.,

$$f_{Vi} = f_{Vi}(D_s, V_s, K_{rs}, C_{rs}, a_u, a_v) \quad . \tag{65}$$

In view of Eq.(65), we now write the RK4 formulas associated with ANA. They are

$$D_i^{k+1} = D_i^k + \frac{1}{6}\left(a_{Di} + 2\, b_{Di} + 2\, c_{Di} + d_{Di}\right)$$

$$V_i^{k+1} = V_i^k + \frac{1}{6}\left(a_{Vi} + 2\, b_{Vi} + 2\, c_{Vi} + d_{Vi}\right);\ (i=1\text{-}m), \tag{66}$$

where

$$a_{Di} = \Delta t * V_i^k$$

$$a_{Vi} = \Delta t * f_{Vi}\left(D_s^k,\ V_s^k,\ K_{rs}^a,\ C_{rs}^a,\ a_u(t_k)\ ,\ a_v(t_k)\ \right)$$

$$b_{Di} = \Delta t * \left(V_i^k + \frac{a_{Vi}}{2}\right)$$

$$b_{Vi} = \Delta t * f_{Vi}\left(D_s^k + \frac{a_{Ds}}{2},\ V_s^k + \frac{a_{Vs}}{2},\ K_{rs}^b,\ C_{rs}^b,\right.$$
$$\left. a_u(t_k + \frac{\Delta t}{2}),\ a_v(t_k + \frac{\Delta t}{2})\ \right)$$

$$c_{Di} = \Delta t * \left(V_i^k + \frac{b_{Vi}}{2}\right) \tag{67}$$

$$c_{Vi} = \Delta t * f_{Vi}\left(D_s^k + \frac{b_{Ds}}{2},\ V_s^k + \frac{b_{Vs}}{2},\ K_{rs}^c,\ C_{rs}^c,\right.$$
$$\left. a_u(t_k + \frac{\Delta t}{2}),\ a_v(t_k + \frac{\Delta t}{2})\ \right)$$

$$d_{Di} = \Delta t * \left(V_i^k + c_{Vi}\right)$$

$$d_{Vi} = \Delta t * f_{Vi}\left(D_s^k + c_{Ds}\ ,\ V_s^k + c_{Vs},\ K_{rs}^d,\ C_{rs}^d,\right.$$
$$\left. a_u(t_k + \Delta t),\ a_v(t_k + \Delta t)\ \right).$$

Here the superscript k is again used to designate the values at the time point t_k. The hysteretic behavior of wall elements is described by the variables K_{rs}^{α} and C_{rs}^{α} (α=a,b,c,d) in Eqs.(67). These variables are defined as follows:

K_{rs}^{a} and C_{rs}^{a} are the values of K_{rs} and C_{rs} corresponding to G^k and G'^k, where G^k and G'^k designate the G and G' values of wall elements at the time t_k. G^k and G'^k values are assumed to be determined (for all of the wall elements) from the analysis of the previous time step using the loading and unloading characteristics of G and G'.

K_{rs}^{b} and C_{rs}^{b} are to be determined as follows: (i) Compute a_{Di}'s using the first of Eqs.(67). (ii) Calculate the master point (MP) displacement values ($D_i^k+a_{Di}/2$). (iii) Corresponding to these MP displacements find the assembly displacements from Eq.(13) and then using the last of Eqs.(30) compute the inplane shear strain γ_e for each wall element. (iv) Employing these shear strain values and the loading and unloading properties of G and G', determine G and G' values for all of the wall elements (it may be noted that these G and G' values correspond to the deformation state associated with the MP displacements ($D_i^k+a_{Di}/2$)). (v) Finally, calculate stiffness (K_{rs}) and damping (C_{rs}) coefficients corresponding to the G and G' values found in part (iv), which will respectively establish K_{rs}^{b} and C_{rs}^{b} values.

K^c_{rs} and C^c_{rs} can be found by using exactly the same procedure described above for K^b_{rs} and C^b_{rs}; but, in this case the MP displacements should be computed from $(D^k_i+b_{Di}/2)$, where the b_{Di}'s are to be determined from the third of Eqs.(67).

K^d_{rs} and C^d_{rs} are to be computed by using again the aforementioned procedure with MP displacements determined from (D_i+c_{Di}), where c_{Di}'s are to be calculated by employing the fifth of Eqs.(67).

Starting from the initial time point t_0 and using Eqs.(66) and (67), the response quantities D_i and V_i predicted by ANM can be computed at the time points $t_1, t_2, \ldots$.

In view of discussions presented above, we now summarize, in an algorithm form, the numerical integration procedure used in this study for ANA:

i) Set k=0 and let

$$D^k_i = 0 \quad , \; V^k_i = 0 \quad , \quad \gamma^k_e = 0$$
$$G^k = \bar{G} \quad , \quad G'^k = \bar{G}' \quad . \tag{68}$$

ii) Form K^a_{rs} and C^a_{rs} using $G=G^k$ and $G'=G'^k$ and compute a_{Di} and a_{Vi} from the first two of Eqs.(67).

iii) Find MP displacements

$$D^k_i + \frac{a_{Di}}{2} \quad , \tag{69}$$

and associated with them determine the inplane shear strain γ_e for each wall element. Using these γ_e values, and loading and unloading properties of G and G', determine G and G' values for all of the wall elements (which are compatible with the deformation state described by MP displacements in Eq.(69)). Find K^b_{rs} and C^b_{rs}'s by employing the G and G' values computed above. Finally, determine b_{Di} and b_{Vi}'s from the third and fourth of Eqs.(67).

iv) Repeat the procedure in (iii) with MP displacements

$$D_i^k + \frac{b_{Di}}{2} \quad , \tag{70}$$

which will determine K^c_{rs} and C^c_{rs}'s; and find c_{Di} and c_{Vi}'s from the fifth and sixth of Eqs.(67).

v) Again, repeat the procedure in (iii), but in this case, with MP displacements

$$D_i^k + c_{Di} \quad , \tag{71}$$

which will establish K^d_{rs} and C^d_{rs} values, and then determine d_{Di} and d_{Vi}'s from the last two of Eqs.(67).

vi) From Eqs.(66), compute the response quantities D_i^{k+1} and V_i^{k+1} at the time point t_{k+1}. Using displacements D_i^{k+1} compute the shear strain γ_e^{k+1} in each wall element. Employing γ_e^{k+1} values, and loading and unloading properties of G

and G′ compute G and G′ values at the time point t_{k+1}, i.e., G^{k+1} and G'^{k+1}, for all of the wall elements.

vii) For the computations at the next time point set k=k+1 and go to step (ii).

5. COMPUTER PROGRAMS

Based on the formulations and numerical methods discussed in previous chapters, two computer programs are developed, which will be named as MAS1 and MAS2 in this study. The programs are prepared in Fortran 77 and have both their PC and main frame versions available in the Civil Engineering Department, Cukurova University, Adana, Turkey. The first program, MAS1, performs free vibration, earthquake spectrum, linear static, linear time history analyses of masonry buildings as well as nonlinear time history analysis by ELM. The second program, MAS2, carries out the nonlinear time history analysis by using the actual nonlinear model (ANM).

The programs have some data generation capabilities, which will be discussed in later sections, by which one can shorten the input data considerably when the masonry building has a complicated geometry. The programs use free format in reading the data from input files.

The source as well as execution programs of MAS1 and MAS2 are given in the attached 1.2 MB floppy disk. In what follows, we discuss in detail these two programs.

5.1 Computer Program for Linear Analysis and for the Nonlinear Analysis by ELM (MAS1)

MAS1 has the options to perform

- linear static
- free vibration
- earthquake spectrum
- linear time history
- nonlinear time history (by ELM)

analyses. The program is based on the formulations and methods discussed in Chapters 3 and 4. The first option performs the analysis when the MP's are subjected to static loads. It may be noted that even though the equations presented in Section 3.2 are obtained for the dynamic case, they are also valid for the static case provided that the master point displacements are found from

$$\underset{\sim}{K}\ \underset{\sim}{D} = \underset{\sim}{P} \quad , \tag{72}$$

where $\underset{\sim}{P}$ describes the static loads applied to the MP's.

Flow chart of MAS1 is given in Fig.7. The programs calls the subroutines shown in Fig.8, which have the functions listed below.

FILE : reads the name of input data file and generates the names of output and intermediate files

NG : computes the number of entries in an input line, which is needed for data generations

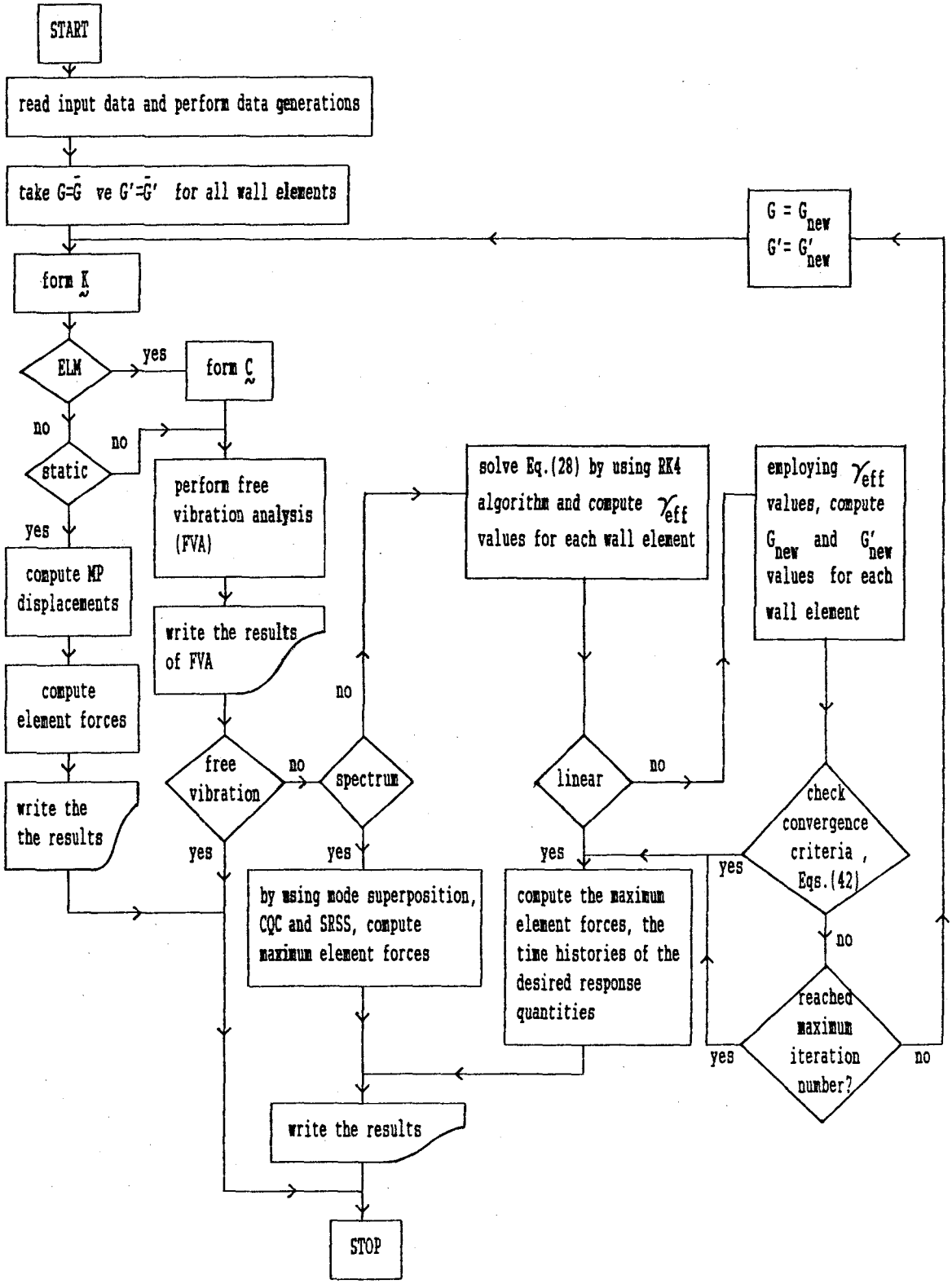

Figure 7 Flow chart of MAS1

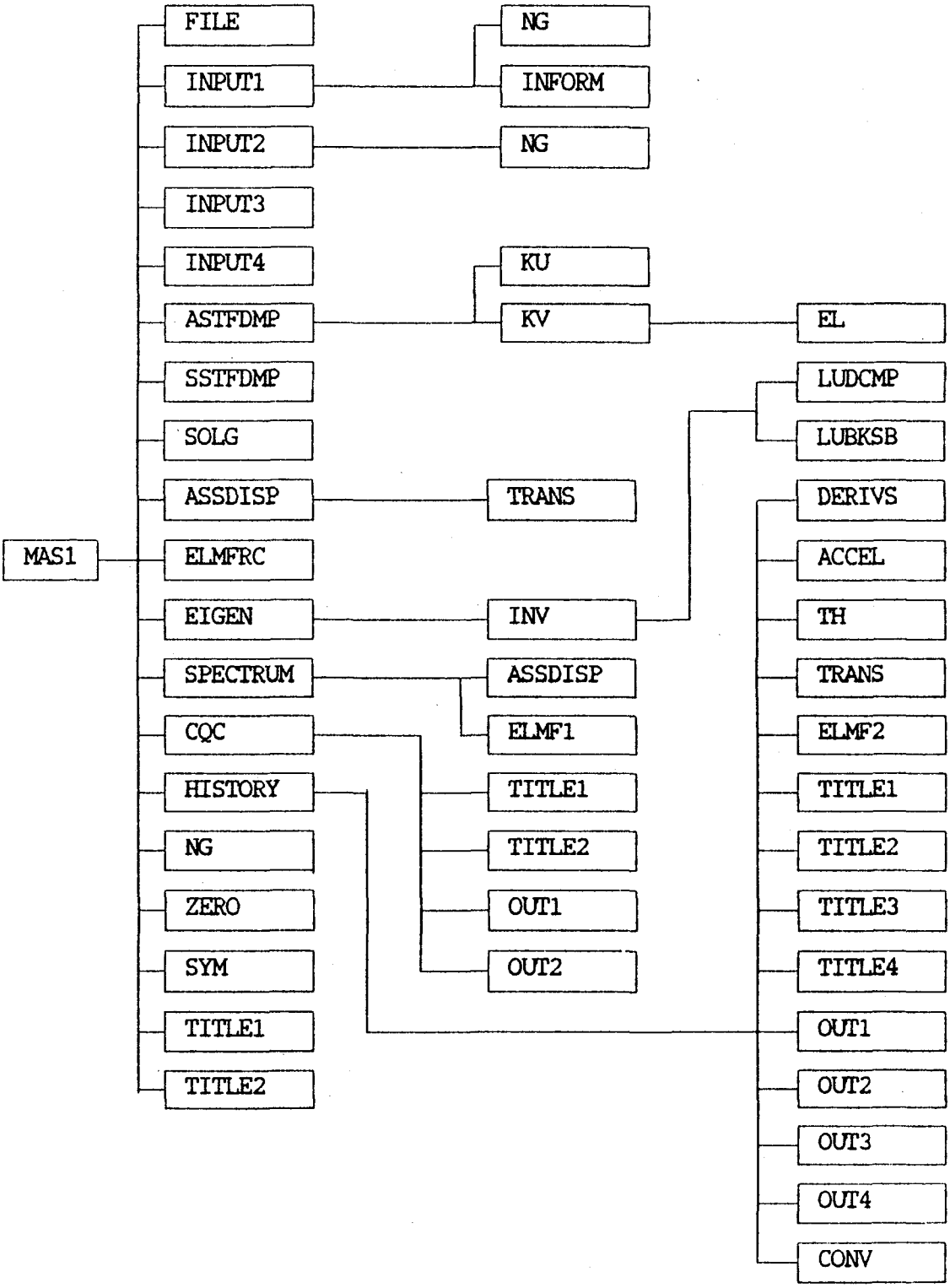

Figure 8 The subroutines used in the computer program MAS1

INPUT1 : reads the contents of the data blocks

GENERAL INFORMATION

STORY HEIGHTS

COORDINATES

PROP. OF ASSEMBLIES

MASSES

LOADS

COORD. OF MP

MATERIAL PROP.

INFORM : writes the input values on the screen

INPUT2 : reads the content of the data block

SPECTRUM

INPUT3 : reads the content of the data block

TIME HISTORY

INPUT4 : reads the earthquake acceleration record

KU : forms $\underset{\sim}{k}_u$ and $\underset{\sim}{k}_\theta$ matrices for each assembly

KV : forms $\underset{\sim}{k}_v$ matrix for each assembly for reinforced case

EL : forms $\underset{\sim}{k}_e$ matrix for each wall element for reinforced case

ZERO : initializes a square matrix

ASTFDMP: forms the stiffness and damping matrices ($\underset{\sim}{k}$, $\underset{\sim}{c}$) for each assembly of the masonry building

TRANS : computes transformation matrix $\underset{\sim}{B}$ for each assembly

SSTFDMP: forms the system stiffness and damping matrices ($\underset{\sim}{K}$, $\underset{\sim}{C}$) using Eqs.(26)

SYM : forms a symmetric matrix completely by using its upper triangular part

SOLG : computes the MP displacements for linear static case by solving

$$\underset{\sim}{K}\ \underset{\sim}{D} = \underset{\sim}{P} ,$$

where $\underset{\sim}{P}$ is the static forces applied to MP's

ELMFRC : computes element forces for linear static case

EIGEN : solves the eigenvalue problem by using the inverse iteration method

INV : performs the inverse iterations in free vibration analysis

LUDCMP : computes $\underset{\sim}{L}$ and $\underset{\sim}{U}$ parts of a square matrix

LUBKSB : computes the solution of a linear algebraic system by LU decomposition method

SPECTRUM: computes the maximum modal displacements $(Y_i)_{max}$ in earthquake spectrum analysis

CQC : combines the modal contributions to the response quantities by CQC and SRSS method as discussed in Section 4.1.2

ELMF1 : computes element forces in earthquake spectrum analysis

HISTORY: performs time history analysis by RK4

DERIVS : in each step of RK4, computes f_{Vi}'s in Eqs.(61)

ASSDISP: computes assembly displacements by using Eq.(13)

ACCEL : using D_i^k and V_i^k computed by RK4, calculates $\ddot{D}_i^k$ of MP's from Eq.(28)

TH : writes the time histories of desired displacements and element forces into the output files

CONV : writes, into an output file, T and T' values in Eqs.(42) for each iteration of ELA and gives information with regard to the satisfaction of the convergence criteria, Eqs.(42)

ELMF2 : computes element forces in time history analysis

TITLE1-4:write the titles for outputs in a suitable format

OUT1-4 : write the outputs in a suitable format

MS-DOS version of MAS1 is given in the attached floppy disk. The execution program can be found in the file

MAS1.EXE

and the listing, in the files

MAS1A.FOR

MAS1B.FOR

MAS1C.FOR .

For MAS1, we now present the manual for input data and give information about output files.

5.1.1 Manual for Input Data

The input data is to be read from a file whose name is specified interactively when MAS1 is run. The name of the input file should have no extension.

The structure of input data for various analysis options are shown in Table 1.

The first line in these data files is a data line indicating the mode of analysis, which should be

STATIC for static analysis

VIBRATION for free vibration analysis

SPECTRUM for earthquake spectrum analysis

LINEAR for linear time history analysis

NONLINEAR for nonlinear time history analysis by ELM

The other lines in Table 1 are the names of some data blocks. These names should be included in the input data file. The data blocks should be entered in the order shown in Table 1. The data in each block should be entered below the block name and should be prepared according to the information given below.

"GENERAL INFORMATION" block:

This block contains a single data line in the format

nru ns nass [mod] [nit] [eps] [c] (73)

Here, square brackets are used to indicate that the variable which they enclose is optional and

nru : an integer indicating whether the masonry

Table 1 The structure of input data for various analysis options of MAS1

linear static analysis	free vibration analysis	earthquake spectrum analysis
STATIC GENERAL INFORMATION STORY HEIGHTS COORDINATES PROP.OF ASSEMBLIES LOADS COORD.OF MP MATERIAL PROP.	VIBRATION GENERAL INFORMATION STORY HEIGHTS COORDINATES PROP.OF ASSEMBLIES MASSES COORD.OF MP MATERIAL PROP.	SPECTRUM GENERAL INFORMATION STORY HEIGHTS COORDINATES PROP.OF ASSEMBLIES MASSES COORD.OF MP MATERIAL PROP. SPECTRUM

linear time history analysis	nonlinear time history analysis
LINEAR GENERAL INFORMATION STORY HEIGHTS COORDINATES PROP.OF ASSEMBLIES MASSES COORD.OF MP MATERIAL PROP. TIME HISTORY	NONLINEAR GENERAL INFORMATION STORY HEIGHTS COORDINATES PROP.OF ASSEMBLIES MASSES COORD.OF MP MATERIAL PROP. TIME HISTORY

structure is reinforced or unreinforced (nru=0 for unreinforced and nru=1 for reinforced case)

ns : number of stories

nass: number of assemblies

mod : number of vibration modes to be considered in the analysis

nit : maximum iteration number

eps : convergence factor being used in ELA (see Eqs.(42))

c : the coefficient which appears in the definition of γ_{eff} (it stands for "c" in Eq.(41))

For the linear static case, the first three; free vibration, earthquake spectrum and linear time history analyses, the first four; nonlinear time history analysis by ELM, all of the data items in the data line, Eq.(73), should be specified.

"STORY HEIGHTS" block:

It contains the data lines of the format

$$n_1 \quad [,n_2] \quad h \tag{74}$$

by which, starting from the first story, the story heights are specified in increasing order in upwards direction. Here,

n_1, n_2: story numbers

h : story height.

The data line in Eq.(74) has a data generation capability and expresses that the story heights from n_1 th to n_2 th stories (n_1 and n_2 are inclusive) are "h". If the optional variable n_2 in Eq.(74) is ignored, i.e., if the data line is entered as

$$n_1 \quad h \quad ,$$

it specifies only the height of the n_1 th story as "h". For example, if the story heights of a five- story masonry building are h_1=4 mt, h_2=h_3=h_4=3 mt and h_5=2.8 mt, the "STORY HEIGHTS" block may be entered as

```
STORY HEIGHTS
1       4.0
2,4     3.0
5       2.8
```

"COORDINATES" block:

In this block the x and y coordinates of the assemblies are given in the data lines of the format

$$n_a \quad x \quad y \qquad (75)$$

where

n_a: assembly number

x : x coordinate of the assembly n_a

y : y coordinate of the assembly n_a .

"PROP.OF ASSEMBLIES" block:

In this block, for each assembly, the data lines having the format

$$\begin{array}{l} n_a \quad \text{theta} \\ n_1 \quad [,n_2] \quad hh \quad b \quad k \end{array} \tag{76}$$

are entered, where

n_a : assembly number

theta: the angle (in degrees) of the local u axis of the assembly n_a with the global x axis (it is the angle "Θ" in Fig.3)

n_1,n_2: story numbers

hh : the width of the assembly n_a in u direction (it is "H" in Fig.3)

b : the thickness of the assembly n_a in v direction (it is "B" in Fig.3)

k : shear area coefficient for the assembly n_a (it is the coefficient "k" in Eq.(11))

The data generation option indicated in the second line of Eqs.(76) states that the width, thickness and shear area coefficient of the assembly n_a from n_1 th to n_2 th stories (n_1 and n_2 are inclusive) are respectively hh, b and k. From the structure of the data lines in Eqs.(76) it may be seen that different values of hh, b and k may be assigned to each story of an assembly. The assembly geometric properties in Eqs.(76) should be entered for each assembly with the order n_a=1,2,...,nass.

"LOADS" block:

It contains the data lines of the format

$$n_1 \quad [,n_2] \quad f_x \quad f_y \quad c \tag{77}$$

by which the static loads applied to MP's are given. Here

n_1, n_2: story numbers

f_x, f_y: x and y components of the static load applied to the MP

c : static moment about z axis applied to the MP

It may be noted that the data line in Eq.(77) has a data generation option which was explained previously. The program assumes that the default values of f_x, f_y and c are zero.

"MASSES" block:

In this block the mass properties of the floors are given by the data lines of the format

$$n_1 \quad [,n_2] \quad m_x \quad m_y \quad i_m \tag{78}$$

where

n_1, n_2: story numbers

m_x, m_y: masses of the floor participating in the motions in x and y directions respectively

i_m : mass inertia moment of the floor

The comments given for the "LOADS" block hold also for this block.

"COORD.OF MP" block:

It has data lines of the format

$$n_1 \quad [,n_2] \quad x_m \quad y_m \tag{79}$$

by which the coordinates of the MP's are specified. Here

n_1, n_2: story numbers

x_m, y_m: x and y coordinates of MP. The form of the data line in Eq.(79) implies that it contains a generation option discussed previously.

"MATERIAL PROP." block:

For the static, free vibration, earthquake spectrum and linear time history analyses, this block contains a single data line having the format

for static analysis:

$$g \tag{80}$$

for free vibration analysis:

$$g \quad [gp] \tag{81}$$

for earthquake spectrum and linear time history analyses

$$g \quad gp \tag{82}$$

where

g : linear value of the shear modulus G (it corresponds to $\bar{G}$ in Fig.1)

gp: linear value of viscous shear modulus G' (it corresponds to $\bar{G}'$ in Fig.1)

If gp in Eq.(81) is given, the program computes not only the free vibration frequencies and vibration shapes, but also the damping ratio for each mode by using Eq.(58).

For nonlinear time history analysis by ELM, the "MATERIAL.PROP." block contains five data lines of the format

$$\gamma_i \quad g_i \quad gp_i \tag{83}$$

where i=1-5. The data lines in Eq.(83) describes the variations of G and G′ with $|\gamma|$ shown in Fig.1, and, in view of this figure,

$\gamma_1 := 0$
$\gamma_2 := \bar{\gamma}$
$\gamma_3 := \gamma_c$
$\gamma_4 := 2\gamma_c$
γ_5: a large $|\gamma|$ value greater than $2\gamma_c$
g_i, gp_i: the values of G and G′ at γ_i

It may be noted that g_5 and gp_5 have respectively the values zero and $\overset{*}{G}'$ (see Fig.1).

"SPECTRUM" block:

This block exists only for earthquake spectrum analysis and gives the spectrum values in tabular form by the data lines of the format

alpha
n_s (84)
t s_{au} $[s_{av}]$

where

alpha : angle (in degrees) defining the propagation direction of earthquake excitation (it is "α" in Fig.3)

n_s : number of periods for which spectrum values are given

t : period

s_{au}, s_{av}: acceleration spectrum values in U and V directions (see Fig.3)

It may be noted that the first two lines in Eqs.(84) are single data lines whereas the third line describes n_s data lines giving the spectrum values in tabular form. Thus, the total number of data lines in Eqs.(84) is n_s+2. In the program it is assumed that the default value of s_{av} is zero. MAS1 uses interpolation for the computation of the spectrum value at an intermediate period value of the spectrum table.

"TIME HISTORY" block:

This block exists for time history analysis (linear or nonlinear (ELM)). It is composed of data lines of the format

(1) (one data line) ... **alpha**
(2) (one data line) ... **nd**
(3) (nd data lines) ... **nda ndf**
(4) (one data line) ... **nf**
(5) (nf data lines) ... **nfa nfs** (85)
(6) (one data line) ... **na**
(7) (na data lines) ... **naf**
(8) (one data line) ... **ts tf dtp**
(9) (one data line) ... **dt nar nr sc**
(10) (one data line) ... **file**

where

alpha : angle (in degrees) of earthquake propagation direction which is already defined in the "SPECTRUM" block

nd : number of displacements whose time histories to be printed (if no prints are desired enter "0" for nd)

nda, ndf: the assembly and floor numbers for nd displacements (the data part (3) in which these numbers are given has nd data lines; skip this part if nd=0)

nf : number of forces whose time histories to be printed (if no prints are desired enter "0" for nf)

nfa,nfs : the assembly and story numbers for nf forces (the data part (5) in which these numbers are given has nf data lines; skip this part if nf=0)

na : number of MP accelerations whose time histories to be printed (if no prints are desired enter "0" for na)

naf : the floor numbers for na accelerations the data part (7) in which these numbers are given has na data lines; skip this part if na=0)

ts, tf : lower and upper bounds of the time interval in which the time histories are to be printed

dtp : the time increment used in printing the time histories

dt : time increment of the ground acceleration record (the same time increment is also used in computations)

nar : length of the ground acceleration record (the number of time points in the record)

nr : an integer which takes either the value 1 or 2 and defines the number of ground acceleration components to which the structure is subjected (if nr=1, the ground acceleration will be in U direction; on the other hand, if nr=2, the

ground acceleration will have both U and V components (see Fig.3))

sc : scale factor

file : name of the file from which the ground acceleration record will be read

If nd=nf=na=0, the data part (8) must be skipped. The time increment dtp used for printing should be an integer multiple of the time increment dt which is employed in computations.

When nr=2 in (9), the acceleration records in U and V directions should be given successively in the data part (10). The displacements and forces whose time histories are printed describe respectively the inplane displacements and shear forces (in u direction (see Fig.3)) of the wall assemblies. The positive sign of the shear force in the time history print corresponds to the positive direction of the shear force at the lower end of the story.

Let us explain the preparation of this data block by an example. Suppose that we wish to perform the nonlinear time history analysis (by ELM) of a masonry building having 3 stories and 26 assemblies. Further suppose that we wish to print the time histories of

- the inplane displacement of the second assembly at the third floor
- the inplane shear force of the fifth assembly in the second story
- the MP accelerations of the third floor

Assume that the ground acceleration record is in file "ACC" and has the time increment 0.02s. The length of the record (i.e., the number of time points in the record) is 1000. The angle α describing the propagation direction of earthquake is 90^{o}. Suppose that we apply this ground acceleration to the building in the U direction only by magnifying the record values by the factor 2.5. In order to obtain the aforementioned time history prints in the time interval $2 \leq t \leq 5$ with the printing time increment 0.1s, the "TIME HISTORY" block should be prepared as follows.

```
TIME HISTORY
90.
1
2   3
1
5   2
1
3
2.0   5.0   0.1
0.02   1000   1   2.5
ACC
```

5.1.2 Description of Output Files

MAS1 writes the results into some output files with a common root name, which is the same as that of the input file, but having different extensions for various types of results. These output files are listed below:

NAME.FRE : contains the results of free vibration analysis

NAME.ELA : contains the results for the change of frequencies and damping ratios during the iterations of ELA

NAME.ELF : contains the element forces for static case, and absolute maximum values of element forces for earthquake spectrum and time history (linear or nonlinear) analyses; for nonlinear case, this file also contains the damage ratios and effective shear strains for wall elements which are computed using Eqs.(2) and (41)

NAME.MDA : contains MP displacements for static case, absolute maximum MP displacements for earthquake spectrum analysis, and absolute maximum MP displacements and accelerations for time history analysis

NAME.TDS : contains time histories of the desired assembly displacements (in linear or nonlinear case)

NAME.TFR : contains time histories of the desired inplane shear forces (in linear or nonlinear case)

NAME.TAC : contains time histories of the desired MP accelerations (in linear or nonlinear case)

NAME.COE : contains the results for the change of the values of T and T' (in Eq.(42)) during the iterations of ELA

where NAME stands for the name used for the input file.

The results of the static and time history analyses for the element forces are printed according to the sign convention shown in Fig.9.

The assembly displacements in NAME.TDS describe the relative displacements of the assembly at floor levels and in the direction of the local u axis (see Fig.3).

The MP displacements in NAME.MDA represent the relative displacements of MP's in x and y directions and the rotation about z axis.

The MP accelerations in NAME.MDA and NAME.TAC describe the total accelerations of MP's in U and V directions and angular acceleration about z axis.

The damping ratios printed in NAME.ELA, representing the change of these ratios during the iterations of ELA, are computed by employing Eq.(56). Since the proportionality of the damping matrix to $\underset{\sim}{K}$ does no longer hold in the iterations of ELA, the damping ratio values in NAME.ELA, except those in the first iteration (in which the system is linear), are approximate.

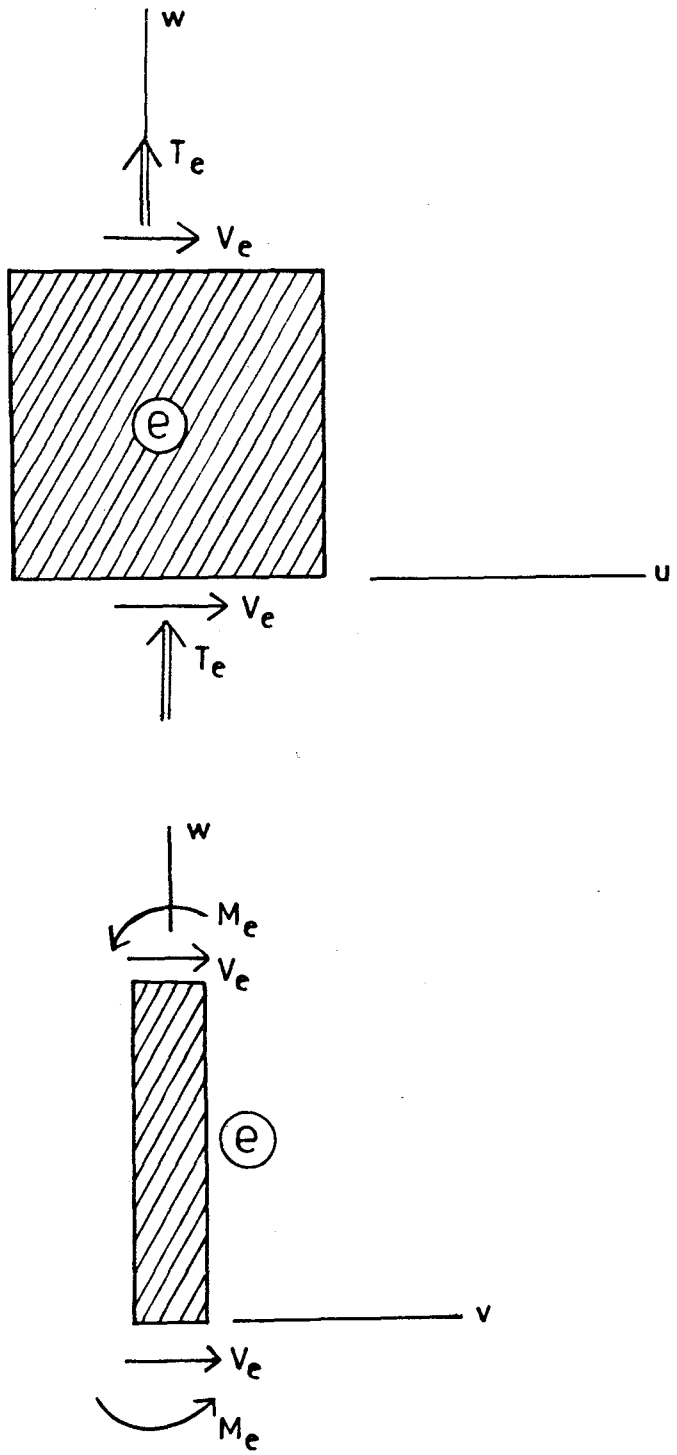

Figure 9 Sign convention for element forces

5.2 Computer Program for Actual Nonlinear Analysis (MAS2)

MAS2 performs the nonlinear analysis by solving the equations of the actual nonlinear model (ANM), presented in Chapter 3, with the aid of a step-by-step procedure, based on RK4, whose algorithm is given in Chapter 4 (Section.4.2).

Flow chart of MAS2 is given in Fig.10. The program calls the subroutines shown in Fig.11, having the functions listed below.

FILE : reads the name of input data file and generates the names of output and intermediate files

NG : computes the number of entries in an input line, which is needed for data generations

INFORM : writes the input values on the screen

ZERO : initializes a square matrix

ASTFDMP : forms the stiffness and damping matrices ($\underset{\sim}{k}$, $\underset{\sim}{c}$) for each assembly of the masonry building

KU : forms $\underset{\sim}{k}_u$ and $\underset{\sim}{k}_\theta$ matrices for each assembly

KV : forms $\underset{\sim}{k}_v$ matrix, for each assembly, for reinforced case

EL : forms $\underset{\sim}{k}_e$ matrix for each wall element for reinforced case

TRANS : computes transformation matrix $\underset{\sim}{B}$ for each assembly

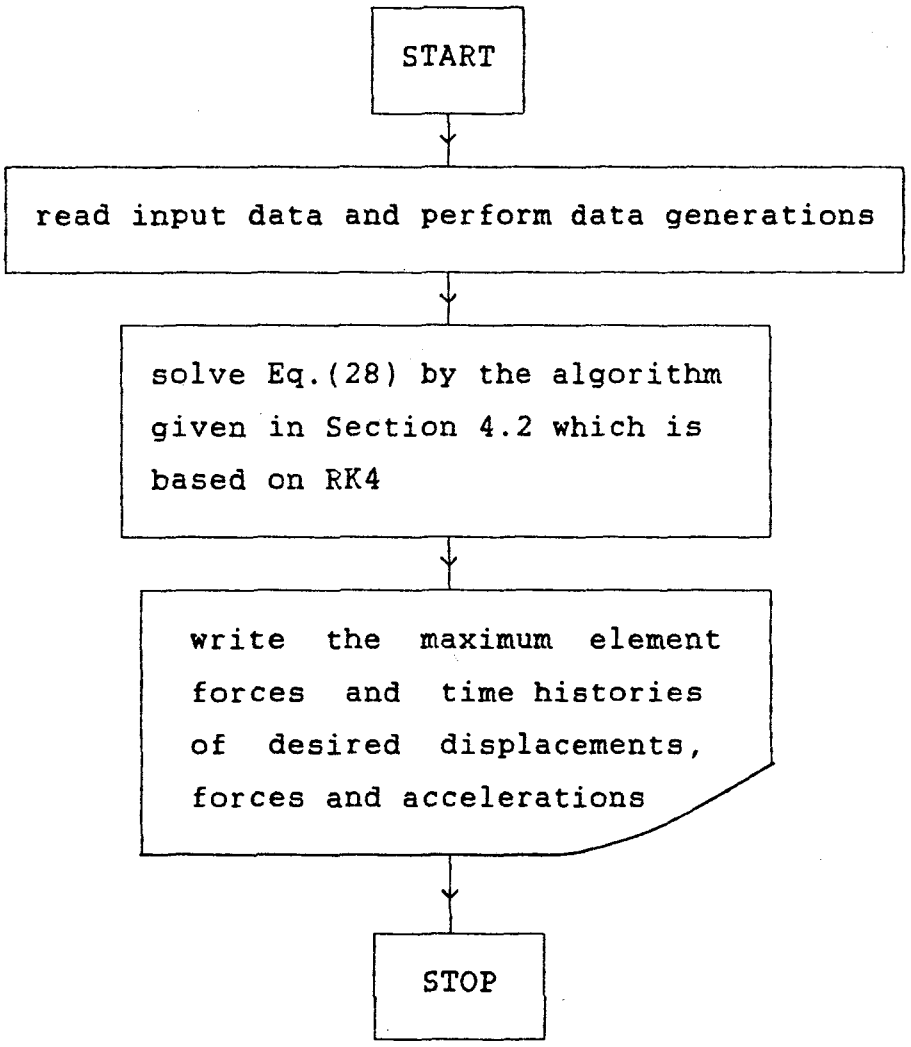

Figure 10 Flow chart of MAS2

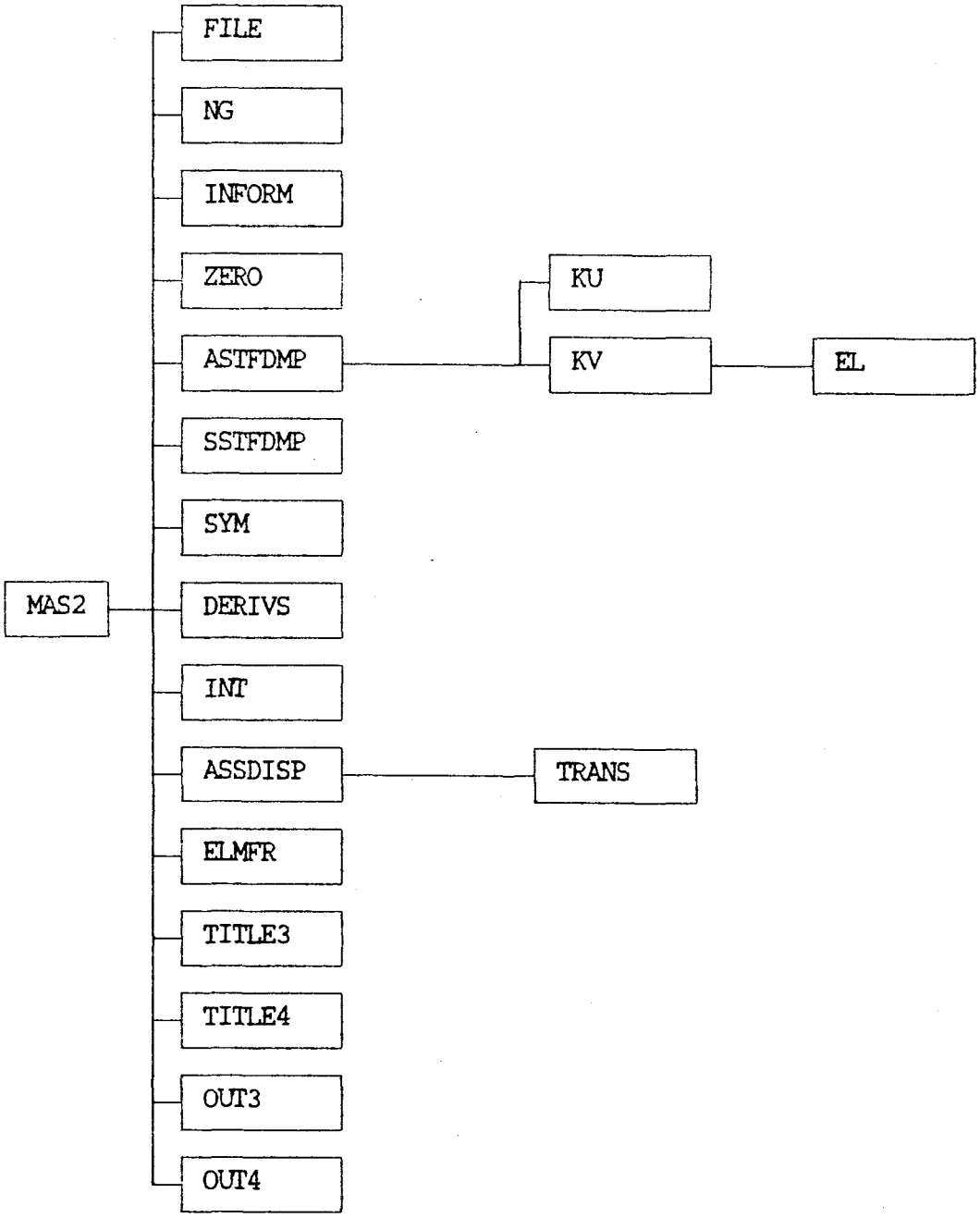

Figure 11 The subroutines used in the computer program MAS2

SSTFDMP : forms the system stiffness and damping matrices ($\underset{\sim}{K}$, $\underset{\sim}{C}$) using Eqs.(26)

SYM : forms a symmetric matrix completely by using its upper triangular part

DERIVS : in each step of RK4, computes f_{Vi}'s in Eqs.(61)

INT : computes, for each wall element, G^k and G'^k values in each step of RK4 by using loading and unloading properties of G and G'

ASSDISP : computes assembly displacements employing Eq.(13)

ELMFR : evaluates element forces for unreinforced and reinforced cases

TITLE3-4: write the titles for outputs in a suitable format

OUT3-4 : write the outputs in a suitable format

MS-DOS version of MAS2 is given in the attached floppy disk. The program MAS2 can be run either by executing the execution files separately in the order

MAS2A.EXE

MAS2B.EXE

MAS2C.EXE

or using the batch file

MAS2.BAT .

Listing of the program can be found in the files

MAS2A.FOR

MAS2B.FOR

MAS2C.FOR .

5.2.1 Manual for Input Data

The input data is to be read from a file whose name is specified interactively when MAS2A is run. The name of the input file should have no extension.

The structure of input data is shown in Table 2. Each line in Table 2 is the name of a data block. These names should be included in the input data file. The data blocks should be entered in the same order as that shown in Table 2.

Table 2 The structure of input data for the program MAS2

GENERAL INFORMATION
STORY HEIGHTS
COORDINATES
PROP.OF ASSEMBLIES
MASSES
COORD.OF MP
MATERIAL PROP.
TIME HISTORY

The data in each block should be entered below the block name and should be prepared according to the information given below.

"GENERAL INFORMATION" block:

This block contains a single data line in the format

nru ns nass (86)

where

nru : an integer indicating whether the masonry structure is reinforced or unreinforced (nru=0 for unreinforced and nru=1 for reinforced case)

ns : number of stories

nass : number of assemblies

"STORY HEIGHTS", "COORDINATES", "PROP. OF ASSEMBLIES", "MASSES", "COORD. OF MP" blocks:

They are the same as those of MAS1.

"MATERIAL PROP." block:

This data block contains five data lines of the format

$$\gamma_i \quad g_i \quad gp_i \tag{87}$$

where i=1-5. The data lines in Eq.(87) describe the variations of G and G' with $|\gamma|$ shown in Fig.1. The

definitions of the variables appearing in Eq.(87) are given as, in view of Fig.1,

$\gamma_1, \gamma_2, \gamma_3, \gamma_4 := 0, \bar{\gamma}, \gamma_c, 2\gamma_c$

γ_5: a large $|\gamma|$ value greater than $2\gamma_c$

g_i, gp_i: the values of G and G' at γ_i

It may be noted that g_5 and gp_5 have respectively the values zero and $\overset{*}{G}'$.

"TIME HISTORY" block:

It is the same as that of MAS1.

5.2.2 Description of Output Files

MAS2 writes the results into some output files with a common root name, which is the same as that of the input file, but having different extensions for various types of results. These output files are listed below:

NAME.ELF : contains absolute maximum values of element forces, shear strains and the damage ratios for wall elements, where the latter two are computed by Eqs.(30) and (2)

NAME.MDA : contains absolute maximum displacements and accelerations of MP's

NAME.TDS : contains time histories of the desired assembly displacements

NAME.TFR : contains time histories of the inplane shear forces and shear strains of the desired wall elements

NAME.TAC : contains time histories of the desired MP accelerations

where NAME designates the name used for the input file.

The sign convention and other matters regarding the output files listed above are the same as those given for MAS1.

6. NUMERICAL EXAMPLES AND DISCUSSIONS

Here, we present some examples involving two different masonry structures. These two structures will be named as Structure 1 and Structure 2 in this study. In what follows we first present the geometric and physical properties of these structures and describe the types of earthquake inputs to which the structures are subjected in the examples.

Description of Structure 1

It is a single story adobe house which was investigated experimentally in [11] and has a plan shown in Fig.12. All of the dimensions in Fig.12 are given in cm. The circled numbers in the figure designate the wall assembly numbers used in the theoretical analysis. The roof mass of the adobe house is about 1 ton and its height is 2.40 mt. The mass density of its wall material is 1.80 t/mt^3 . Using this data and the xyz global coordinate system shown in Fig.12, the location of the mass center, the mass and the mass inertia moment of the top floor can be computed as

$$x_m=1.625 \text{ mt} \ , \quad y_m=1.7328 \text{ mt}$$
$$M= 7.0912 \text{ tons} \tag{88}$$
$$I_m=23.1932 \text{ ton-mt}^2$$

In obtaining these results, half of the wall masses are lumped at the top floor.

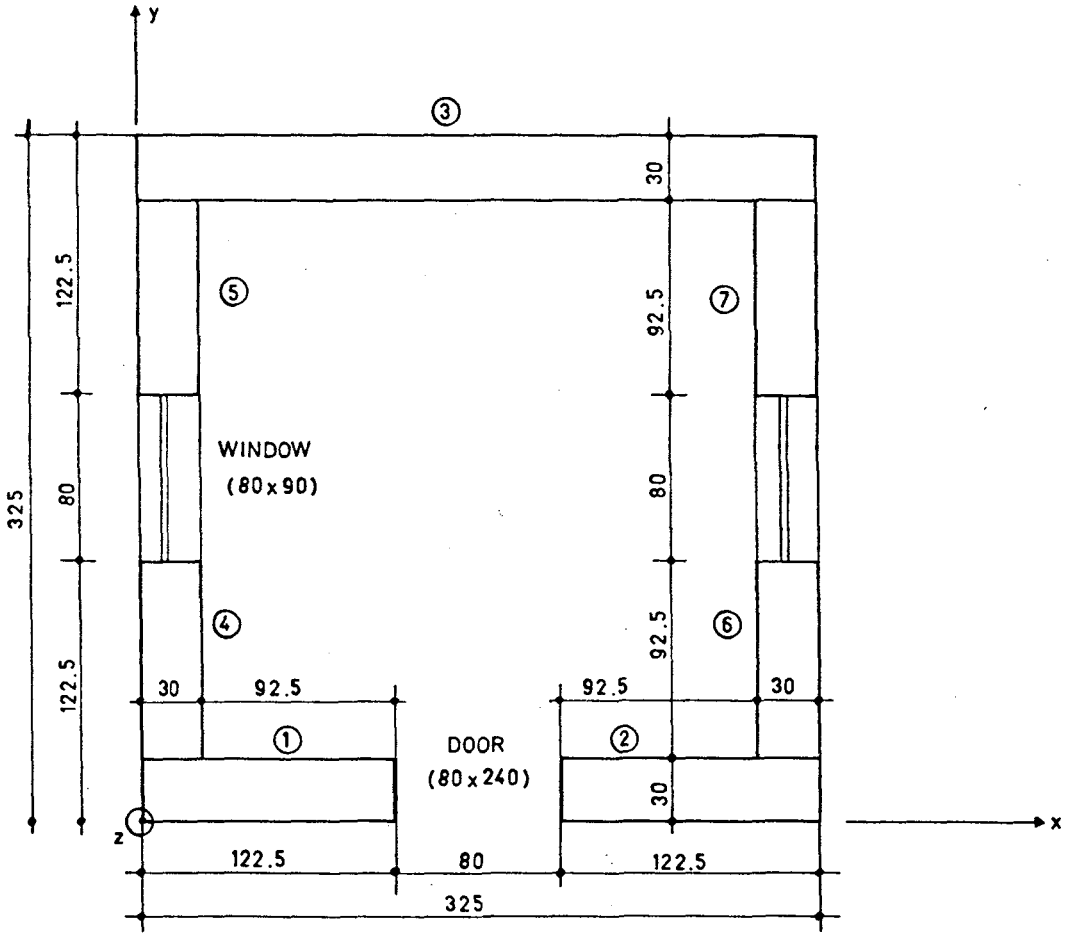

Figure 12 Plan view of the single story adobe house (Structure 1)

In [11], the linear value of the shear modulus G for the adobe material (used in constructing the houses) was determined from some static tests. It is

$$\bar{G} = 95000 \text{ kN/mt}^2 \ . \tag{89}$$

Description of Structure 2

The Structure 2 is a 3-story brick masonry building having the plan shown in Fig.13. The dimensions in the figure are given in mt. The circled numbers designate the wall assembly numbers. Story height is taken to be 3 mt for all of the three stories. The mass density of the wall material is assumed to be 1.75 ton/mt^3. The mass per unit area of the floors is 0.59 ton/mt^2. The building is referred to the xyz coordinate system shown in Fig.13. The locations of the mass centers, the masses and the mass inertia moments of the floors are computed by lumping the wall masses at floor levels (using lump mass assumption). They are

for the first and second floors:

$$\begin{aligned} x_m &= 5.09 \text{ mt} \ , \ y_m = 4.80 \text{ mt} \\ M &= 114.04 \text{ tons} \\ I_m &= 2191.34 \text{ ton-mt}^2 \end{aligned} \tag{90}$$

for the third floor:

$$\begin{aligned} x_m &= 5.14 \text{ mt} \ , \ y_m = 4.70 \text{ mt} \\ M &= 84.80 \text{ tons} \\ I_m &= 1539.34 \text{ ton-mt}^2 \end{aligned}$$

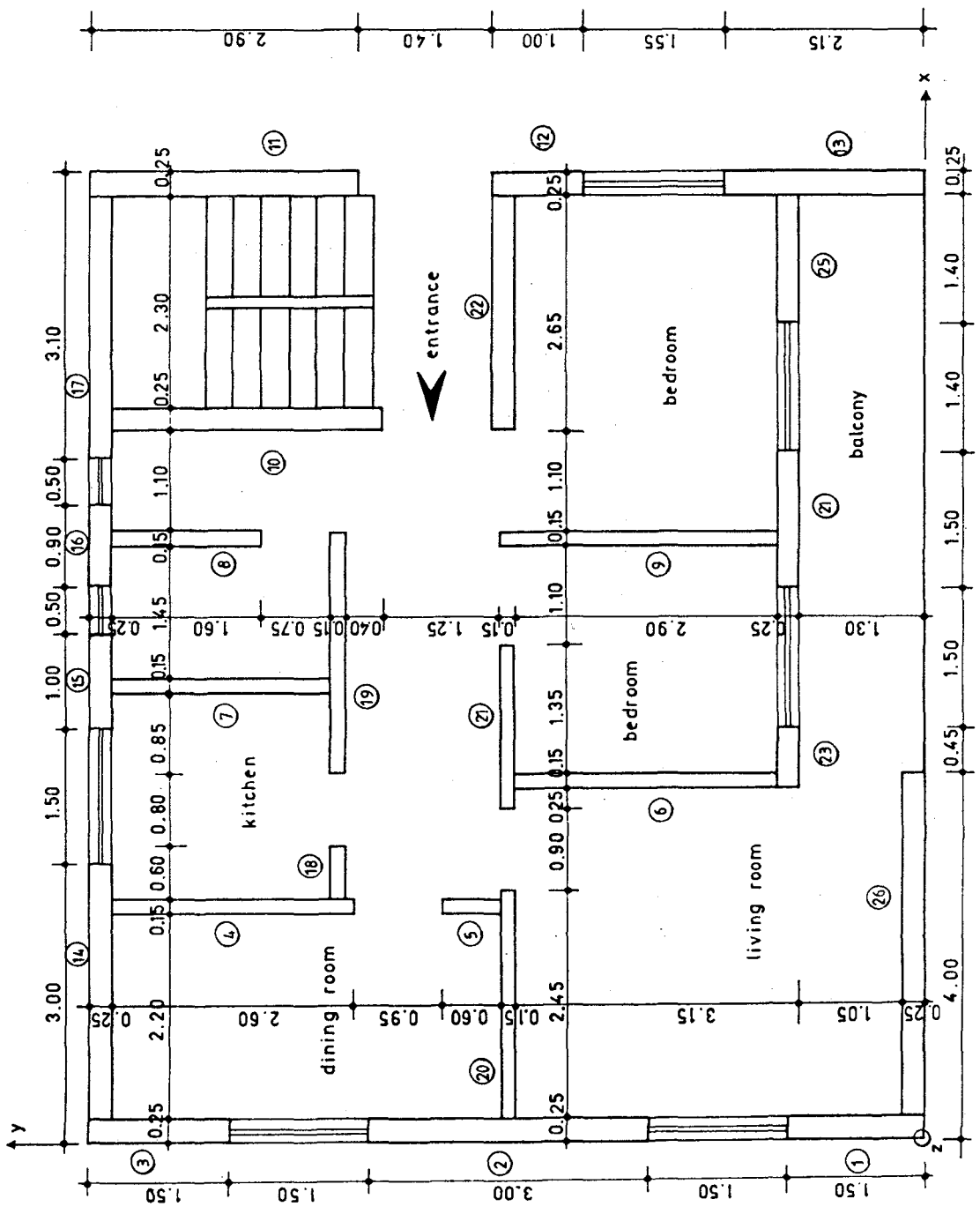

Figure 13 Plan view of the 3-story brick masonry building (Structure 2)

It will be assumed that the wall material properties of the building are described by G and G' curves in Fig.1 having the parameter values defined in Eqs.(1). These values represent the dynamic values for fired clay brick masonry walls obtained in [4] using shaking table experiments.

Earthquake inputs used in the analyses

Structure 1 is not subjected to any earthquake input. Only free vibration analysis is performed for this structure with the object of assessing the linear dynamic model experimentally.

Structure 2, on the other hand, is subjected to an earthquake input whose propagation direction is in y direction (see Fig.13 for the definition of y axis). The earthquake input has only one ground acceleration component which is in y direction. The time variation of the single earthquake acceleration component is chosen to be described by the S16E component of Pacoima earthquake record which is modified in the analysis so that its peak acceleration value is 1.07 mt/s^2. The variation of this record is shown in Fig.14, and its absolute Fourier spectrum, in Fig.15. The Fourier spectrum is obtained by using the FFT algorithm [12,13]. Fig.15 shows that the major portion of the excitation frequencies "f" lies in the interval $0 \leq f \leq 5$ Hz. The earthquake input described above is used in the examples by multiplying it by various scale factors.

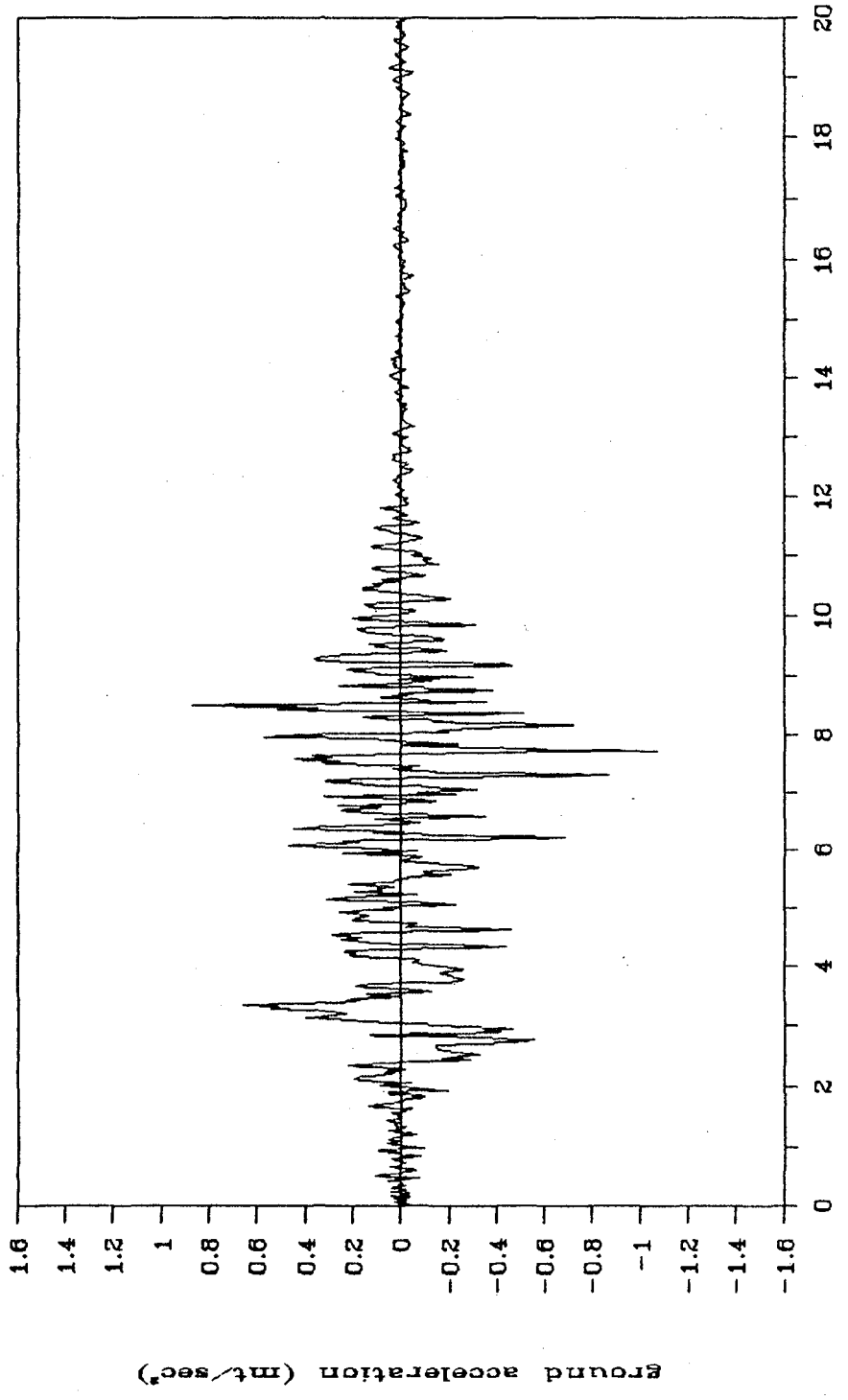

Figure 14 Time history of the S16E component of Pacoima earthquake record

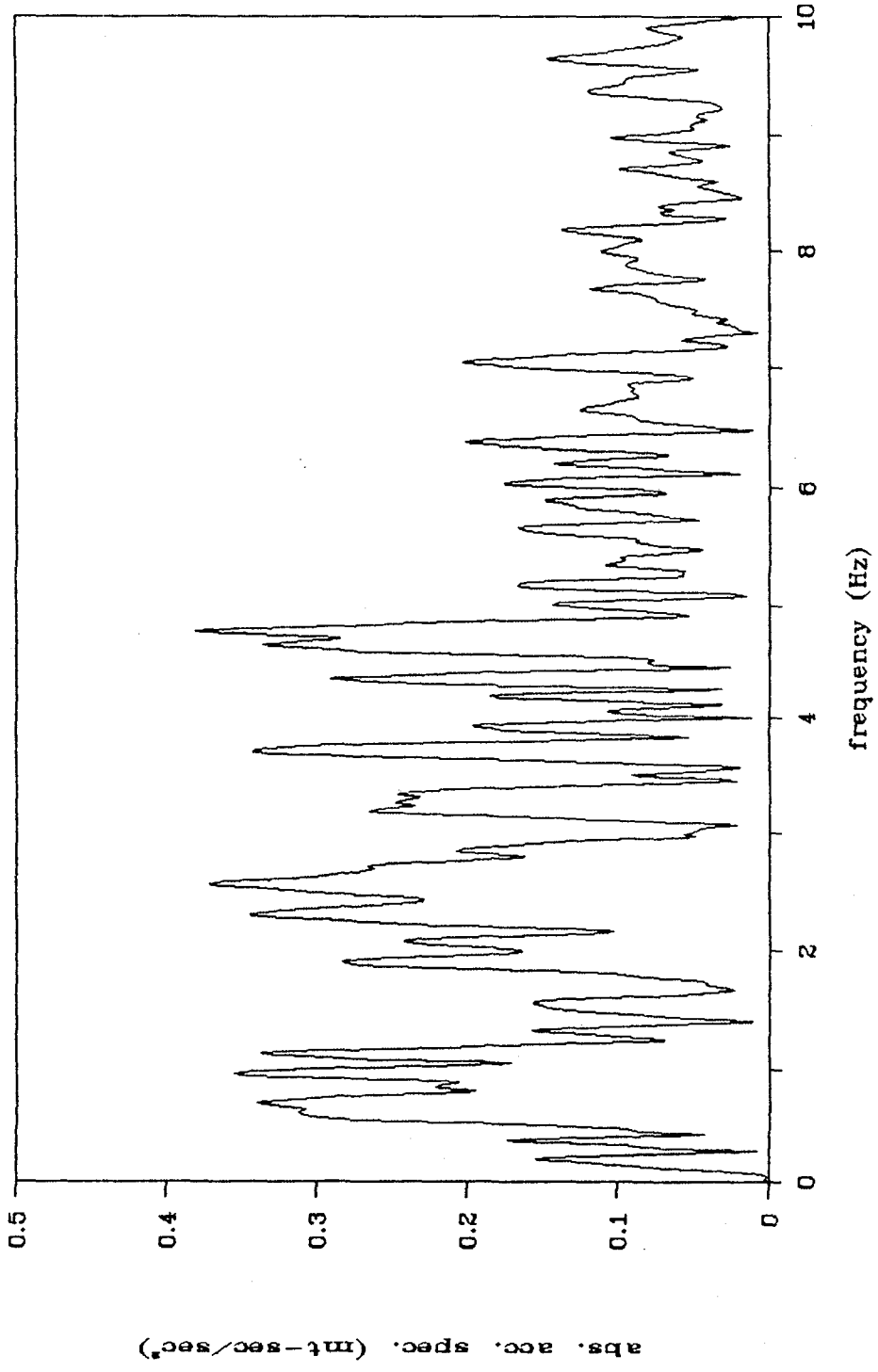

Figure 15 Absolute Fourier spectrum of the S16E component of Pacoima earthquake record

We now start discussing some examples involving Structure 1 and 2 defined above.

Example 1

Here, we perform free vibration analysis of Structure 1 by using the computer program MAS1. We do this with the object of comparing the prediction of the linear dynamic model for the free vibration frequency of the Structure 1 in y direction (see Fig.12) with that obtained experimentally in [11], which is about 11.50 Hz. The input file of this example is given in Fig.16 and also in the file EXMPL1 of the attached floppy disk. The results of the analysis taken from the output file EXMPL1.FRE are listed in Table 3. The mode shape (eigenvector) values in the table correspond to the displacements (DX, DY) and the rotation RZ of the master point. The table shows that the first (lowest) frequency involves the motion only in the y direction while the other two frequencies are coupled with each other, and involve both the translation in x direction and the rotation about z axis. From the results we see that the theoretical value of the frequency associated with the vibrations in the y direction is 12.52 Hz., which agrees quite well with the experimental value, 11.50 Hz.

Example 2

In this example, the free vibration analysis for Structure 2 (3-story masonry building) is performed by employing MAS1. The input data can be found, in the

```
VIBRATION
GENERAL INFORMATION
0     1      7      3
STORY HEIGHTS
1      2.40
COORDINATES
1    0.6125    0.15
2    2.6375    0.15
3    1.625     3.10
4    0.15      0.7625
5    0.15      2.4875
6    3.10      0.7625
7    3.10      2.4875
PROP.OF ASSEMBLIES
1       0
1    1.225     0.30    1.0
2       0
1    1.225     0.30    1.0
3       0
1    3.250     0.30    1.0
4      90
1    0.925     0.30    1.0
5      90
1    0.925     0.30    1.0
6      90
1    0.925     0.30    1.0
7      90
1    0.925     0.30    1.0
MASSES
1    7.0912    7.0912    23.1932
COORD.OF MP
1    1.625     1.7328
MATERIAL PROP
95000.0
```

Figure 16 Input data for Example 1

Table 3 Theoretical results for the free vibration frequencies and mode shapes of the adobe house (Structure 1)

FREQUENCY (# 1)= 12.52 (HZ)
PERIOD (# 1)= .08 (SEC)

MODE SHAPE (# 1) (MASTER POINT)

FLOOR	DX	DY	RZ
1	.4514E-03	.3755E+00	.4171E-04

FREQUENCY (# 2)= 15.35 (HZ)
PERIOD (# 2)= .07 (SEC)

MODE SHAPE (# 2) (MASTER POINT)

FLOOR	DX	DY	RZ
1	.3435E+00	-.4435E-03	.8394E-01

FREQUENCY (# 3)= 16.48 (HZ)
PERIOD (# 3)= .06 (SEC)

MODE SHAPE (# 3) (MASTER POINT)

FLOOR	DX	DY	RZ
1	.1518E+00	-.1135E-03	-.1899E+00

attached floppy disk, in the file EXMPL2U for unreinforced case and EXMPL2R for reinforced case. The results for the first three modes extracted from the output files (of the extension FRE) are shown in Tables 4 and 5 for unreinforced and reinforced cases respectively. As the higher modes are of minor importance in the time history analyses presented in subsequent examples, they are not given in the tables. This is because these higher modes have frequencies larger than 10 Hz, which are out of the excitation interval of the Pacoima earthquake (see Fig.15) used in time history analyses.

From the results in the tables we see that the frequencies of the first three modes are closely spaced and lie in the interval $3.9 \leq f \leq 5.1$ Hz, which indicate that these three modes can all contribute to the response greatly when they are excited by an earthquake input. The frequencies for reinforced case are slightly higher than those for unreinforced case. Tables contain also a damping ratio value for each mode which is computed by MAS1 using Eq.(58). Examination of these values shows that the damping ratios are close to each other for the first three modes and have an avarage value of about 7% for unreinforced case and of about 7.5% for reinforced case.

Example 3

This example concerns with the earthquake spectrum analysis of unreinforced Structure 2. The earthquake

Table 4 Free vibration characteristics and damping ratios of 3-story masonry building (Structure 2) for unreinforced case

FREQUENCY (# 1)= 3.93 (HZ)
PERIOD (# 1)= .25 (SEC)
DAMPING RATIO (# 1)= 6.59 (PERCENT)

MODE SHAPE (# 1) (MASTER POINT)

FLOOR	DX	DY	RZ
1	.3373E-01	-.3783E-02	.7446E-03
2	.5973E-01	-.6698E-02	.1326E-02
3	.7220E-01	-.7993E-02	.1619E-02

FREQUENCY (# 2)= 4.01 (HZ)
PERIOD (# 2)= .25 (SEC)
DAMPING RATIO (# 2)= 6.74 (PERCENT)

MODE SHAPE (# 2) (MASTER POINT)

FLOOR	DX	DY	RZ
1	.4244E-02	.3360E-01	-.1076E-02
2	.7504E-02	.5948E-01	-.1893E-02
3	.8800E-02	.7158E-01	-.2255E-02

FREQUENCY (# 3)= 4.84 (HZ)
PERIOD (# 3)= .21 (SEC)
DAMPING RATIO (# 3)= 8.13 (PERCENT)

MODE SHAPE (# 3) (MASTER POINT)

FLOOR	DX	DY	RZ
1	.3167E-02	-.4704E-02	-.7822E-02
2	.5479E-02	-.8412E-02	-.1380E-01
3	.4667E-02	-.1115E-01	-.1654E-01

Table 5 Free vibration characteristics and damping ratios of Structure 2 for reinforced case

FREQUENCY (# 1)= 4.19 (HZ)
PERIOD (# 1)= .24 (SEC)
DAMPING RATIO (# 1)= 7.03 (PERCENT)

MODE SHAPE (# 1) (MASTER POINT)

FLOOR	DX	DY	RZ
1	.3364E-01	-.5243E-02	.1025E-02
2	.5976E-01	-.9308E-02	.1824E-02
3	.7067E-01	-.1086E-01	.2200E-02

FREQUENCY (# 2)= 4.29 (HZ)
PERIOD (# 2)= .23 (SEC)
DAMPING RATIO (# 2)= 7.19 (PERCENT)

MODE SHAPE (# 2) (MASTER POINT)

FLOOR	DX	DY	RZ
1	.5958E-02	.3352E-01	-.1232E-02
2	.1057E-01	.5952E-01	-.2171E-02
3	.1215E-01	.6995E-01	-.2545E-02

FREQUENCY (# 3)= 5.06 (HZ)
PERIOD (# 3)= .20 (SEC)
DAMPING RATIO (# 3)= 8.49 (PERCENT)

MODE SHAPE (# 3) (MASTER POINT)

FLOOR	DX	DY	RZ
1	.4065E-02	-.5707E-02	-.7808E-02
2	.7083E-02	-.1023E-01	-.1380E-01
3	.6294E-02	-.1299E-01	-.1628E-01

acceleration spectrum (EAS) values used in the example are derived from Pacoima earthquake record (with the scale factor sc=1.0) by taking the damping ratio as 7% (this value corresponds to the avarage damping ratio for the first three modes of unreinforced Structure 2). The variation of this EAS with the period T is shown, in smoothed form, in Fig.17. It may be noted that earthquake spectrum analysis assumes that the structure behaves linearly during earthquake excitation. This assumption is justified in this example in view of the fact that the nonlinear time history analyses performed in subsequent examples indicated that the behavior of Structure 2 remains in linear range when it is subjected to Pacoima earthquake with sc=1.0.

The input data to MAS1 for the analysis under consideration is given in Fig.18 and also in the file EXMPL3 of the attached floppy disk. EAS values appearing in the data block "SPECTRUM" in Fig.18 are taken from Fig.17. The results for maximum element forces extracted from the file EXMPL3.ELF are given in Table 6 for the assemblies 2, 4 and 26 (see Fig.13). With the object of comparison , the time history analysis of the same problem is also performed by using the linear dynamic model together with Pacoima earthquake input with sc=1.0. The results of this latter analysis are shown in parantheses in Table 6. Examination of Table 6 shows that the results obtained from earthquake spectrum and time history analyses are fairly close and the difference between them is at most 17% (with respect to the values from earthquake spectrum analysis).

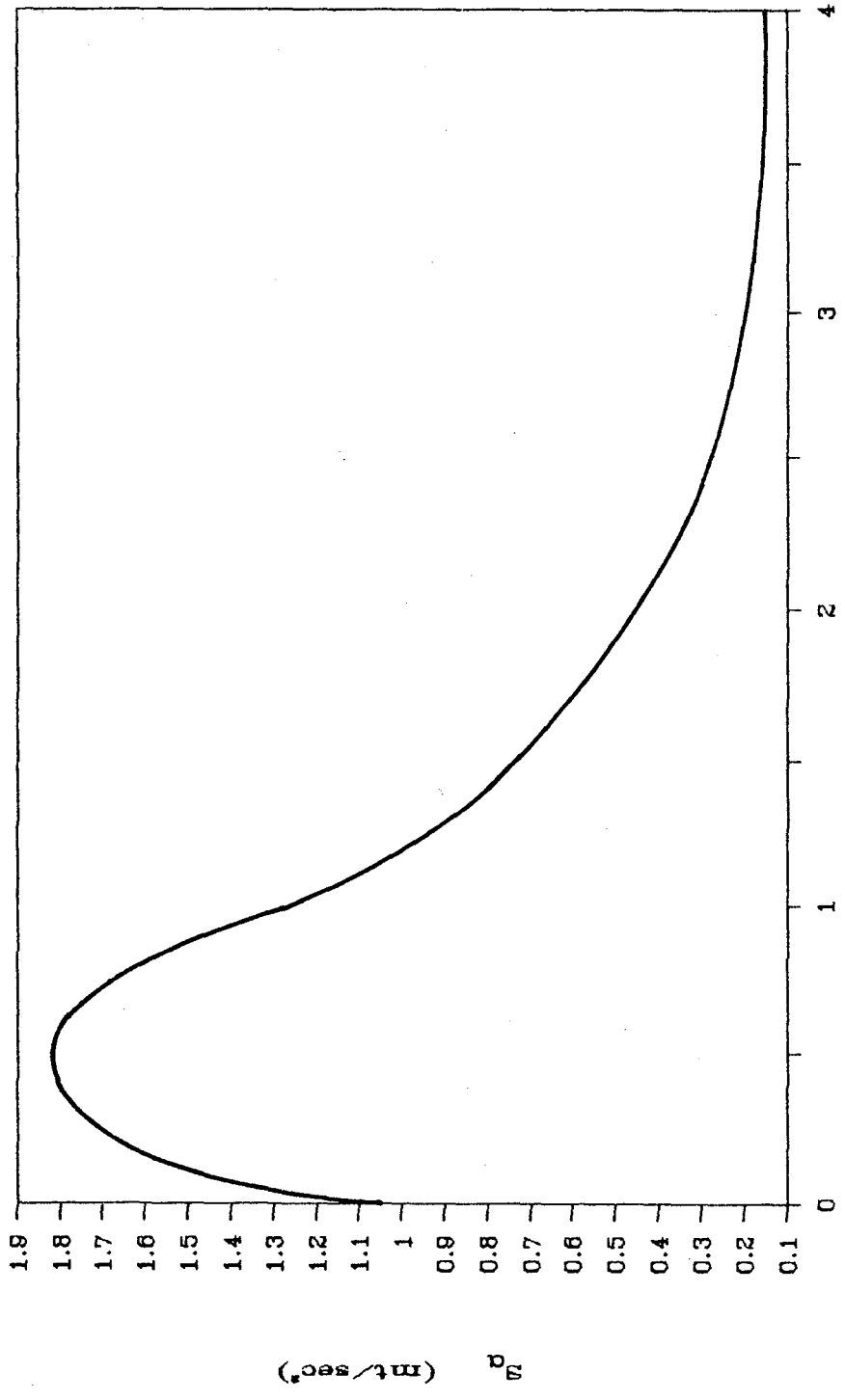

Figure 17 The earthquake acceleration spectrum used in Example 3

```
SPECTRUM
GENERAL INFORMATION
0   3   26   9
STORY HEIGHTS
1,3    3.0
COORDINATES
1     0.125     0.750
2     0.125     4.500
3     0.125     8.250
4     2.525     7.450
5     2.525     4.900
6     3.925     3.000
7     4.925     7.525
8     6.525     7.950
9     6.525     3.075
10    7.825     7.300
11   10.375     7.550
12   10.375     4.200
13   10.375     1.075
14    1.625     8.875
15    5.000     8.875
16    6.450     8.875
17    8.825     8.875
18    2.900     6.325
19    5.300     6.325
20    1.475     4.525
21    4.475     4.525
22    8.975     4.575
23    4.150     1.425
24    6.700     1.425
25    9.550     1.425
26    2.125     0.125
PROP.OF ASSEMBLIES
1     90
1,3    1.50    0.25    1.0
2     90
1,3    3.00    0.25    1.0
3     90
1,3    1.50    0.25    1.0
4     90
1,3    2.60    0.15    1.0
5     90
1,3    0.60    0.15    1.0
6     90
1,3    2.90    0.15    1.0
7     90
1,3    2.35    0.15    1.0
8     90
1,3    1.60    0.15    1.0
9    90
1,3    3.05    0.15    1.0
10    90
1,3    2.90    0.25    1.0
11    90
1,3    2.90    0.25    1.0
12    90
1,3    1.00    0.25    1.0
13    90
1,3    2.15    0.25    1.0
14     0
1,3    2.75    0.25    1.0
15     0
1,3    1.00    0.25    1.0
16     0
1,3    0.90    0.25    1.0
17     0
1,3    2.85    0.25    1.0
18     0
1,3    0.60    0.15    1.0
19     0
1,3    2.60    0.15    1.0
20     0
1,3    2.45    0.15    1.0
21     0
1,3    1.75    0.15    1.0
22     0
1,3    2.55    0.25    1.0
23     0
1,3    0.60    0.25    1.0
24     0
1,3    1.50    0.25    1.0
25     0
1,3    1.40    0.25    1.0
26     0
1,3    3.75    0.25    1.0
MASSES
1,2   114.04   114.04   2191.34
3      84.80    84.80   1539.34
COORD. OF MP
1,2      5.09    4.80
3        5.14    4.70
MATERIAL PROP.
168000.00      896.9
SPECTRUM
90.
10
0.000          1.07
0.250          1.75
0.500          1.85
0.750          1.71
1.000          1.30
1.500          0.77
2.000          0.46
2.500          0.27
3.000          0.21
4.000          0.12
```

Figure 18 Input data for Example 3

Table 6 The maximum values of element forces for the assemblies 2, 4 and 26 of Structure 2 as obtained from earthquake spectrum and linear time history analyses

(the values in parantheses correspond to time history analysis; forces are given in kN and torques in kN-mt; sc=1.0)

MEMBER FORCES FOR WALL ASSEMBLY # 2

STORY	U-Z PLANE SHEAR	TORQUE
1	74.93 (68.94)	.04 (.04)
2	57.51 (52.84)	.03 (.03)
3	27.37 (24.94)	.02 (.01)

MEMBER FORCES FOR WALL ASSEMBLY # 4

STORY	U-Z PLANE SHEAR	TORQUE
1	36.67 (34.38)	.01 (.01)
2	28.16 (26.36)	.01 (.01)
3	13.44 (12.47)	.00 (.00)

MEMBER FORCES FOR WALL ASSEMBLY # 26

STORY	U-Z PLANE SHEAR	TORQUE
1	12.50 (10.59)	.06 (.05)
2	9.56 (8.05)	.04 (.03)
3	4.44 (3.67)	.02 (.02)

Example 4

Nonlinear time history analysis is carried out for Structure 2 by ELM and by using the scale factors sc=1.0, 1.5, 2.0, 2.5 in Pacoima earthquake input. The constant "c" in Eq.(41) is chosen to be c=1. The input data to MAS1 for reinforced Structure 2 and sc=2.5 is given in Fig.19, and is also given, in the attached floppy disk, in the file EXMPL4U for unreinforced case and in the file EXMPL4R for reinforced case.

The results of the analyses indicated that the building behaves linearly for the scale factor sc=1.0 and nonlinearly for the other scale factors sc=1.5, 2.0, 2.5. In what follows we first present some typical results of the analysis for the scale factor sc=2.5.

Tables 7 and 8 show, for unreinforced and reinforced cases respectively, the variations of the free vibration frequencies and the damping ratios of the first three modes during iterations of ELM. From the tables we see that (a) as expected, the converged values of free vibration frequencies for reinforced case are somewhat higher than those for unreinforced case while damping ratios for these two cases are considerably close (b) the converged values of free vibration frequencies decreased compared to their linear values shown in the first lines of Tables 7 and 8, which is due to the loss in the rigidity of the building caused by the damages occuring in the wall elements during earthquake excitation (c) the converged values of the

```
NONLINEAR
GENERAL INFORMATION
1   3   26   3   9   0.01   1.0
STORY HEIGHTS
1,3    3.0
COORDINATES
1     0.125     0.750
2     0.125     4.500
3     0.125     8.250
4     2.525     7.450
5     2.525     4.900
6     3.925     3.000
7     4.925     7.525
8     6.525     7.950
9     6.525     3.075
10    7.825     7.300
11   10.375     7.550
12   10.375     4.200
13   10.375     1.075
14    1.625     8.875
15    5.000     8.875
16    6.450     8.875
17    8.825     8.875
18    2.900     6.325
19    5.300     6.325
20    1.475     4.525
21    4.475     4.525
22    8.975     4.575
23    4.150     1.425
24    6.700     1.425
25    9.550     1.425
26    2.125     0.125
PROP.OF ASSEMBLIES
1     90
1,3    1.50    0.25    1.0
2     90
1,3    3.00    0.25    1.0
3     90
1,3    1.50    0.25    1.0
4     90
1,3    2.60    0.15    1.0
5     90
1,3    0.60    0.15    1.0
6     90
1,3    2.90    0.15    1.0
7     90
1,3    2.35    0.15    1.0
8     90
1,3    1.60    0.15    1.0
9    90
1,3    3.05    0.15    1.0
10    90
1,3    2.90    0.25    1.0
11    90
1,3    2.90    0.25    1.0
12    90
1,3    1.00    0.25    1.0
13    90
1,3    2.15    0.25    1.0
14     0
1,3    2.75    0.25    1.0
15     0
1,3    1.00    0.25    1.0
16     0
1,3    0.90    0.25    1.0
17     0
1,3    2.85    0.25    1.0
18     0
1,3    0.60    0.15    1.0
19     0
1,3    2.60    0.15    1.0
20     0
1,3    2.45    0.15    1.0
21     0
1,3    1.75    0.15    1.0
22     0
1,3    2.55    0.25    1.0
23     0
1,3    0.60    0.25    1.0
24     0
1,3    1.50    0.25    1.0
25     0
1,3    1.40    0.25    1.0
26     0
1,3    3.75    0.25    1.0
MASSES
1,2   114.04   114.04   2191.34
3      84.80    84.80   1539.34
COORD. OF MP
1,2    5.09    4.80
3      5.14    4.70
MATERIAL PROP.
0.0          168000.00     896.9
0.000513     168000.00     896.9
0.001580     100279.60    1855.8
0.003160          0.00    1855.8
0.010000          0.00    1855.8
TIME HISTORY
90.0
1
2   3
1
2   1
1
3
0.0    10.0    0.02
0.02   1000    1  2.5
PACOIMA
```

Figure 19 Input data for Example 4

(for reinforced case)

Table 7 The free vibration frequencies and damping ratios of unreinforced Structure 2 as predicted by ELM

iteration number	mode 1		mode 2		mode 3	
	freq.(Hz)	damping ratio(%)	freq.(Hz)	damping ratio(%)	freq.(Hz)	damping ratio(%)
1	3.929	6.59	4.015	6.74	4.843	8.13
2	3.530	12.52	3.927	6.66	4.533	11.60
3	3.469	13.52	3.927	6.68	4.502	12.02

Table 8 The free vibration frequencies and damping ratios of reinforced Structure 2 as predicted by ELM

iteration number	mode 1		mode 2		mode 3	
	freq.(Hz)	damping ratio(%)	freq.(Hz)	damping ratio(%)	freq.(Hz)	damping ratio(%)
1	4.192	7.03	4.288	7.19	5.061	8.49
2	3.841	12.39	4.191	7.14	4.786	11.52
3	3.829	12.69	4.191	7.14	4.782	11.61

damping ratios increased, in general, considerably compared to their linear values. From the tables it may be noted that the damping ratio for the first mode is about 13%, which appears to be a realistic value for masonry structures.

Maximum element forces, damages ratios and effective inplane shear strains are presented for the assemblies 2, 4 and 26 in Tables 9 and 10 for unreinforced and reinforced cases respectively. From these tables we observe that (a) the results obtained for unreinforced and reinforced cases do not differ appreciably (b) the assemblies 2 and 4, which are parallel to the earthquake excitation direction (see Fig.13), undergo considerable damages while the assembly 26, which is perpendicular to the earthquake direction, behaves linearly (c) the damage ratios for unreinforced case are slightly higher than those for reinforced case (which may be expected in view of physical considerations) (d) the amount of damage in wall elements decreases as the story number increases.

The time histories of the inplane relative displacement at the third floor of the assembly 2, of the inplane shear force in the first story of the assembly 2 and of the total acceleration (in y direction) at the master point of the third floor are shown respectively in Figs.20, 21 and 22 for unreinforced case, and they are compared with those for reinforced case in Figs. 23, 24 and 25. The figures indicate that the time history results for unreinforced and

Table 9 The maximum values of element forces predicted by ELM for the wall assemblies 2, 4 and 26 of Structure 2 for unreinforced case
(forces are in kN and torques in kN-mt; sc=2.5)

MEMBER FORCES FOR WALL ASSEMBLY # 2

STORY	U-Z PLANE SHEAR	TORQUE	SHEAR STRAIN	DAMAGE(%)
1	125.57	.08	.150E-02	37.45
2	97.45	.06	.917E-03	15.28
3	46.24	.02	.358E-03	.00

MEMBER FORCES FOR WALL ASSEMBLY # 4

STORY	U-Z PLANE SHEAR	TORQUE	SHEAR STRAIN	DAMAGE(%)
1	64.35	.02	.142E-02	34.17
2	49.54	.01	.865E-03	13.29
3	23.23	.00	.348E-03	.00

MEMBER FORCES FOR WALL ASSEMBLY # 26

STORY	U-Z PLANE SHEAR	TORQUE	SHEAR STRAIN	DAMAGE(%)
1	36.68	.15	.232E-03	.00
2	21.78	.09	.136E-03	.00
3	8.05	.03	.502E-04	.00

Table 10 The maximum values of element forces predicted by ELM for the wall assemblies 2, 4 and 26 of Structure 2 for reinforced case
(forces are in kN, torques and moments in kN-mt; sc=2.5)

MEMBER FORCES FOR WALL ASSEMBLY # 2

STORY	U-Z PLANE SHEAR	V-Z PLANE SHEAR	MOMENT	TORQUE	SH.STRAIN	DAMAGE(%)
1	126.76	4.57	6.85	.08	.146E-02	35.74
2	97.59	.04	.06	.06	.918E-03	15.29
3	38.46	.02	.02	.02	.302E-03	.00

MEMBER FORCES FOR WALL ASSEMBLY # 4

STORY	U-Z PLANE SHEAR	V-Z PLANE SHEAR	MOMENT	TORQUE	SH.STRAIN	DAMAGE(%)
1	64.66	.84	1.27	.02	.137E-02	32.44
2	49.35	.02	.03	.01	.864E-03	13.25
3	19.26	.01	.01	.00	.286E-03	.00

MEMBER FORCES FOR WALL ASSEMBLY # 26

STORY	U-Z PLANE SHEAR	V-Z PLANE SHEAR	MOMENT	TORQUE	SH.STRAIN	DAMAGE(%)
1	34.08	3.69	5.54	.14	.216E-03	.00
2	20.69	1.87	2.80	.09	.131E-03	.00
3	6.85	.64	.96	.03	.433E-04	.00

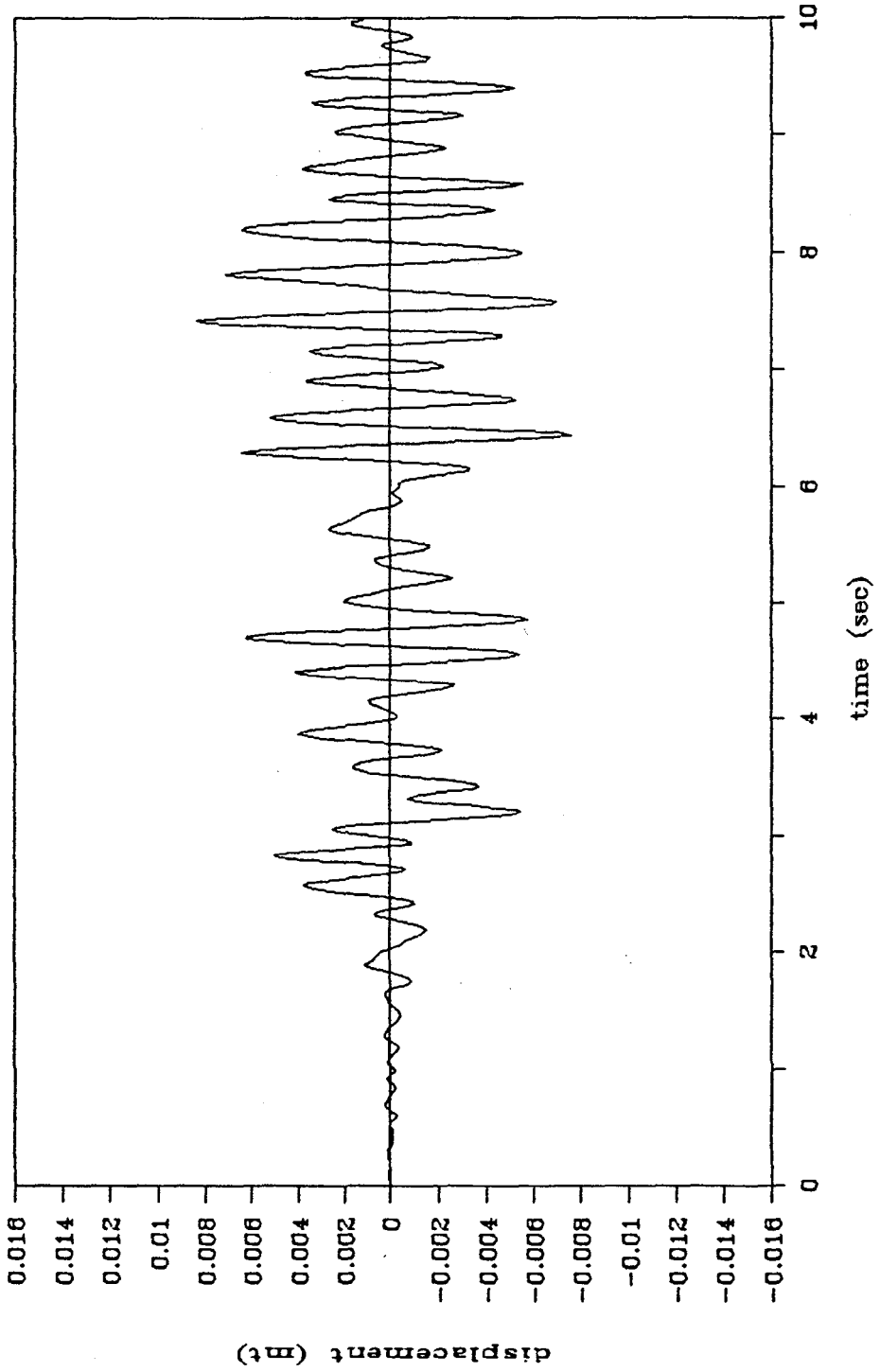

Figure 20 Time history of the relative inplane displacement at the third floor of the assembly 2 (computed by ELM; unreinforced case; sc=2.5; Structure 2)

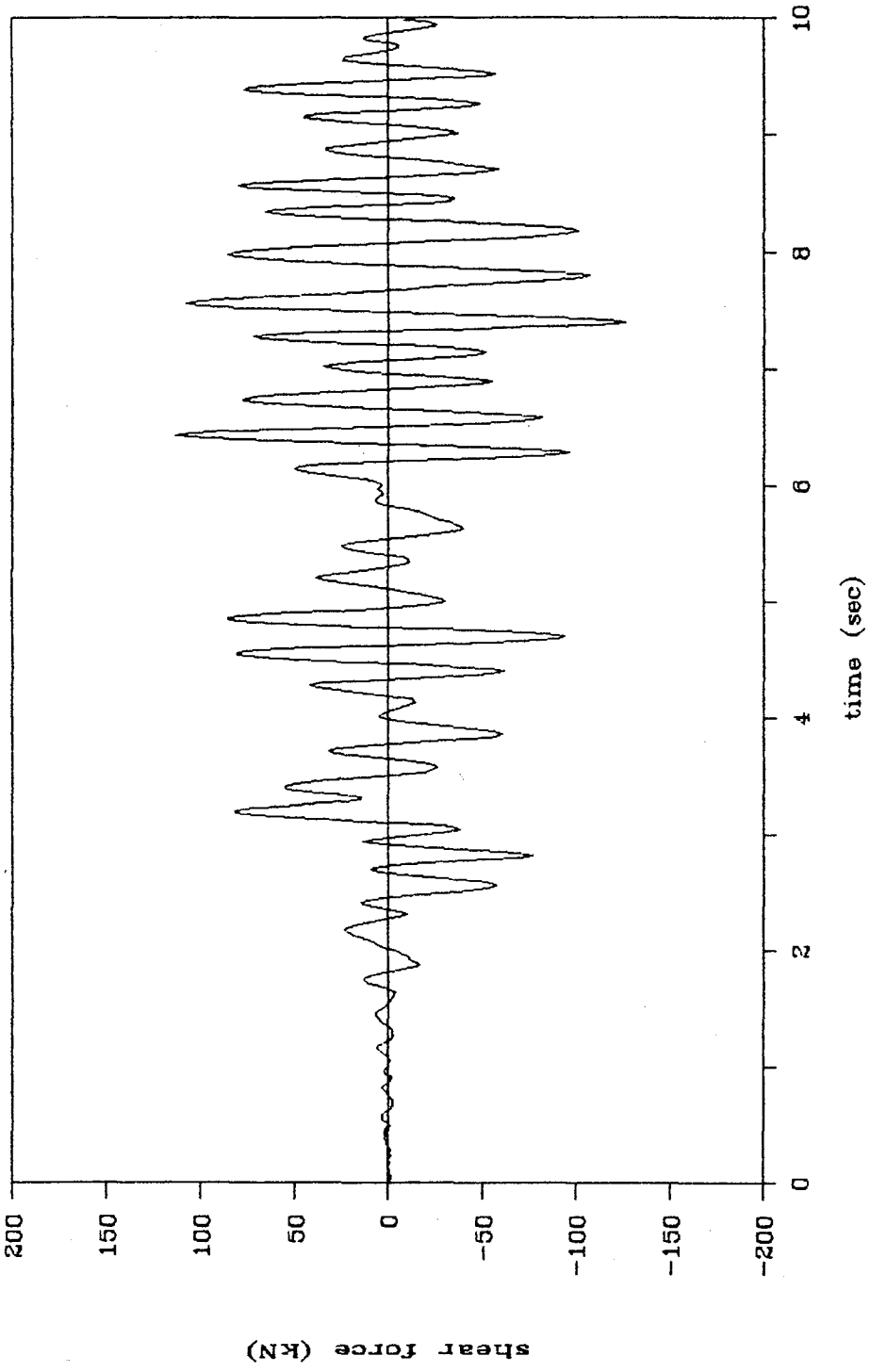

Figure 21 Time history of inplane shear force in the first story of the assembly 2 (computed by ELM; unreinforced case; sc=2.5; Structure 2)

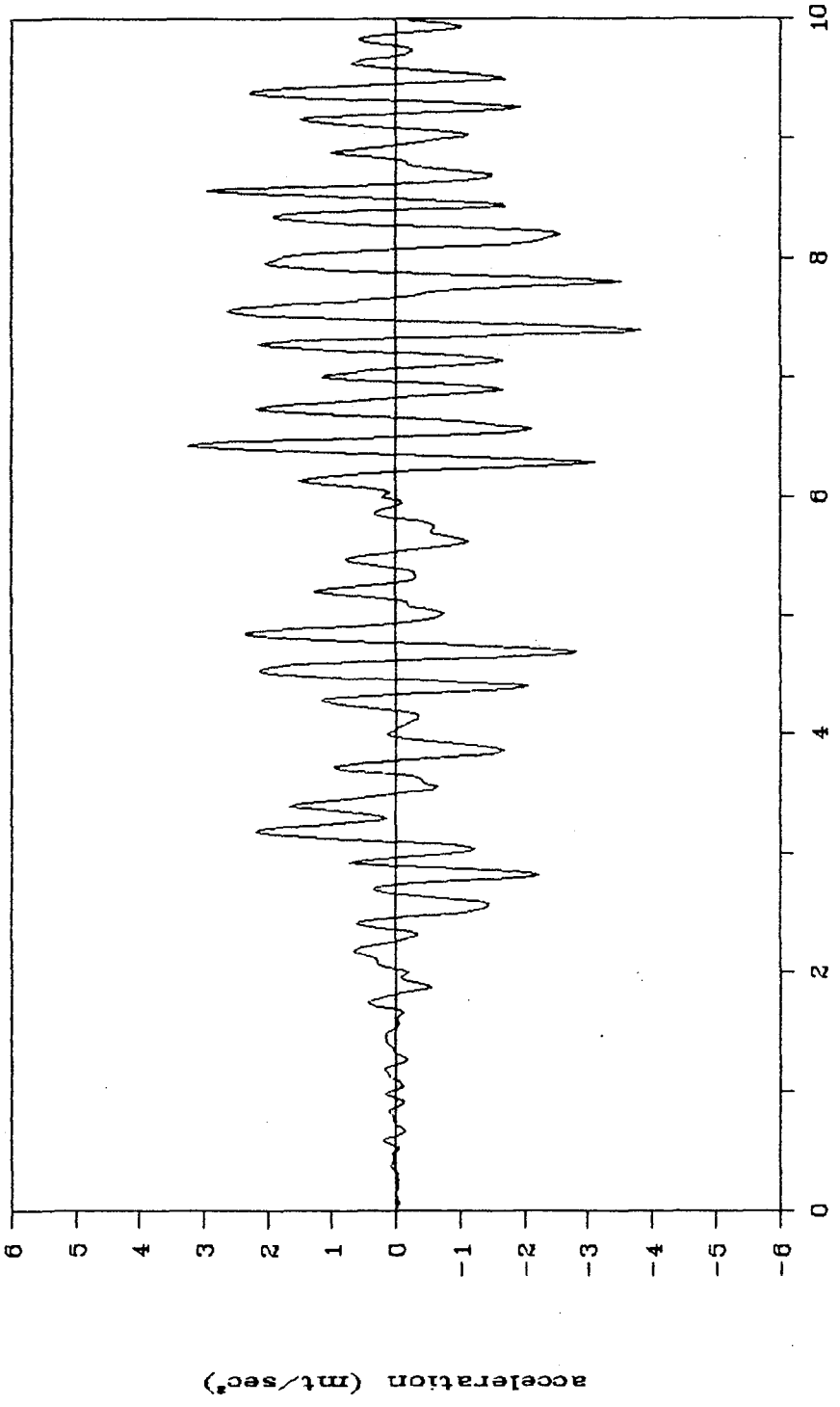

Figure 22 Time history of the total acceleration (in y direction) of the master point at the third floor (computed by ELM; unreinforced case; sc=2.5; Structure 2)

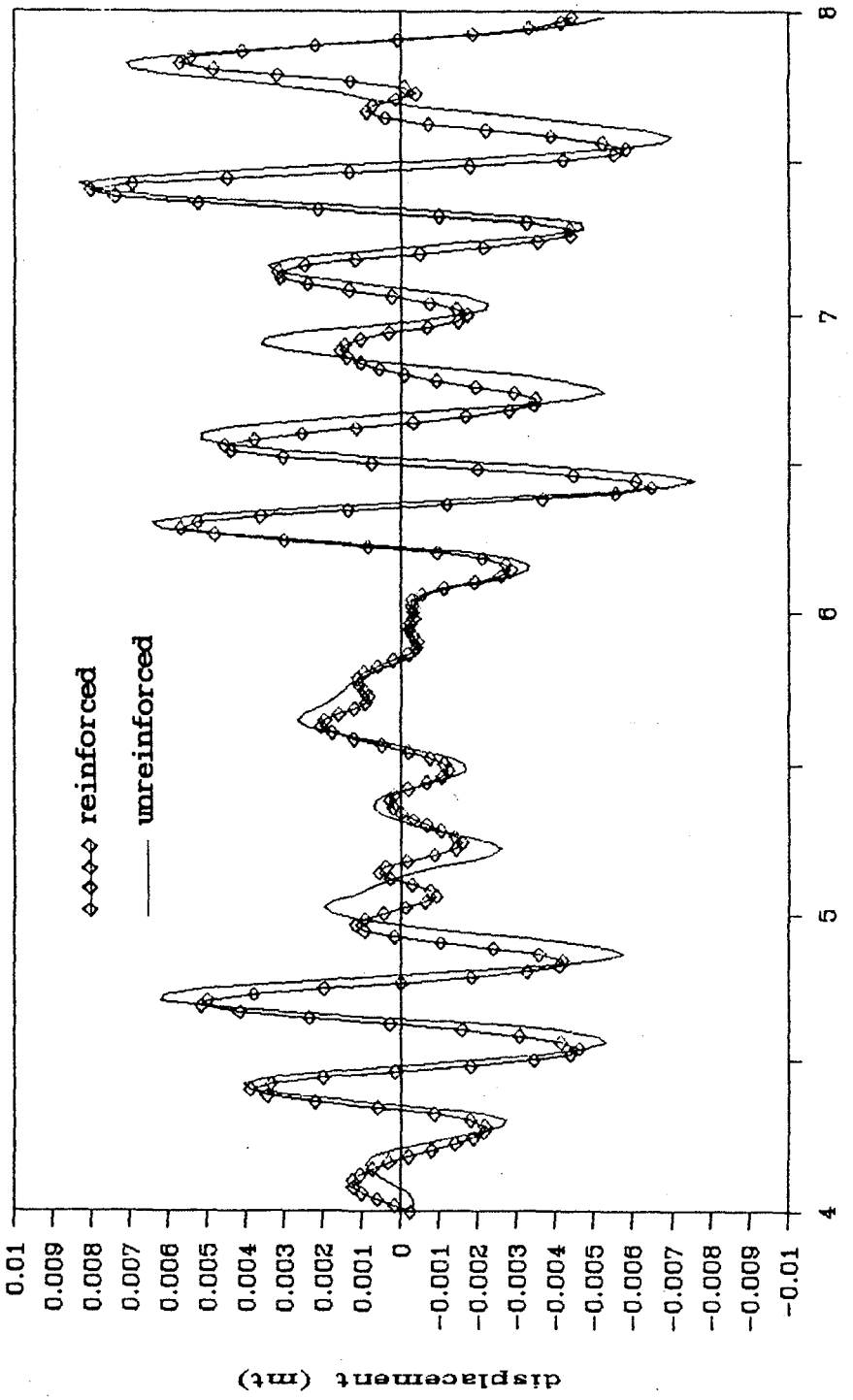

Figure 23 Comparison of the time histories of the relative inplane displacements at the third floor of the assembly 2 for unreinforced and reinforced cases (computed by ELM; sc=2.5; Structure 2)

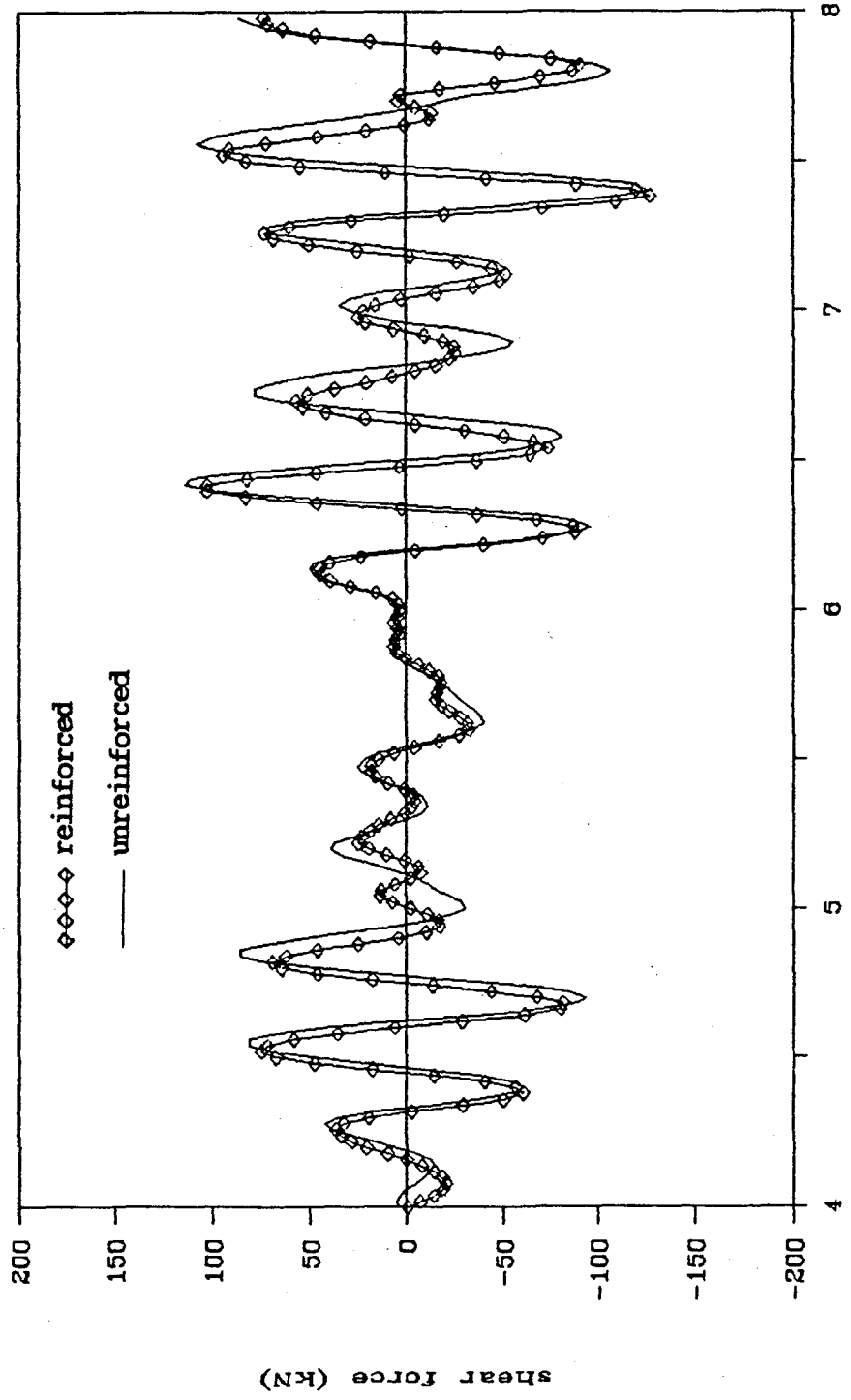

Figure 24 Comparison of the time histories of the inplane shear forces in the first story of the assembly 2 for unreinforced and reinforced cases (computed by ELM; sc=2.5; Structure 2)

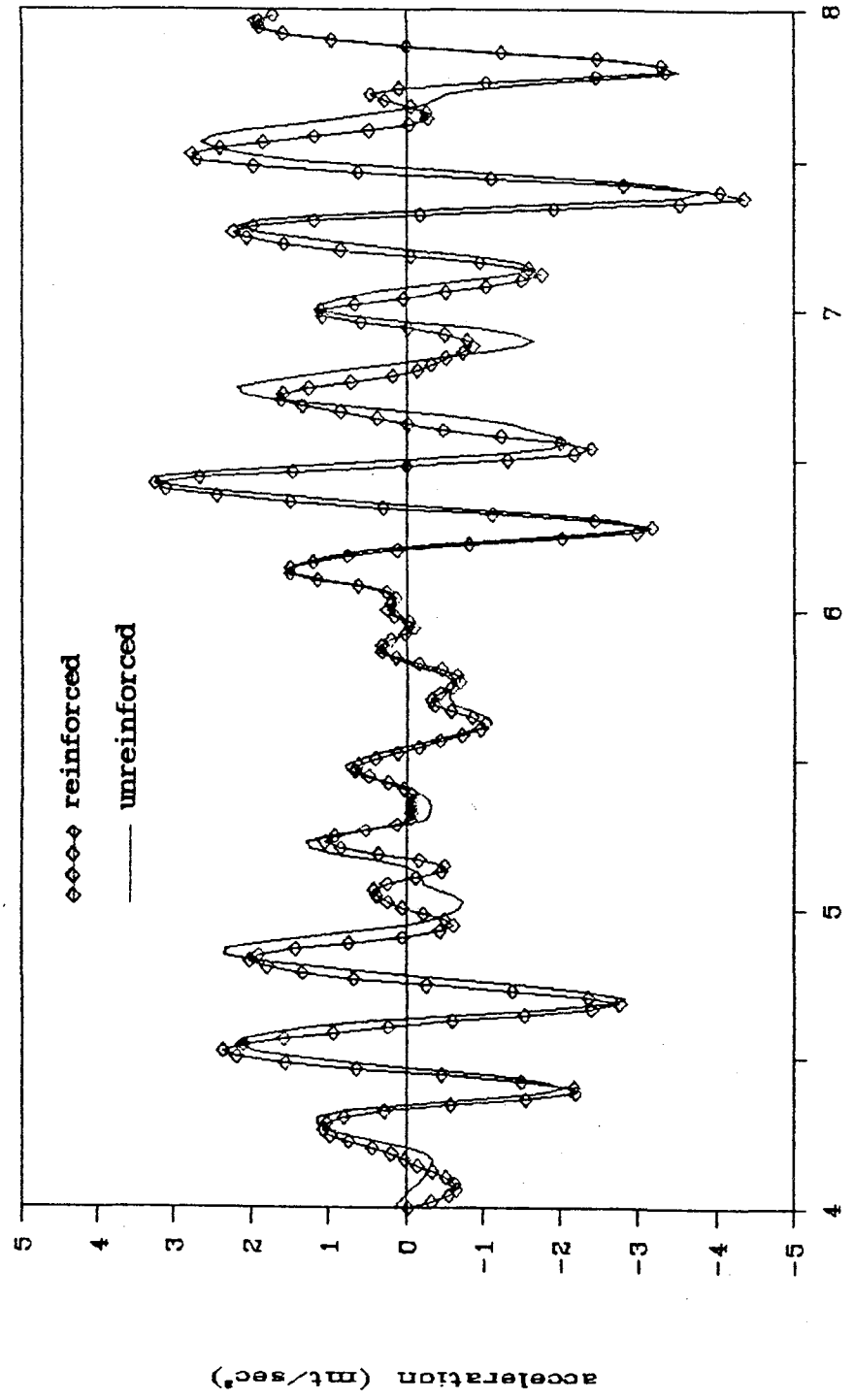

Figure 25 Comparison of the time histories of the total accelerations (in y direction) of the master point at the third floor for unreinforced and reinforced cases (computed by ELM; sc=2.5; Structure 2)

reinforced cases are close to each other. The maximum value of the inplane relative displacement is about 8 mm, which appears to be a reasonable value in view of the rigidity of the masonry building under consideration and the assumed earthquake input.

We now study the influence of the amplitude of the ground acceleration (i.e.,of scale factor) on the amplification curves (defined in frequency space) for unreinforced and reinforced cases. We do this study for the amplification of the absolute acceleration (in y direction) at the MP of the third floor with respect to the ground acceleration by using the formula

$$D = \frac{| a_t^F |}{| a_g^F |} \tag{91}$$

where superscript F designates Fourier transform; a_t and a_g are respectively top and ground accelerations and D is the amplification. Using this equation together with the FFT algorithm [12,13], the variation of D with the frequency "f" are computed for the scale factors sc=1.0, 1.5, 2.0, 2.5 and the resulting amplification curves are presented in Figs.26 and 27 for unreinforced and reinforced cases respectively. Figures show that (a) the results of unreinforced and reinforced cases are close (b) as the scale factor (i.e.,the amplitude of the ground acceleration) increases the peak amplitude value and its corresponding frequency decrease, which are due to the degradation effects in the building

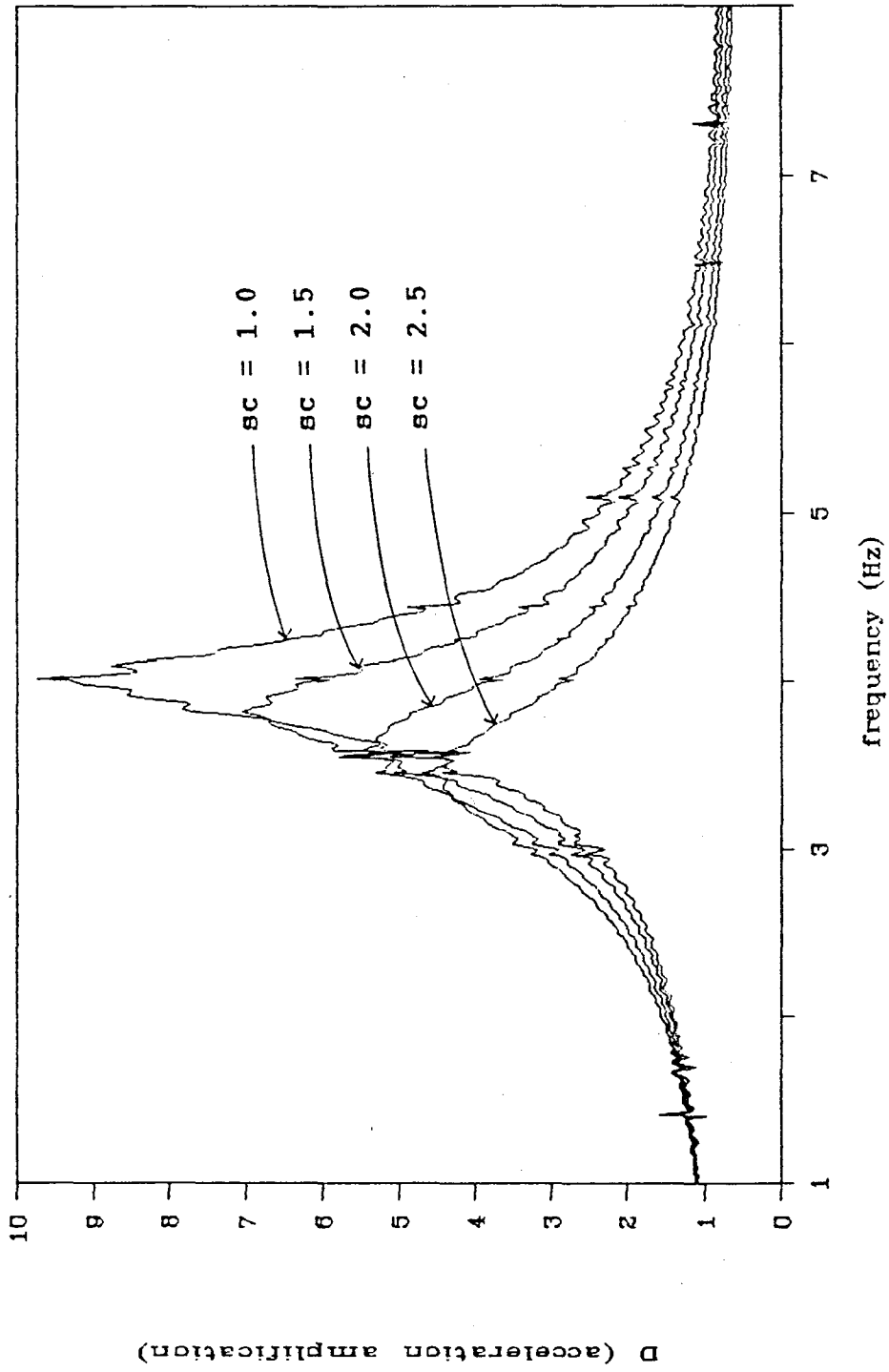

Figure 26 Acceleration amplification curve for unreinforced case (obtained from the results of ELA; Structure 2)

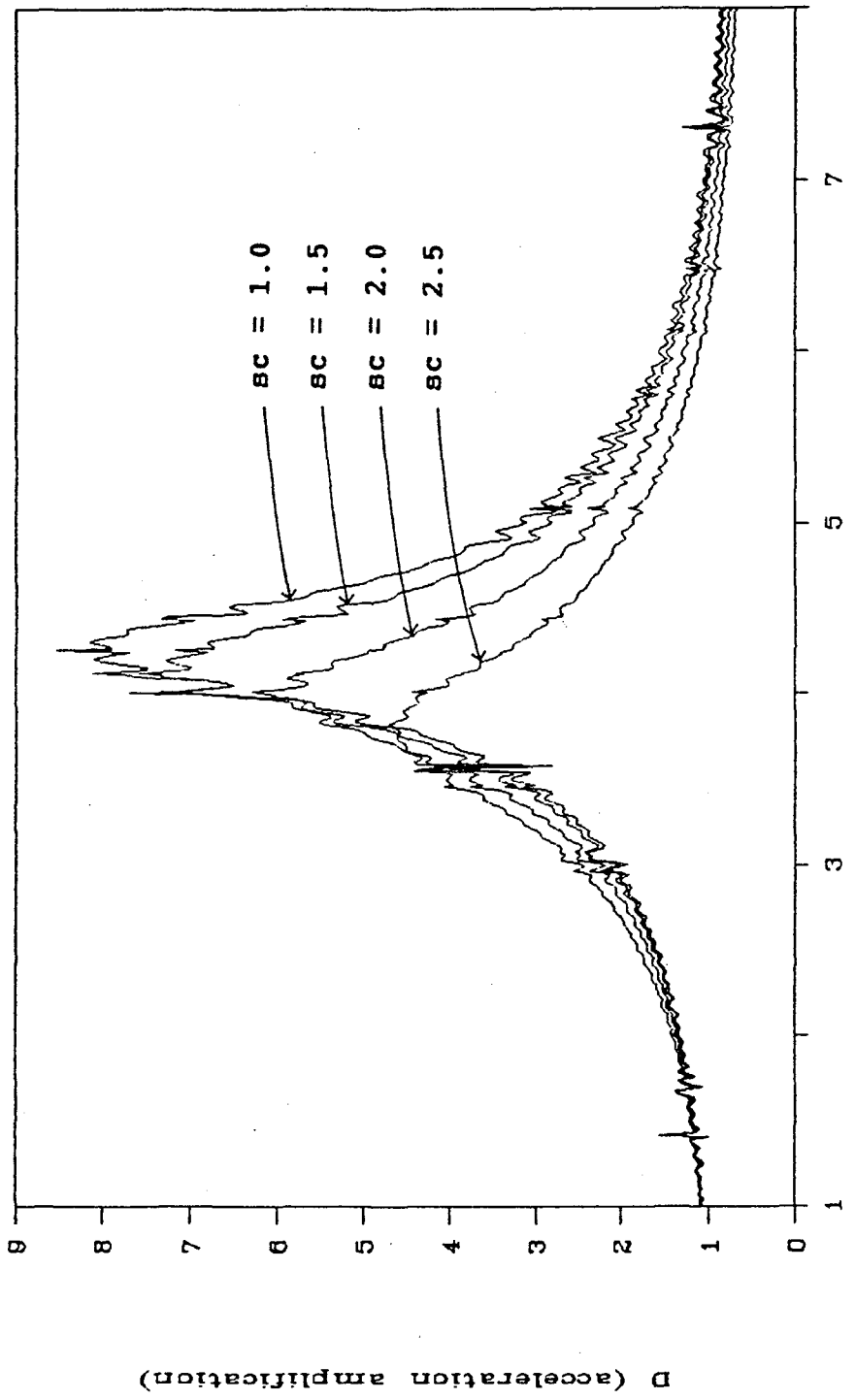

Figure 27 Acceleration amplification curve for reinforced case (obtained from the results of ELA; Structure 2)

caused by the amount of damages in wall elements which increase with the intensity of earthquake excitation. It may further be noted that the portion of the curves containing peak amplifications in Figs. 26 and 27 corresponds approximately to the frequency interval in which the first three free vibration frequencies of the building lie (see Tables 4 and 5).

Example 5

This last example involves the nonlinear time history analysis of Structure 2 by using the actual nonlinear model (ANM), i.e., by the computer program MAS2. The results will be presented for two different scale factors, namely, sc=2.5 and 3.0. The use of the first scale factor sc=2.5 is aimed at the comparison of the results with those of ELM. The second scale factor sc=3.0, on the other hand, is used in presenting the results for the hysteresis curves predicted by ANM. In order to see the degradation effects on hysteresis curves clearly, the second scale factor is selected to be larger than the first.

We first present the results for sc=2.5. The input data to MAS2 is given in Fig.28 for reinforced case, and can be found also in the files EXMPL5U and EXMPL5R of the attached floppy disk for unreinforced and reinforced cases respectively.

Maximum element forces, damage ratios and maximum shear strains predicted by ANM (MAS2) for the wall assemblies 2, 4

```
GENERAL INFORMATION
1   3   26
STORY HEIGHTS
1,3    3.0
COORDINATES
1     0.125     0.750
2     0.125     4.500
3     0.125     8.250
4     2.525     7.450
5     2.525     4.900
6     3.925     3.000
7     4.925     7.525
8     6.525     7.950
9     6.525     3.075
10    7.825     7.300
11   10.375     7.550
12   10.375     4.200
13   10.375     1.075
14    1.625     8.875
15    5.000     8.875
16    6.450     8.875
17    8.825     8.875
18    2.900     6.325
19    5.300     6.325
20    1.475     4.525
21    4.475     4.525
22    8.975     4.575
23    4.150     1.425
24    6.700     1.425
25    9.550     1.425
26    2.125     0.125
PROP.OF ASSEMBLIES
1     90
1,3    1.50    0.25    1.0
2     90
1,3    3.00    0.25    1.0
3     90
1,3    1.50    0.25    1.0
4     90
1,3    2.60    0.15    1.0
5     90
1,3    0.60    0.15    1.0
6     90
1,3    2.90    0.15    1.0
7     90
1,3    2.35    0.15    1.0
8     90
1,3    1.60    0.15    1.0
9    90
1,3    3.05    0.15    1.0
10    90
1,3    2.90    0.25    1.0
11    90
1,3    2.90    0.25    1.0
12    90
1,3    1.00    0.25    1.0
13    90
1,3    2.15    0.25    1.0
14     0
1,3    2.75    0.25    1.0
15     0
1,3    1.00    0.25    1.0
16     0
1,3    0.90    0.25    1.0
17     0
1,3    2.85    0.25    1.0
18     0
1,3    0.60    0.15    1.0
19     0
1,3    2.60    0.15    1.0
20     0
1,3    2.45    0.15    1.0
21     0
1,3    1.75    0.15    1.0
22     0
1,3    2.55    0.25    1.0
23     0
1,3    0.60    0.25    1.0
24     0
1,3    1.50    0.25    1.0
25     0
1,3    1.40    0.25    1.0
26     0
1,3    3.75    0.25    1.0
MASSES
1,2    114.04   114.04   2191.34
3       84.80    84.80   1539.34
COORD. OF MP
1,2     5.09    4.80
3       5.14    4.70
MATERIAL PROP.
0.0          168000.00     896.9
0.000513     168000.00     896.9
0.001580     100279.60    1855.8
0.003160          0.00    1855.8
0.010000          0.00    1855.8
TIME HISTORY
90.0
1
2   3
1
2   1
1
3
0.0     10.0    0.02
0.02    1000    1  2.5
PACOIMA
```

Figure 28 Input data for Example 5

(sc=2.5, for reinforced case)

and 26 are listed in the Tables 11 and 12 for unreinforced and reinforced cases respectively. The comparison of the results in Tables 11 and 12 with those in Tables 9 and 10 obtained by ELM shows that the results from ANM and ELM are close and they differ at most 14% (with respect to ANM values). This observation indicates that ELM can be used reliably in nonlinear time history analysis of masonry buildings without causing any major error in the results. Since the use of ELM requires less computer time compared to ANM, if no convergence problem arises, we recommend in view of the aforementioned observation that ELM (instead of ANM) be used in the nonlinear time history analysis of masonry buildings.

The time histories of

- the inplane relative displacement at the third floor of the assembly 2
- the inplane shear force in the first story of the assembly 2
- the total MP acceleration (in y direction) at the top (third) floor

are obtained by ANM and, since the results are similar for reinforced and unreinforced cases, they are presented only for unreinforced Structure 2 in Figs. 29, 30 and 31. These time histories are compared in Figs. 32, 33 and 34 with those obtained by ELM in Example 4. The comparison indicates that the results of ELM and ANM are close and the agreement between the two improves as time increases. We

Table 11 The maximum values of element forces predicted by ANM for the wall assemblies 2, 4 and 26 of Structure 2 for unreinforced case (forces are in kN and torques in kN-mt; sc=2.5)

MEMBER FORCES FOR WALL ASSEMBLY # 2

STORY	U-Z PLANE SHEAR	TORQUE	SHEAR STRAIN	DAMAGE(%)
1	134.58	.08	.166E-02	43.33
2	106.96	.06	.100E-02	18.56
3	52.51	.03	.415E-03	.00

MEMBER FORCES FOR WALL ASSEMBLY # 4

STORY	U-Z PLANE SHEAR	TORQUE	SHEAR STRAIN	DAMAGE(%)
1	69.54	.02	.155E-02	39.26
2	53.51	.01	.959E-03	16.84
3	26.01	.00	.399E-03	.00

MEMBER FORCES FOR WALL ASSEMBLY # 26

STORY	U-Z PLANE SHEAR	TORQUE	SHEAR STRAIN	DAMAGE(%)
1	42.96	.17	.266E-03	.00
2	22.62	.09	.144E-03	.00
3	8.24	.03	.520E-04	.00

Table 12 The maximum values of element forces predicted by ANM for the wall assemblies 2, 4 and 26 of Structure 2 for reinforced case
(forces are in kN, torques and moments in kN-mt; sc=2.5)

MEMBER FORCES FOR WALL ASSEMBLY # 2

STORY	U-Z PLANE SHEAR	V-Z PLANE SHEAR	MOMENT	TORQUE	SH.STRAIN	DAMAGE(%)
1	126.39	4.52	6.78	.07	.139E-02	33.28
2	99.69	.01	.01	.06	.876E-03	13.73
3	40.90	.01	.01	.02	.317E-03	.00

MEMBER FORCES FOR WALL ASSEMBLY # 4

STORY	U-Z PLANE SHEAR	V-Z PLANE SHEAR	MOMENT	TORQUE	SH.STRAIN	DAMAGE(%)
1	63.98	.84	1.26	.01	.131E-02	29.97
2	49.85	.03	.04	.01	.836E-03	12.19
3	20.25	.04	.06	.00	.304E-03	.00

MEMBER FORCES FOR WALL ASSEMBLY # 26

STORY	U-Z PLANE SHEAR	V-Z PLANE SHEAR	MOMENT	TORQUE	SH.STRAIN	DAMAGE(%)
1	30.34	3.49	5.23	.13	.194E-03	.00
2	18.65	1.86	2.80	.08	.119E-03	.00
3	6.68	.67	1.01	.03	.426E-04	.00

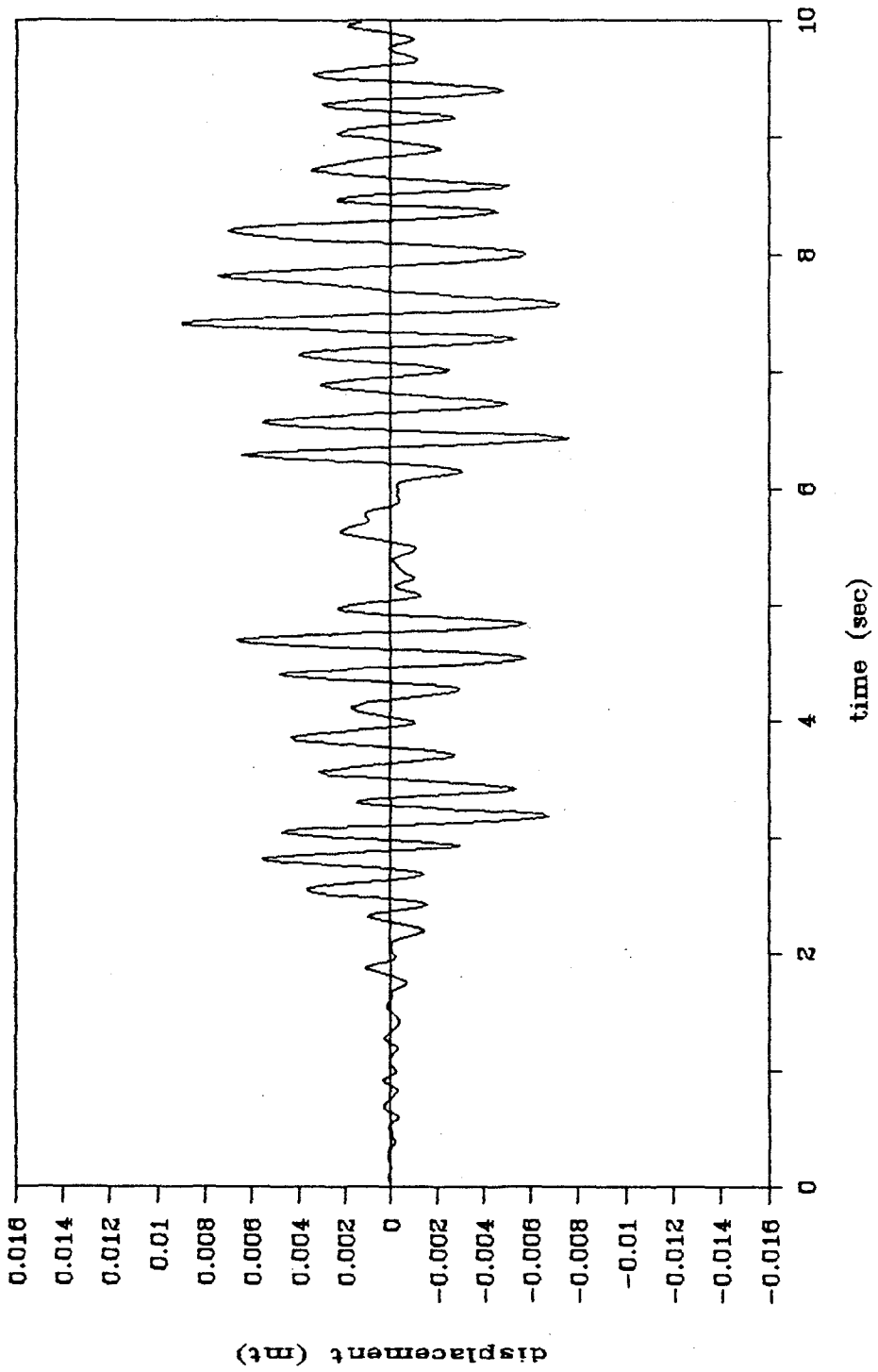

Figure 29 Time history of the relative inplane displacement at the third floor of the assembly 2 (computed by ANM; unreinforced case; sc=2.5; Structure 2)

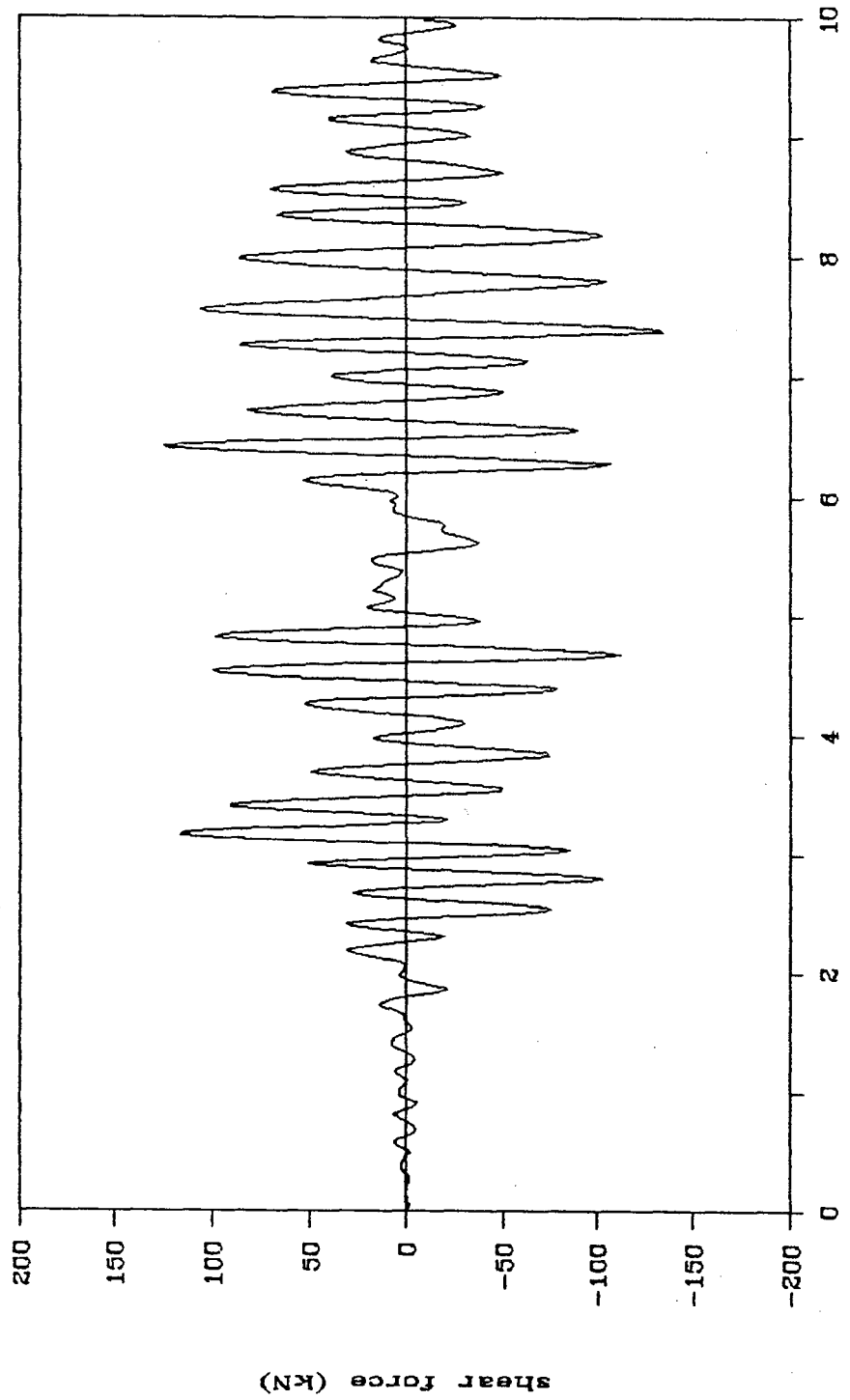

Figure 30 Time history of inplane shear force in the first story of the assembly 2 (computed by ANM; unreinforced case; sc=2.5; Structure 2)

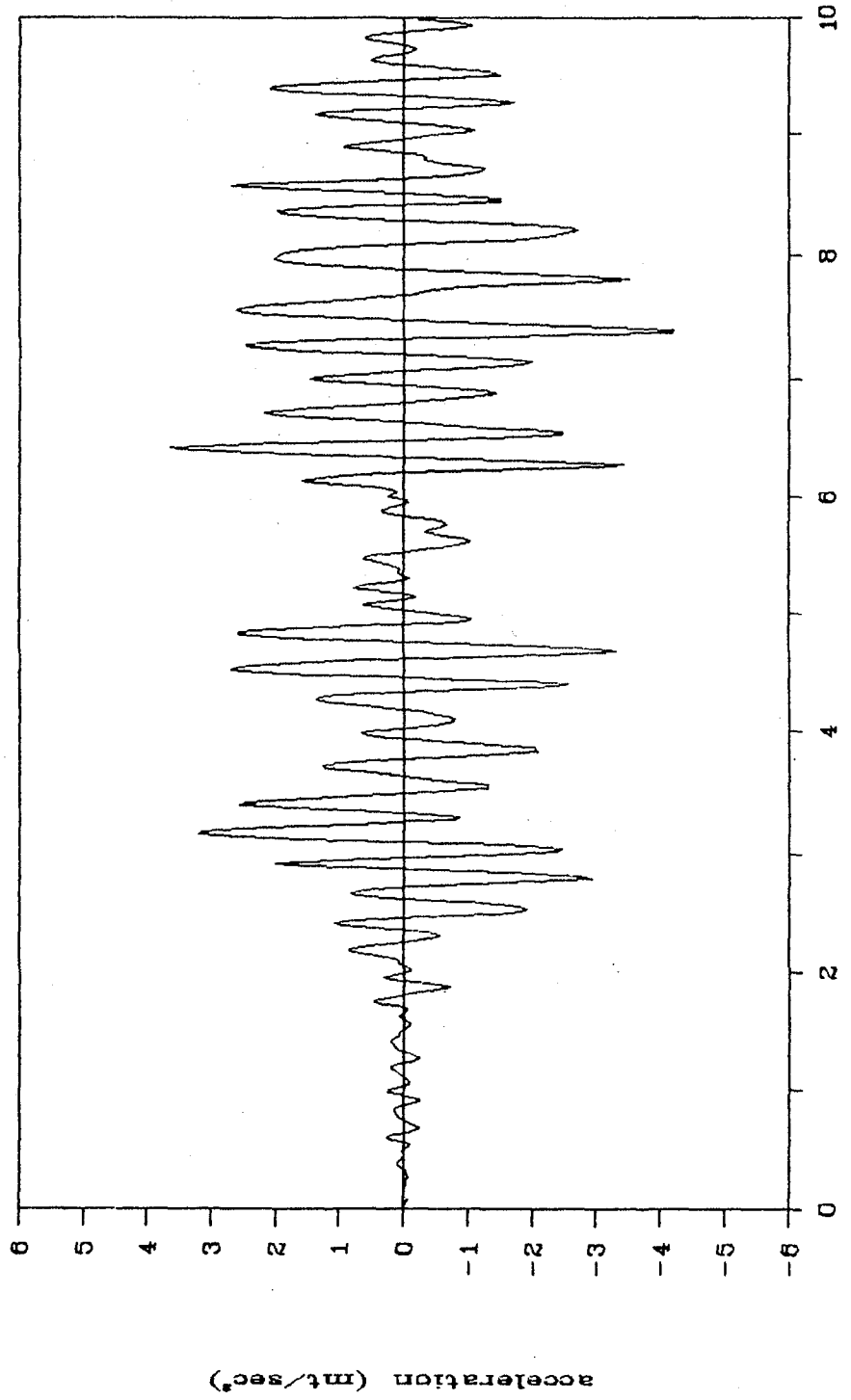

Figure 31 Time history of the total acceleration (in y direction) of the master point at the third floor (computed by ANM; unreinforced case; sc=2.5; Structure 2)

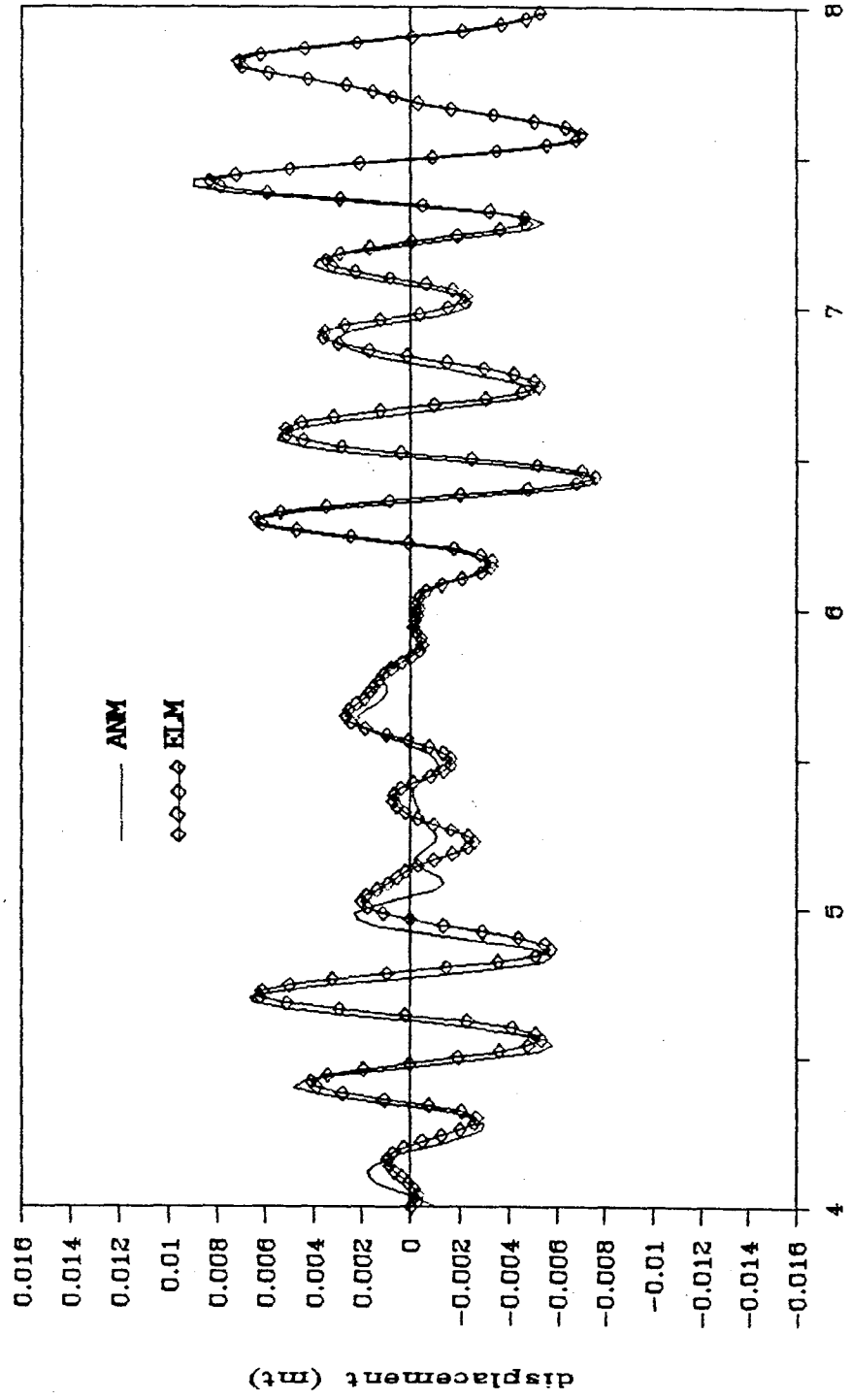

Figure 32 Comparison of the time histories of the relative inplane displacements at the third floor of the assembly 2 computed by ELM and ANM (unreinforced case; sc=2.5; Structure 2)

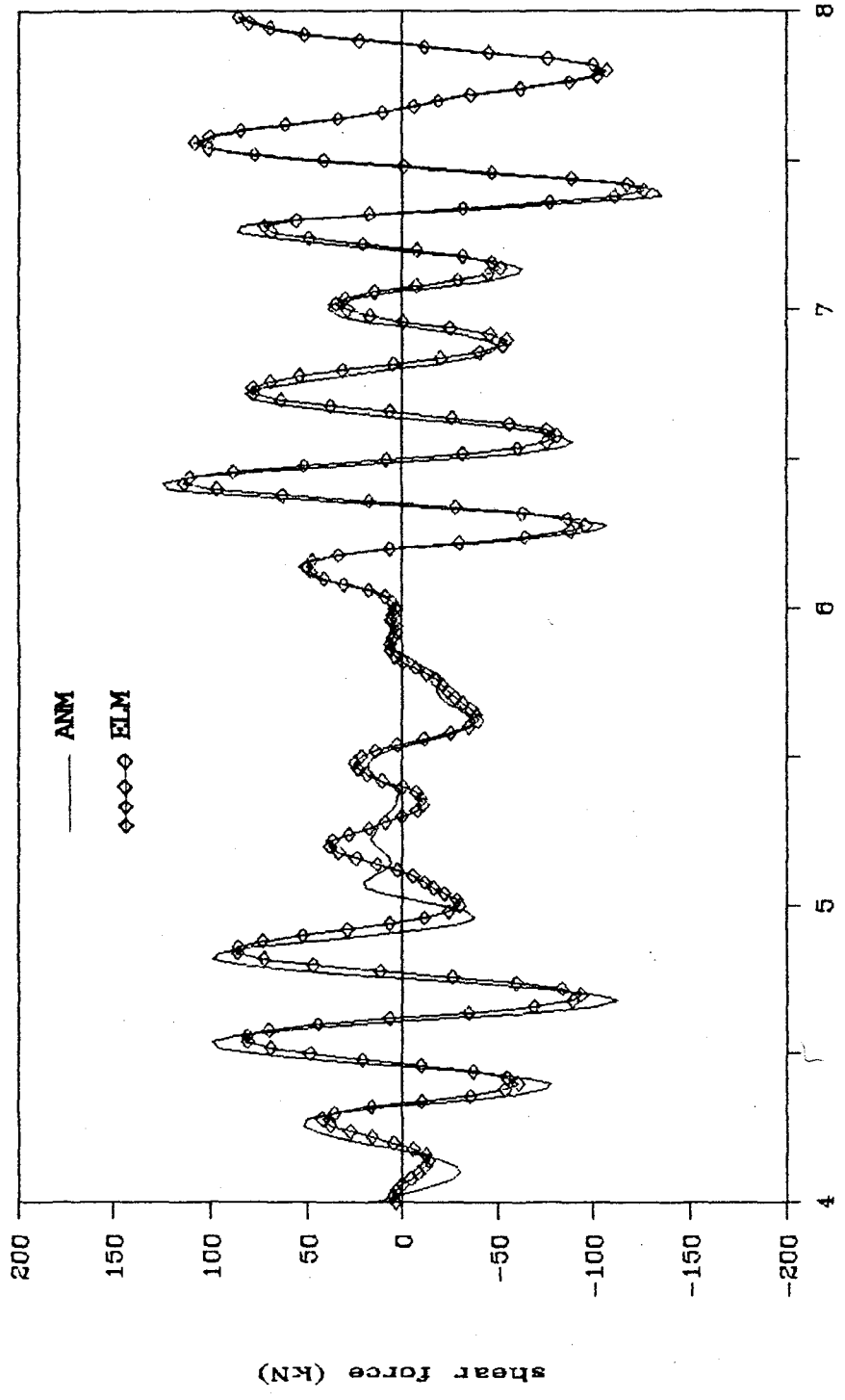

Figure 33 Comparison of the time histories of the inplane shear forces in the first story of the assembly 2 computed by ELM and ANM (unreinforced case; sc=2.5; Structure 2)

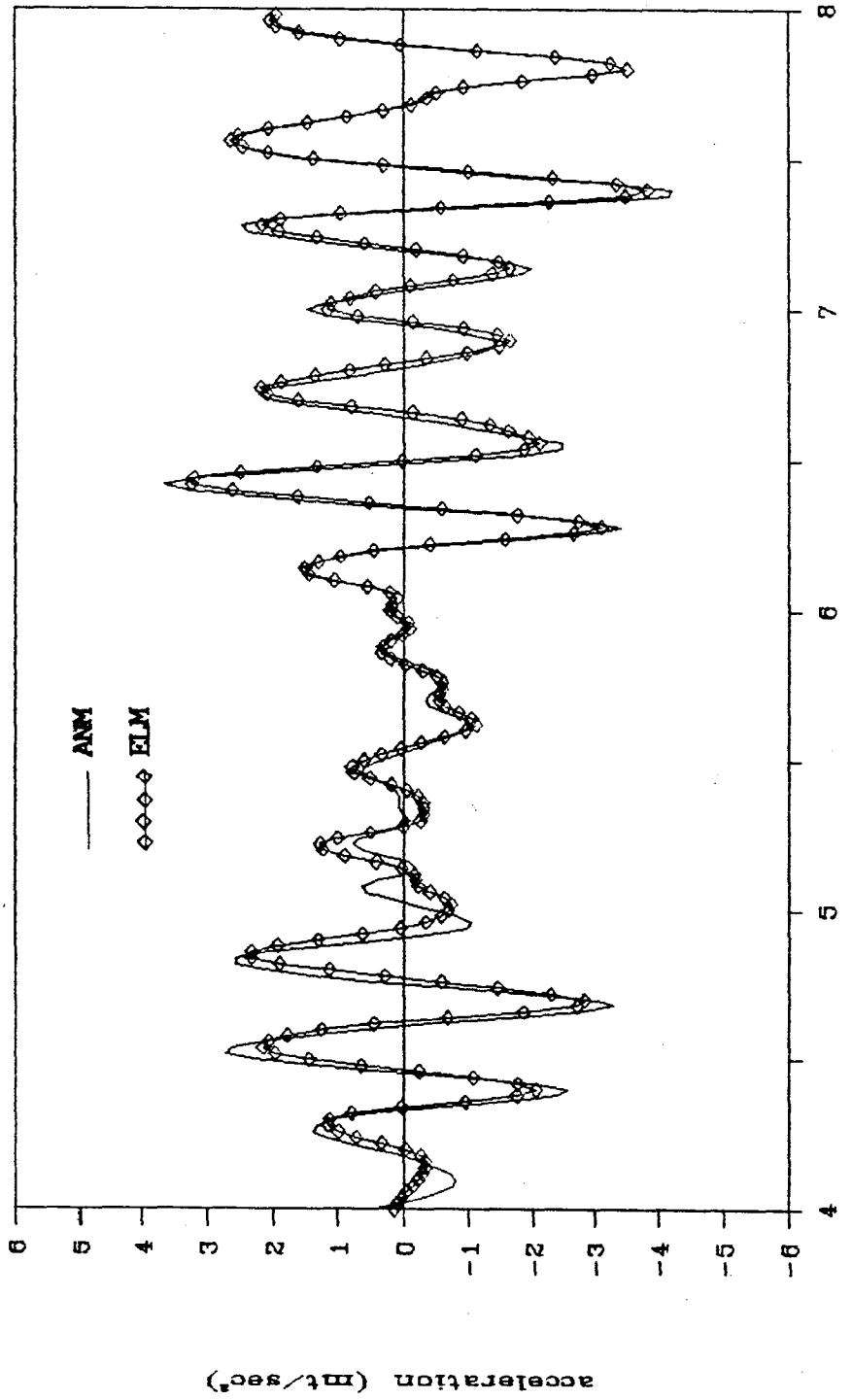

Figure 34 Comparison of the time histories of the total accelerations (in y direction) of the master point at the third floor computed by ELM and ANM (unreinforced case; sc=2.5; Structure 2)

may attribute the reason for getting better agreement for large times to the fact that the damaged state for which ELM results hold is actually reached after a certain time elapses.

We now present the hysteresis curves obtained by ANM with sc=3.0. They are given in Figs. 35 and 36 for unreinforced and reinforced buildings (Structure 2) respectively. The curves in the figures describe, during the earthquake excitation, the variation of the inplane shear force in the first story of the assembly 2 with the shear strain in the same wall element. For unreinforced case, the degradation in the rigidity of the wall element during earthquake excitation is clearly evident in Fig.35: as time increases the slope of the major axis of the hysteresis loops decreases and the areas enclosed by the loops (which correspond to the amount of the energy dissipated during the cycles of hysteresis loops) get larger. It is interesting to note that the shape of hysteresis loops shown in Fig.35 for unreinforced case is very similar to the one obtained in [11] experimentally for an unreinforced adobe house. Comparison of Figs.35 and 36 shows that reinforced masonry buildings retain, as anticipated, their rigidity during earthquake excitations better than that of unreinforced buildings.

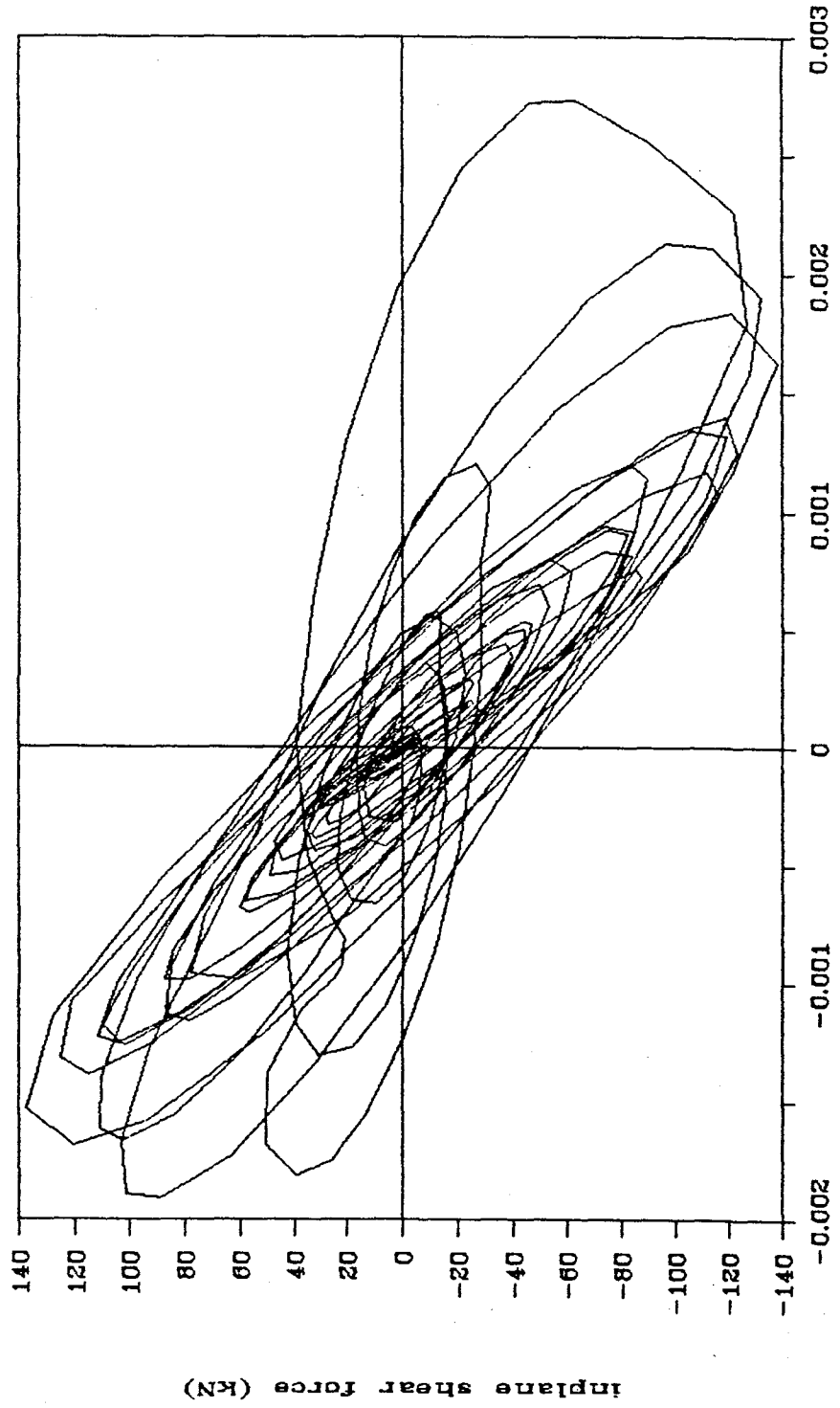

Figure 35 Hysteresis curve for the wall element in the first story of the assembly 2 for unreinforced case (sc=3.0; Structure 2)

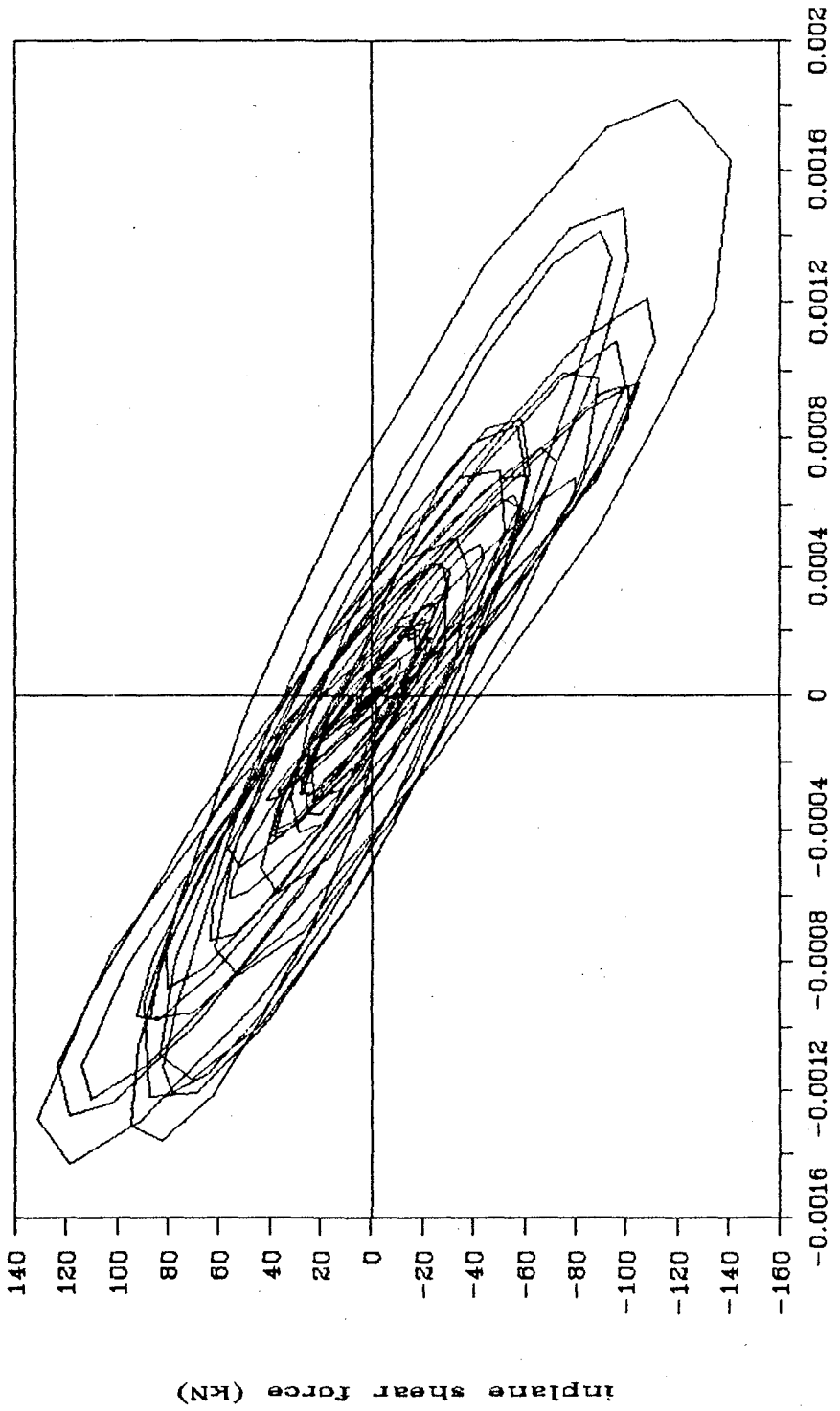

Figure 36 Hysteresis curve for the wall element in the first story of the assembly 2 for reinforced case (sc=3.0; Structure 2)

7. ASSESSMENT OF THE MODELS AND CONCLUSIONS

In this chapter we assess the models proposed in this study and reach some conclusions in view of the numerical results and discussions presented in the previous chapter.

1) The model for the earthquake behavior of the reinforced masonry building was established in Chapter 3 by using the following assumption: the nonlinear behavior of a masonry building is caused only by the inplane deformations of wall elements and the behavior of a wall element in its out-of-plane direction remains linear during an earthquake excitation. Here, we verify this assumption using the results obtained in Example 5 in which Structure 2 is subjected to a strong ground motion, namely Pacoima earthquake input with a scale factor of 2.5, and the building is analyzed by using the actual nonlinear model. As seen from Table 12, the wall elements undergo considerable damages with regard to their inplane deformations. The results not presented in the section of Example 5 (in order to save space) indicate that the maximum bending strain caused by out-of-plane moment (i.e., by the moment acting in vz plane (see Fig.3)) occurs in the first story of the assembly 3, which is equal to 0.07%. This value is well below the upper bound of the linear range of a reinforced concrete slab, which is about 0.1% [14]. This observation may be interpreted as an indication for the validity of the aforementioned assumption if one speculates that the linear upper bounds are close

for reinforced concrete slabs and reinforced masonry walls.

2) The shape of hysteresis loops predicted by ANM for unreinforced masonry buildings (during an earthquake excitation) are similar to the ones observed experimentally. This may be considered as an evidence concerning the correctness of the proposed models.

3) In linear dynamic analysis, the model does not assume preassigned values for damping ratios; instead, it predicts the damping ratios provided that the shear modulus and its viscous counterpart are specified. It also computes the damping ratios approximately for the nonlinear case if the equivalent linear model is used in the analysis. The values of damping ratios predicted by the models for Structure 2 in the example problems are about 7% for linear analysis and may increase up to about 12% for nonlinear case. These values appear to be reasonable for masonry structures and are in good agreement with the ranges being assumed for them in practice.

4) The first three free vibration frequencies of Structure 2 computed by the linear model in the previous chapter are found to be closely spaced and to lie approximately in the frequency interval [4,5] Hz. The frequency values in this interval represent typical values for stiff structures and appear to be realistic for masonry buildings. Closeness of the first three frequencies suggest that all of them may be excited by an earthquake input and thus, in order to obtain meaningful results, at least the first three frequencies of

the masonry building should be considered in the earthquake analysis.

5) In the analysis of example problems presented in the previous chapter, we observed that, when the intensity of the earthquake excitation is very large, the iterations of the equivalent linear method may lead to divergent values. When this is the case, the nonlinear analysis must be performed by using the actual nonlinear model.

6) For the reinforced case the models were established by using the assumption that the rotations of wall elements at floor levels in out-of-plane directions (in vz plane (see Fig.3)) are restrained . It appears that it is possible to improve the models by releasing these restraint conditions. However, we suspect that this modification will not influence the prediction of the models greatly in view of the closeness of the results obtained for reinforced and unreinforced cases in the previous chapter.

SUMMARY

Mathematical models are proposed for the three - dimensional earthquake analysis of reinforced and unreinforced masonry buildings. In the formulation it is assumed that for unreinforced case the earthquake forces are resisted by the inplane shear rigidities of the wall elements while for reinforced case the rigidities of wall elements in out-of-plane directions are also taken into account (in addition to their inplane shear rigidities). It is further assumed that the floors are infinitely rigid in their own planes, which makes it possible to simplify the formulation by using rigid diaphragm modelling. The hysteretic behavior of wall elements are formulated by using experimental data obtained from shaking table experiments. In view of this data, a bilinear form is assumed for the skeleton curve of the inplane shear modulus G of wall elements and a trilinear form for its associated viscous coefficient G'.

For the nonlinear earthquake analysis of masonry buildings by the models described above, two different approaches are adopted. The first one uses the "equivalent linear method" (ELM) which had been used previously by some researchers in soil-structure interaction analysis. ELM performs the nonlinear analysis by employing iterations. Each iteration of ELM involves linear analysis with G and G' values adjusted to the state of the deformation in the previous iteration by using the skeleton curves of G and G'. The second approach employs the actual nonlinear model (ANM)

in which the nonlinear earthquake analysis of the building is carried out by taking into account the actual hysteretic behavior of wall elements (i.e., by considering the loading and unloading properties of G and G'). Both in the iteration of ELM and in the approach involving ANM, the equations are integrated through the use of Runge Kutta's method of order 4.

Based on the proposed models and the methods used in the analysis, two computer programs of the names MAS1 and MAS2 are developed. The first program MAS1 performs linear static, free vibration and linear earthquake analyses as well as nonlinear earthquake analysis by ELM. The second program MAS2 carries out the nonlinear earthquake analysis by using ANM.

To appraise the models, some example problems are presented. The results indicated that the models are capable to predict hysteresis loops observed experimentally for masonry structures and they can be used with confidence in linear or nonlinear earthquake analysis of masonry buildings.

REFERENCES

1. A.Ghali and A.M.Neville, Structural Analysis, Chapman and Hall, London (1978).
2. H.B.Seed and I.M.Idriss. Influence of Soil Conditions on Ground Motions During Earthquakes. Journal of the Soil Mechanics and Foundations Division, ASCE, 94, (1969).
3. Y.Mengi and H.D.McNiven. A Mathematical Model for the In-Plane Non-Linear Earthquake Behaviour of Unreinforced Masonry Walls, Part 1: Experiments and Proposed Model. Earthquake Engineering and Structural Dynamics, 18, 233-247 (1989).
4. H.D.McNiven and Y.Mengi. A Mathematical Model for the In-Plane Non-Linear Earthquake Behaviour of Unreinforced Masonry Walls,Part 2: Completion of the Model. Earthquake Engineering and Structural Dynamics, 18, 249-261 (1989).
5. J.Lysmer, T.Udaka, C.Tsai and H.B.Seed, FLUSH, a Computer Program for Approximate 3-D Dynamic Analysis of Soil-Structure Problems. Report of Earthquake Engineering Research Center, University of California, Berkeley, Report No. EERC-75-30 (1970).
6. G.Dahlquist and A.Bjorck,Numerical Methods,Prentice-Hall, N.J. (1974).
7. K. J. Bathe and E. L. Wilson, Numerical Methods in Finite Element Analysis, Prentice Hall, London (1976).
8. R.W.Clough and J.Penzien, Dynamics of Structures, McGraw Hill, Tokyo (1982).

9. R. R. Craig, Structural Dynamics: An Introduction to Computer Methods, John Wiley, New York (1981).

10. C. L. Kan and A. K. Chopra, Coupled Lateral Torsional Response of Buildings to Ground Shaking. Report of Earthquake Engineering Research Center, University of California, Berkeley, Report No. EERC-76-13, (1976).

11. G. Ottazzi, J. Yep, M. Blondet, G. Villa-Garcia and J.Ginocchio, Ensayos de Simulacion Sismica de Viviendas de Adobe. Report of Pontificia Universidad del Peru, Departamento de Ingenieria, Report No. D1-89-01 (1989).

12. E.O.Brigham, The Fast Fourier Transform, Prentice - Hall, Englewood Cliffs, N.J. (1974).

13. J. W. Cooley, P. A. W. Lewis and P. D. Welch. The Fast Fourier Transform and Its Applications. IEEE Trans., Education, 12, 27-34 (1969).

14. Z. P. Bazant and et. al., Finite Element Analysis of Reinforced Concrete, American Society of Civil Engineers, New York (1980).

EARTHQUAKE ENGINEERING RESEARCH CENTER REPORT SERIES

EERC reports are available from the National Information Service for Earthquake Engineering(NISEE) and from the National Technical Information Service(NTIS). Numbers in parentheses are Accession Numbers assigned by the National Technical Information Service; these are followed by a price code. Contact NTIS, 5285 Port Royal Road, Springfield Virginia, 22161 for more information. Reports without Accession Numbers were not available from NTIS at the time of printing. For a current complete list of EERC reports (from EERC 67-1) and availablity information, please contact University of California, EERC, NISEE, 1301 South 46th Street, Richmond, California 94804.

UCB/EERC-82/01 "Dynamic Behavior of Ground for Seismic Analysis of Lifeline Systems," by Sato, T. and Der Kiureghian, A., January 1982, (PB82 218 926)A05.

UCB/EERC-82/02 "Shaking Table Tests of a Tubular Steel Frame Model," by Ghanaat, Y. and Clough, R.W., January 1982, (PB82 220 161)A07.

UCB/EERC-82/03 "Behavior of a Piping System under Seismic Excitation: Experimental Investigations of a Spatial Piping System supported by Mechanical Shock Arrestors," by Schneider, S., Lee, H.-M. and Godden, W. G., May 1982, (PB83 172 544)A09.

UCB/EERC-82/04 "New Approaches for the Dynamic Analysis of Large Structural Systems," by Wilson, E.L., June 1982, (PB83 148 080)A05.

UCB/EERC-82/05 "Model Study of Effects of Damage on the Vibration Properties of Steel Offshore Platforms," by Shahrivar, F. and Bouwkamp, J.G., June 1982, (PB83 148 742)A10.

UCB/EERC-82/06 "States of the Art and Pratice in the Optimum Seismic Design and Analytical Response Prediction of R/C Frame Wall Structures," by Aktan, A.E. and Bertero, V.V., July 1982, (PB83 147 736)A05.

UCB/EERC-82/07 "Further Study of the Earthquake Response of a Broad Cylindrical Liquid-Storage Tank Model," by Manos, G.C. and Clough, R.W., July 1982, (PB83 147 744)A11.

UCB/EERC-82/08 "An Evaluation of the Design and Analytical Seismic Response of a Seven Story Reinforced Concrete Frame," by Charney, F.A. and Bertero, V.V., July 1982, (PB83 157 628)A09.

UCB/EERC-82/09 "Fluid-Structure Interactions: Added Mass Computations for Incompressible Fluid," by Kuo, J.S.-H., August 1982, (PB83 156 281)A07.

UCB/EERC-82/10 "Joint-Opening Nonlinear Mechanism: Interface Smeared Crack Model," by Kuo, J.S.-H., August 1982, (PB83 149 195)A05.

UCB/EERC-82/11 "Dynamic Response Analysis of Techi Dam," by Clough, R.W., Stephen, R.M. and Kuo, J.S.-H., August 1982, (PB83 147 496)A06.

UCB/EERC-82/12 "Prediction of the Seismic Response of R/C Frame-Coupled Wall Structures," by Aktan, A.E., Bertero, V.V. and Piazzo, M., August 1982, (PB83 149 203)A09.

UCB/EERC-82/13 "Preliminary Report on the Smart 1 Strong Motion Array in Taiwan," by Bolt, B.A., Loh, C.H., Penzien, J. and Tsai, Y.B., August 1982, (PB83 159 400)A10.

UCB/EERC-82/14 "Seismic Behavior of an Eccentrically X-Braced Steel Structure," by Yang, M.S., September 1982, (PB83 260 778)A12.

UCB/EERC-82/15 "The Performance of Stairways in Earthquakes," by Roha, C., Axley, J.W. and Bertero, V.V., September 1982, (PB83 157 693)A07.

UCB/EERC-82/16 "The Behavior of Submerged Multiple Bodies in Earthquakes," by Liao, W.-G., September 1982, (PB83 158 709)A07.

UCB/EERC-82/17 "Effects of Concrete Types and Loading Conditions on Local Bond-Slip Relationships," by Cowell, A.D., Popov, E.P. and Bertero, V.V., September 1982, (PB83 153 577)A04.

UCB/EERC-82/18 "Mechanical Behavior of Shear Wall Vertical Boundary Members: An Experimental Investigation," by Wagner, M.T. and Bertero, V.V., October 1982, (PB83 159 764)A05.

UCB/EERC-82/19 "Experimental Studies of Multi-support Seismic Loading on Piping Systems," by Kelly, J.M. and Cowell, A.D., November 1982, (PB90 262 684)A07.

UCB/EERC-82/20 "Generalized Plastic Hinge Concepts for 3D Beam-Column Elements," by Chen, P. F.-S. and Powell, G.H., November 1982, (PB83 247 981)A13.

UCB/EERC-82/21 "ANSR-III: General Computer Program for Nonlinear Structural Analysis," by Oughourlian, C.V. and Powell, G.H., November 1982, (PB83 251 330)A12.

UCB/EERC-82/22 "Solution Strategies for Statically Loaded Nonlinear Structures," by Simons, J.W. and Powell, G.H., November 1982, (PB83 197 970)A06.

UCB/EERC-82/23 "Analytical Model of Deformed Bar Anchorages under Generalized Excitations," by Ciampi, V., Eligehausen, R., Bertero, V.V. and Popov, E.P., November 1982, (PB83 169 532)A06.

UCB/EERC-82/24 "A Mathematical Model for the Response of Masonry Walls to Dynamic Excitations," by Sucuoglu, H., Mengi, Y. and McNiven, H.D., November 1982, (PB83 169 011)A07.

UCB/EERC-82/25 "Earthquake Response Considerations of Broad Liquid Storage Tanks," by Cambra, F.J., November 1982, (PB83 251 215)A09.

UCB/EERC-82/26 "Computational Models for Cyclic Plasticity, Rate Dependence and Creep," by Mosaddad, B. and Powell, G.H., November 1982, (PB83 245 829)A08.

UCB/EERC-82/27 "Inelastic Analysis of Piping and Tubular Structures," by Mahasuverachai, M. and Powell, G.H., November 1982, (PB83 249 987)A07.

UCB/EERC-83/01 "The Economic Feasibility of Seismic Rehabilitation of Buildings by Base Isolation," by Kelly, J.M., January 1983, (PB83 197 988)A05.

UCB/EERC-83/02 "Seismic Moment Connections for Moment-Resisting Steel Frames.," by Popov, E.P., January 1983, (PB83 195 412)A04.

UCB/EERC-83/03 "Design of Links and Beam-to-Column Connections for Eccentrically Braced Steel Frames," by Popov, E.P. and Malley, J.O., January 1983, (PB83 194 811)A04.

UCB/EERC-83/04 "Numerical Techniques for the Evaluation of Soil-Structure Interaction Effects in the Time Domain," by Bayo, E. and Wilson, E.L., February 1983, (PB83 245 605)A09.

UCB/EERC-83/05 "A Transducer for Measuring the Internal Forces in the Columns of a Frame-Wall Reinforced Concrete Structure," by Sause, R. and Bertero, V.V., May 1983, (PB84 119 494)A06.

UCB/EERC-83/06 "Dynamic Interactions Between Floating Ice and Offshore Structures," by Croteau, P., May 1983, (PB84 119 486)A16.

UCB/EERC-83/07 "Dynamic Analysis of Multiply Tuned and Arbitrarily Supported Secondary Systems," by Igusa, T. and Der Kiureghian, A., July 1983, (PB84 118 272)A11.

UCB/EERC-83/08 "A Laboratory Study of Submerged Multi-body Systems in Earthquakes," by Ansari, G.R., June 1983, (PB83 261 842)A17.

UCB/EERC-83/09 "Effects of Transient Foundation Uplift on Earthquake Response of Structures," by Yim, C.-S. and Chopra, A.K., June 1983, (PB83 261 396)A07.

UCB/EERC-83/10 "Optimal Design of Friction-Braced Frames under Seismic Loading," by Austin, M.A. and Pister, K.S., June 1983, (PB84 119 288)A06.

UCB/EERC-83/11 "Shaking Table Study of Single-Story Masonry Houses: Dynamic Performance under Three Component Seismic Input and Recommendations," by Manos, G.C., Clough, R.W. and Mayes, R.L., July 1983, (UCB/EERC-83/11)A08.

UCB/EERC-83/12 "Experimental Error Propagation in Pseudodynamic Testing," by Shiing, P.B. and Mahin, S.A., June 1983, (PB84 119 270)A09.

UCB/EERC-83/13 "Experimental and Analytical Predictions of the Mechanical Characteristics of a 1/5-scale Model of a 7-story R/C Frame-Wall Building Structure," by Aktan, A.E., Bertero, V.V., Chowdhury, A.A. and Nagashima, T., June 1983, (PB84 119 213)A07.

UCB/EERC-83/14 "Shaking Table Tests of Large-Panel Precast Concrete Building System Assemblages," by Oliva, M.G. and Clough, R.W., June 1983, (PB86 110 210/AS)A11.

UCB/EERC-83/15 "Seismic Behavior of Active Beam Links in Eccentrically Braced Frames," by Hjelmstad, K.D. and Popov, E.P., July 1983, (PB84 119 676)A09.

UCB/EERC-83/16 "System Identification of Structures with Joint Rotation," by Dimsdale, J.S., July 1983, (PB84 192 210)A06.

UCB/EERC-83/17 "Construction of Inelastic Response Spectra for Single-Degree-of-Freedom Systems," by Mahin, S. and Lin, J., June 1983, (PB84 208 834)A05.

UCB/EERC-83/18 "Interactive Computer Analysis Methods for Predicting the Inelastic Cyclic Behaviour of Structural Sections," by Kaba, S. and Mahin, S., July 1983, (PB84 192 012)A06.

UCB/EERC-83/19 "Effects of Bond Deterioration on Hysteretic Behavior of Reinforced Concrete Joints," by Filippou, F.C., Popov, E.P. and Bertero, V.V., August 1983, (PB84 192 020)A10.

UCB/EERC-83/20 "Correlation of Analytical and Experimental Responses of Large-Panel Precast Building Systems," by Oliva, M.G., Clough, R.W., Velkov, M. and Gavrilovic, P., May 1988, (PB90 262 692)A06.

UCB/EERC-83/21 "Mechanical Characteristics of Materials Used in a 1/5 Scale Model of a 7-Story Reinforced Concrete Test Structure," by Bertero, V.V., Aktan, A.E., Harris, H.G. and Chowdhury, A.A., October 1983, (PB84 193 697)A05.

UCB/EERC-83/22 "Hybrid Modelling of Soil-Structure Interaction in Layered Media," by Tzong, T.-J. and Penzien, J., October 1983, (PB84 192 178)A08.

UCB/EERC-83/23 "Local Bond Stress-Slip Relationships of Deformed Bars under Generalized Excitations," by Eligehausen, R., Popov, E.P. and Bertero, V.V., October 1983, (PB84 192 848)A09.

UCB/EERC-83/24 "Design Considerations for Shear Links in Eccentrically Braced Frames," by Malley, J.O. and Popov, E.P., November 1983, (PB84 192 186)A07.

UCB/EERC-84/01 "Pseudodynamic Test Method for Seismic Performance Evaluation: Theory and Implementation," by Shing, P.-S.B. and Mahin, S.A., January 1984, (PB84 190 644)A08.

UCB/EERC-84/02 "Dynamic Response Behavior of Kiang Hong Dian Dam," by Clough, R.W., Chang, K.-T., Chen, H.-Q. and Stephen, R.M., April 1984, (PB84 209 402)A08.

UCB/EERC-84/03 "Refined Modelling of Reinforced Concrete Columns for Seismic Analysis," by Kaba, S.A. and Mahin, S.A., April 1984, (PB84 234 384)A06.

UCB/EERC-84/04 "A New Floor Response Spectrum Method for Seismic Analysis of Multiply Supported Secondary Systems," by Asfura, A. and Der Kiureghian, A., June 1984, (PB84 239 417)A06.

UCB/EERC-84/05 "Earthquake Simulation Tests and Associated Studies of a 1/5th-scale Model of a 7-Story R/C Frame-Wall Test Structure," by Bertero, V.V., Aktan, A.E., Charney, F.A. and Sause, R., June 1984, (PB84 239 409)A09.

UCB/EERC-84/06 "Unassigned," by Unassigned, 1984.

UCB/EERC-84/07 "Behavior of Interior and Exterior Flat-Plate Connections Subjected to Inelastic Load Reversals," by Zee, H.L. and Moehle, J.P., August 1984, (PB86 117 629/AS)A07.

UCB/EERC-84/08 "Experimental Study of the Seismic Behavior of a Two-Story Flat-Plate Structure," by Moehle, J.P. and Diebold, J.W., August 1984, (PB86 122 553/AS)A12.

UCB/EERC-84/09 "Phenomenological Modeling of Steel Braces under Cyclic Loading," by Ikeda, K., Mahin, S.A. and Dermitzakis, S.N., May 1984, (PB86 132 198/AS)A08.

UCB/EERC-84/10 "Earthquake Analysis and Response of Concrete Gravity Dams," by Fenves, G.L. and Chopra, A.K., August 1984, (PB85 193 902/AS)A11.

UCB/EERC-84/11 "EAGD-84: A Computer Program for Earthquake Analysis of Concrete Gravity Dams," by Fenves, G.L. and Chopra, A.K., August 1984, (PB85 193 613/AS)A05.

UCB/EERC-84/12 "A Refined Physical Theory Model for Predicting the Seismic Behavior of Braced Steel Frames," by Ikeda, K. and Mahin, S.A., July 1984, (PB85 191 450/AS)A09.

UCB/EERC-84/13 "Earthquake Engineering Research at Berkeley - 1984," by EERC, August 1984, (PB85 197 341/AS)A10.

UCB/EERC-84/14 "Moduli and Damping Factors for Dynamic Analyses of Cohesionless Soils," by Seed, H.B., Wong, R.T., Idriss, I.M. and Tokimatsu, K., September 1984, (PB85 191 468/AS)A04.

UCB/EERC-84/15 "The Influence of SPT Procedures in Soil Liquefaction Resistance Evaluations," by Seed, H.B., Tokimatsu, K., Harder, L.F. and Chung, R.M., October 1984, (PB85 191 732/AS)A04.

UCB/EERC-84/16 "Simplified Procedures for the Evaluation of Settlements in Sands Due to Earthquake Shaking," by Tokimatsu, K. and Seed, H.B., October 1984, (PB85 197 887/AS)A03.

UCB/EERC-84/17 "Evaluation of Energy Absorption Characteristics of Highway Bridges Under Seismic Conditions - Volume I (PB90 262 627)A16 and Volume II (Appendices) (PB90 262 635)A13," by Imbsen, R.A. and Penzien, J., September 1986.

UCB/EERC-84/18 "Structure-Foundation Interactions under Dynamic Loads," by Liu, W.D. and Penzien, J., November 1984, (PB87 124 889/AS)A11.

UCB/EERC-84/19 "Seismic Modelling of Deep Foundations," by Chen, C.-H. and Penzien, J., November 1984, (PB87 124 798/AS)A07.

UCB/EERC-84/20 "Dynamic Response Behavior of Quan Shui Dam," by Clough, R.W., Chang, K.-T., Chen, H.-Q., Stephen, R.M., Ghanaat, Y. and Qi, J.-H., November 1984, (PB86 115177/AS)A07.

UCB/EERC-85/01 "Simplified Methods of Analysis for Earthquake Resistant Design of Buildings," by Cruz, E.F. and Chopra, A.K., February 1985, (PB86 112299/AS)A12.

UCB/EERC-85/02 "Estimation of Seismic Wave Coherency and Rupture Velocity using the SMART 1 Strong-Motion Array Recordings," by Abrahamson, N.A., March 1985, (PB86 214 343)A07.

UCB/EERC-85/03 "Dynamic Properties of a Thirty Story Condominium Tower Building," by Stephen, R.M., Wilson, E.L. and Stander, N., April 1985, (PB86 118965/AS)A06.

UCB/EERC-85/04 "Development of Substructuring Techniques for On-Line Computer Controlled Seismic Performance Testing," by Dermitzakis, S. and Mahin, S., February 1985, (PB86 132941/AS)A08.

UCB/EERC-85/05 "A Simple Model for Reinforcing Bar Anchorages under Cyclic Excitations," by Filippou, F.C., March 1985, (PB86 112 919/AS)A05.

UCB/EERC-85/06 "Racking Behavior of Wood-framed Gypsum Panels under Dynamic Load," by Oliva, M.G., June 1985, (PB90 262 643)A04.

UCB/EERC-85/07 "Earthquake Analysis and Response of Concrete Arch Dams," by Fok, K.-L. and Chopra, A.K., June 1985, (PB86 139672/AS)A10.

UCB/EERC-85/08 "Effect of Inelastic Behavior on the Analysis and Design of Earthquake Resistant Structures," by Lin, J.P. and Mahin, S.A., June 1985, (PB86 135340/AS)A08.

UCB/EERC-85/09 "Earthquake Simulator Testing of a Base-Isolated Bridge Deck," by Kelly, J.M., Buckle, I.G. and Tsai, H.-C., January 1986, (PB87 124 152/AS)A06.

UCB/EERC-85/10 "Simplified Analysis for Earthquake Resistant Design of Concrete Gravity Dams," by Fenves, G.L. and Chopra, A.K., June 1986, (PB87 124 160/AS)A08.

UCB/EERC-85/11 "Dynamic Interaction Effects in Arch Dams," by Clough, R.W., Chang, K.-T., Chen, H.-Q. and Ghanaat, Y., October 1985, (PB86 135027/AS)A05.

UCB/EERC-85/12 "Dynamic Response of Long Valley Dam in the Mammoth Lake Earthquake Series of May 25-27, 1980," by Lai, S. and Seed, H.B., November 1985, (PB86 142304/AS)A05.

UCB/EERC-85/13 "A Methodology for Computer-Aided Design of Earthquake-Resistant Steel Structures," by Austin, M.A., Pister, K.S. and Mahin, S.A., December 1985, (PB86 159480/AS)A10 .

UCB/EERC-85/14 "Response of Tension-Leg Platforms to Vertical Seismic Excitations," by Liou, G.-S., Penzien, J. and Yeung, R.W., December 1985, (PB87 124 871/AS)A08.

UCB/EERC-85/15 "Cyclic Loading Tests of Masonry Single Piers: Volume 4 - Additional Tests with Height to Width Ratio of 1," by Sveinsson, B., McNiven, H.D. and Sucuoglu, H., December 1985, (PB87 165031/AS)A08.

UCB/EERC-85/16 "An Experimental Program for Studying the Dynamic Response of a Steel Frame with a Variety of Infill Partitions," by Yanev, B. and McNiven, H.D., December 1985, (PB90 262 676)A05.

UCB/EERC-86/01 "A Study of Seismically Resistant Eccentrically Braced Steel Frame Systems," by Kasai, K. and Popov, E.P., January 1986, (PB87 124 178/AS)A14.

UCB/EERC-86/02 "Design Problems in Soil Liquefaction," by Seed, H.B., February 1986, (PB87 124 186/AS)A03.

UCB/EERC-86/03 "Implications of Recent Earthquakes and Research on Earthquake-Resistant Design and Construction of Buildings," by Bertero, V.V., March 1986, (PB87 124 194/AS)A05.

UCB/EERC-86/04 "The Use of Load Dependent Vectors for Dynamic and Earthquake Analyses," by Leger, P., Wilson, E.L. and Clough, R.W., March 1986, (PB87 124 202/AS)A12.

UCB/EERC-86/05 "Two Beam-To-Column Web Connections," by Tsai, K.-C. and Popov, E.P., April 1986, (PB87 124 301/AS)A04.

UCB/EERC-86/06 "Determination of Penetration Resistance for Coarse-Grained Soils using the Becker Hammer Drill," by Harder, L.F. and Seed, H.B., May 1986, (PB87 124 210/AS)A07.

UCB/EERC-86/07 "A Mathematical Model for Predicting the Nonlinear Response of Unreinforced Masonry Walls to In-Plane Earthquake Excitations," by Mengi, Y. and McNiven, H.D., May 1986, (PB87 124 780/AS)A06.

UCB/EERC-86/08 "The 19 September 1985 Mexico Earthquake: Building Behavior," by Bertero, V.V., July 1986.

UCB/EERC-86/09 "EACD-3D: A Computer Program for Three-Dimensional Earthquake Analysis of Concrete Dams," by Fok, K.-L., Hall, J.F. and Chopra, A.K., July 1986, (PB87 124 228/AS)A08.

UCB/EERC-86/10 "Earthquake Simulation Tests and Associated Studies of a 0.3-Scale Model of a Six-Story Concentrically Braced Steel Structure," by Uang, C.-M. and Bertero, V.V., December 1986, (PB87 163 564/AS)A17.

UCB/EERC-86/11 "Mechanical Characteristics of Base Isolation Bearings for a Bridge Deck Model Test," by Kelly, J.M., Buckle, I.G. and Koh, C.-G., November 1987, (PB90 262 668)A04.

UCB/EERC-86/12 "Effects of Axial Load on Elastomeric Isolation Bearings," by Koh, C.-G. and Kelly, J.M., November 1987.

UCB/EERC-87/01 "The FPS Earthquake Resisting System: Experimental Report," by Zayas, V.A., Low, S.S. and Mahin, S.A., June 1987, (PB88 170 287)A06.

UCB/EERC-87/02 "Earthquake Simulator Tests and Associated Studies of a 0.3-Scale Model of a Six-Story Eccentrically Braced Steel Structure," by Whittaker, A., Uang, C.-M. and Bertero, V.V., July 1987, (PB88 166 707/AS)A18.

UCB/EERC-87/03 "A Displacement Control and Uplift Restraint Device for Base-Isolated Structures," by Kelly, J.M., Griffith, M.C. and Aiken, I.D., April 1987, (PB88 169 933)A04.

UCB/EERC-87/04 "Earthquake Simulator Testing of a Combined Sliding Bearing and Rubber Bearing Isolation System," by Kelly, J.M. and Chalhoub, M.S., December 1990.

UCB/EERC-87/05 "Three-Dimensional Inelastic Analysis of Reinforced Concrete Frame-Wall Structures," by Moazzami, S. and Bertero, V.V., May 1987, (PB88 169 586/AS)A08.

UCB/EERC-87/06 "Experiments on Eccentrically Braced Frames with Composite Floors," by Ricles, J. and Popov, E., June 1987, (PB88 173 067/AS)A14.

UCB/EERC-87/07 "Dynamic Analysis of Seismically Resistant Eccentrically Braced Frames," by Ricles, J. and Popov, E., June 1987, (PB88 173 075/AS)A16.

UCB/EERC-87/08 "Undrained Cyclic Triaxial Testing of Gravels-The Effect of Membrane Compliance," by Evans, M.D. and Seed, H.B., July 1987, (PB88 173 257)A19.

UCB/EERC-87/09 "Hybrid Solution Techniques for Generalized Pseudo-Dynamic Testing," by Thewalt, C. and Mahin, S.A., July 1987, (PB 88 179 007)A07.

UCB/EERC-87/10 "Ultimate Behavior of Butt Welded Splices in Heavy Rolled Steel Sections," by Bruneau, M., Mahin, S.A. and Popov, E.P., September 1987, (PB90 254 285)A07.

UCB/EERC-87/11 "Residual Strength of Sand from Dam Failures in the Chilean Earthquake of March 3, 1985," by De Alba, P., Seed, H.B., Retamal, E. and Seed, R.B., September 1987, (PB88 174 321/AS)A03.

UCB/EERC-87/12 "Inelastic Seismic Response of Structures with Mass or Stiffness Eccentricities in Plan," by Bruneau, M. and Mahin, S.A., September 1987, (PB90 262 650/AS)A14.

UCB/EERC-87/13 "CSTRUCT: An Interactive Computer Environment for the Design and Analysis of Earthquake Resistant Steel Structures," by Austin, M.A., Mahin, S.A. and Pister, K.S., September 1987, (PB88 173 339/AS)A06.

UCB/EERC-87/14 "Experimental Study of Reinforced Concrete Columns Subjected to Multi-Axial Loading," by Low, S.S. and Moehle, J.P., September 1987, (PB88 174 347/AS)A07.

UCB/EERC-87/15 "Relationships between Soil Conditions and Earthquake Ground Motions in Mexico City in the Earthquake of Sept. 19, 1985," by Seed, H.B., Romo, M.P., Sun, J., Jaime, A. and Lysmer, J., October 1987, (PB88 178 991)A06.

UCB/EERC-87/16 "Experimental Study of Seismic Response of R. C. Setback Buildings," by Shahrooz, B.M. and Moehle, J.P., October 1987, (PB88 176 359)A16.

UCB/EERC-87/17 "The Effect of Slabs on the Flexural Behavior of Beams," by Pantazopoulou, S.J. and Moehle, J.P., October 1987, (PB90 262 700)A07.

UCB/EERC-87/18 "Design Procedure for R-FBI Bearings," by Mostaghel, N. and Kelly, J.M., November 1987, (PB90 262 718)A04.

UCB/EERC-87/19 "Analytical Models for Predicting the Lateral Response of R C Shear Walls: Evaluation of their Reliability," by Vulcano, A. and Bertero, V.V., November 1987, (PB88 178 983)A05.

UCB/EERC-87/20 "Earthquake Response of Torsionally-Coupled Buildings," by Hejal, R. and Chopra, A.K., December 1987.

UCB/EERC-87/21 "Dynamic Reservoir Interaction with Monticello Dam," by Clough, R.W., Ghanaat, Y. and Qiu, X-F., December 1987, (PB88 179 023)A07.

UCB/EERC-87/22 "Strength Evaluation of Coarse-Grained Soils," by Siddiqi, F.H., Seed, R.B., Chan, C.K., Seed, H.B. and Pyke, R.M., December 1987, (PB88 179 031)A04.

UCB/EERC-88/01 "Seismic Behavior of Concentrically Braced Steel Frames," by Khatib, I., Mahin, S.A. and Pister, K.S., January 1988, (PB91 210 898/AS)A11.

UCB/EERC-88/02 "Experimental Evaluation of Seismic Isolation of Medium-Rise Structures Subject to Uplift," by Griffith, M.C., Kelly, J.M., Coveney, V.A. and Koh, C.G., January 1988, (PB91 217 950/AS)A09.

UCB/EERC-88/03 "Cyclic Behavior of Steel Double Angle Connections," by Astaneh-Asl, A. and Nader, M.N., January 1988, (PB91 210 872)A05.

UCB/EERC-88/04 "Re-evaluation of the Slide in the Lower San Fernando Dam in the Earthquake of Feb. 9, 1971," by Seed, H.B., Seed, R.B., Harder, L.F. and Jong, H.-L., April 1988, (PB91 212 456/AS)A07.

UCB/EERC-88/05 "Experimental Evaluation of Seismic Isolation of a Nine-Story Braced Steel Frame Subject to Uplift," by Griffith, M.C., Kelly, J.M. and Aiken, I.D., May 1988, (PB91 217 968/AS)A07.

UCB/EERC-88/06 "DRAIN-2DX User Guide.," by Allahabadi, R. and Powell, G.H., March 1988, (PB91 212 530)A12.

UCB/EERC-88/07 "Theoretical and Experimental Studies of Cylindrical Water Tanks in Base-Isolated Structures," by Chalhoub, M.S. and Kelly, J.M., April 1988, (PB91 217 976/AS)A05.

UCB/EERC-88/08 "Analysis of Near-Source Waves: Separation of Wave Types Using Strong Motion Array Recording," by Darragh, R.B., June 1988, (PB91 212 621)A08.

UCB/EERC-88/09 "Alternatives to Standard Mode Superposition for Analysis of Non-Classically Damped Systems," by Kusainov, A.A. and Clough, R.W., June 1988, (PB91 217 992/AS)A04.

UCB/EERC-88/10 "The Landslide at the Port of Nice on October 16, 1979," by Seed, H.B., Seed, R.B., Schlosser, F., Blondeau, F. and Juran, I., June 1988, (PB91 210 914)A05.

UCB/EERC-88/11 "Liquefaction Potential of Sand Deposits Under Low Levels of Excitation," by Carter, D.P. and Seed, H.B., August 1988, (PB91 210 880)A15.

UCB/EERC-88/12 "Nonlinear Analysis of Reinforced Concrete Frames Under Cyclic Load Reversals," by Filippou, F.C. and Issa, A., September 1988, (PB91 212 589)A07.

UCB/EERC-88/13 "Implications of Recorded Earthquake Ground Motions on Seismic Design of Building Structures," by Uang, C.-M. and Bertero, V.V., November 1988, (PB91 212 548)A06.

UCB/EERC-88/14 "An Experimental Study of the Behavior of Dual Steel Systems," by Whittaker, A.S. , Uang, C.-M. and Bertero, V.V., September 1988, (PB91 212 712)A16.

UCB/EERC-88/15 "Dynamic Moduli and Damping Ratios for Cohesive Soils," by Sun, J.I., Golesorkhi, R. and Seed, H.B., August 1988, (PB91 210 922)A04.

UCB/EERC-88/16 "Reinforced Concrete Flat Plates Under Lateral Load: An Experimental Study Including Biaxial Effects," by Pan, A. and Moehle, J.P., October 1988, (PB91 210 856)A13.

UCB/EERC-88/17 "Earthquake Engineering Research at Berkeley - 1988," by EERC, November 1988, (PB91 210 864)A10.

UCB/EERC-88/18 "Use of Energy as a Design Criterion in Earthquake-Resistant Design," by Uang, C.-M. and Bertero, V.V., November 1988, (PB91 210 906/AS)A04.

UCB/EERC-88/19 "Steel Beam-Column Joints in Seismic Moment Resisting Frames," by Tsai, K.-C. and Popov, E.P., November 1988, (PB91 217 984/AS)A20.

UCB/EERC-88/20 "Base Isolation in Japan, 1988," by Kelly, J.M., December 1988, (PB91 212 449)A05.

UCB/EERC-89/01 "Behavior of Long Links in Eccentrically Braced Frames," by Engelhardt, M.D. and Popov, E.P., January 1989, (PB92 143 056)A18.

UCB/EERC-89/02 "Earthquake Simulator Testing of Steel Plate Added Damping and Stiffness Elements," by Whittaker, A., Bertero, V.V., Alonso, J. and Thompson, C., January 1989, (PB91 229 252/AS)A10.

UCB/EERC-89/03 "Implications of Site Effects in the Mexico City Earthquake of Sept. 19, 1985 for Earthquake-Resistant Design Criteria in the San Francisco Bay Area of California," by Seed, H.B. and Sun, J.I., March 1989, (PB91 229 369/AS)A07.

UCB/EERC-89/04 "Earthquake Analysis and Response of Intake-Outlet Towers," by Goyal, A. and Chopra, A.K., July 1989, (PB91 229 286/AS)A19.

UCB/EERC-89/05 "The 1985 Chile Earthquake: An Evaluation of Structural Requirements for Bearing Wall Buildings," by Wallace, J.W. and Moehle, J.P., July 1989, (PB91 218 008/AS)A13.

UCB/EERC-89/06 "Effects of Spatial Variation of Ground Motions on Large Multiply-Supported Structures," by Hao, H., July 1989, (PB91 229 161/AS)A08.

UCB/EERC-89/07 "EADAP - Enhanced Arch Dam Analysis Program: Users's Manual," by Ghanaat, Y. and Clough, R.W., August 1989, (PB91 212 522)A06.

UCB/EERC-89/08 "Seismic Performance of Steel Moment Frames Plastically Designed by Least Squares Stress Fields," by Ohi, K. and Mahin, S.A., August 1989, (PB91 212 597)A05.

UCB/EERC-89/09 "Feasibility and Performance Studies on Improving the Earthquake Resistance of New and Existing Buildings Using the Friction Pendulum System," by Zayas, V., Low, S., Mahin, S.A. and Bozzo, L., July 1989, (PB92 143 064)A14.

UCB/EERC-89/10 "Measurement and Elimination of Membrane Compliance Effects in Undrained Triaxial Testing," by Nicholson, P.G., Seed, R.B. and Anwar, H., September 1989, (PB92 139 641/AS)A13.

UCB/EERC-89/11 "Static Tilt Behavior of Unanchored Cylindrical Tanks," by Lau, D.T. and Clough, R.W., September 1989, (PB92 143 049)A10.

UCB/EERC-89/12 "ADAP-88: A Computer Program for Nonlinear Earthquake Analysis of Concrete Arch Dams," by Fenves, G.L., Mojtahedi, S. and Reimer, R.B., September 1989, (PB92 139 674/AS)A07.

UCB/EERC-89/13 "Mechanics of Low Shape Factor Elastomeric Seismic Isolation Bearings," by Aiken, I.D., Kelly, J.M. and Tajirian, F.F., November 1989, (PB92 139 732/AS)A09.

UCB/EERC-89/14 "Preliminary Report on the Seismological and Engineering Aspects of the October 17, 1989 Santa Cruz (Loma Prieta) Earthquake," by EERC, October 1989, (PB92 139 682/AS)A04.

UCB/EERC-89/15 "Experimental Studies of a Single Story Steel Structure Tested with Fixed, Semi-Rigid and Flexible Connections," by Nader, M.N. and Astaneh-Asl, A., August 1989, (PB91 229 211/AS)A10.

UCB/EERC-89/16 "Collapse of the Cypress Street Viaduct as a Result of the Loma Prieta Earthquake," by Nims, D.K., Miranda, E., Aiken, I.D., Whittaker, A.S. and Bertero, V.V., November 1989, (PB91 217 935/AS)A05.

UCB/EERC-90/01 "Mechanics of High-Shape Factor Elastomeric Seismic Isolation Bearings," by Kelly, J.M., Aiken, I.D. and Tajirian, F.F., March 1990.

UCB/EERC-90/02 "Javid's Paradox: The Influence of Preform on the Modes of Vibrating Beams," by Kelly, J.M., Sackman, J.L. and Javid, A., May 1990, (PB91 217 943/AS)A03.

UCB/EERC-90/03 "Earthquake Simulator Testing and Analytical Studies of Two Energy-Absorbing Systems for Multistory Structures," by Aiken, I.D. and Kelly, J.M., October 1990.

UCB/EERC-90/04 "Damage to the San Francisco-Oakland Bay Bridge During the October 17, 1989 Earthquake," by Astaneh-Asl, A., June 1990.

UCB/EERC-90/05 "Preliminary Report on the Principal Geotechnical Aspects of the October 17, 1989 Loma Prieta Earthquake," by Seed, R.B., Dickenson, S.E., Riemer, M.F., Bray, J.D., Sitar, N., Mitchell, J.K., Idriss, I.M., Kayen, R.E., Kropp, A., Harder, L.F., Jr. and Power, M.S., April 1990.

UCB/EERC-90/06 "Models of Critical Regions in Reinforced Concrete Frames Under Seismic Excitations," by Zulfiqar, N. and Filippou, F.C., May 1990.

UCB/EERC-90/07 "A Unified Earthquake-Resistant Design Method for Steel Frames Using ARMA Models," by Takewaki, I., Conte, J.P., Mahin, S.A. and Pister, K.S., June 1990.

UCB/EERC-90/08 "Soil Conditions and Earthquake Hazard Mitigation in the Marina District of San Francisco," by Mitchell, J.K., Masood, T., Kayen, R.E. and Seed, R.B., May 1990.

UCB/EERC-90/09 "Influence of the Earthquake Ground Motion Process and Structural Properties on Response Characteristics of Simple Structures," by Conte, J.P., Pister, K.S. and Mahin, S.A., July 1990.

UCB/EERC-90/10 "Experimental Testing of the Resilient-Friction Base Isolation System," by Clark, P.W. and Kelly, J.M., July 1990, (PB92 143 072)A08.

UCB/EERC-90/11 "Seismic Hazard Analysis: Improved Models, Uncertainties and Sensitivities," by Araya, R. and Der Kiureghian, A., March 1988.

UCB/EERC-90/12 "Effects of Torsion on the Linear and Nonlinear Seismic Response of Structures," by Sedarat, H. and Bertero, V.V., September 1989.

UCB/EERC-90/13 "The Effects of Tectonic Movements on Stresses and Deformations in Earth Embankments," by Bray, J. D., Seed, R. B. and Seed, H. B., September 1989.

UCB/EERC-90/14 "Inelastic Seismic Response of One-Story, Asymmetric-Plan Systems," by Goel, R.K. and Chopra, A.K., October 1990.

UCB/EERC-90/15 "Dynamic Crack Propagation: A Model for Near-Field Ground Motion.," by Seyyedian, H. and Kelly, J.M., 1990.

UCB/EERC-90/16 "Sensitivity of Long-Period Response Spectra to System Initial Conditions," by Blasquez, R., Ventura, C. and Kelly, J.M., 1990.

UCB/EERC-90/17 "Behavior of Peak Values and Spectral Ordinates of Near-Source Strong Ground-Motion over a Dense Array," by Niazi, M., June 1990.

UCB/EERC-90/18 "Material Characterization of Elastomers used in Earthquake Base Isolation," by Papoulia, K.D. and Kelly, J.M., 1990.

UCB/EERC-90/19 "Cyclic Behavior of Steel Top-and-Bottom Plate Moment Connections," by Harriott, J.D. and Astaneh-Asl, A., August 1990, (PB91 229 260/AS)A05.

UCB/EERC-90/20 "Seismic Response Evaluation of an Instrumented Six Story Steel Building," by Shen, J.-H. and Astaneh-Asl, A., December 1990, (PB91 229 294/AS)A04.

UCB/EERC-90/21 "Observations and Implications of Tests on the Cypress Street Viaduct Test Structure," by Bollo, M., Mahin, S.A., Moehle, J.P., Stephen, R.M. and Qi, X., December 1990.

UCB/EERC-91/01 "Experimental Evaluation of Nitinol for Energy Dissipation in Structures," by Nims, D.K., Sasaki, K.K. and Kelly, J.M., 1991.

UCB/EERC-91/02 "Displacement Design Approach for Reinforced Concrete Structures Subjected to Earthquakes," by Qi, X. and Moehle, J.P., January 1991.

UCB/EERC-91/03 "A Long-Period Isolation System Using Low-Modulus High-Damping Isolators for Nuclear Facilities at Soft-Soil Sites," by Kelly, J.M., March 1991.

UCB/EERC-91/04 "Dynamic and Failure Characteristics of Bridgestone Isolation Bearings," by Kelly, J.M., April 1991.

UCB/EERC-91/05 "Base Sliding Response of Concrete Gravity Dams to Earthquakes," by Chopra, A.K. and Zhang, L., May 1991.

UCB/EERC-91/06 "Computation of Spatially Varying Ground Motion and Foundation-Rock Impedance Matrices for Seismic Analysis of Arch Dams," by Zhang, L. and Chopra, A.K., May 1991.

UCB/EERC-91/07 "Estimation of Seismic Source Processes Using Strong Motion Array Data," by Chiou, S.-J., July 1991.

UCB/EERC-91/08 "A Response Spectrum Method for Multiple-Support Seismic Excitations," by Der Kiureghian, A. and Neuenhofer, A., August 1991.

UCB/EERC-91/09 "A Preliminary Study on Energy Dissipating Cladding-to-Frame Connection," by Cohen, J.M. and Powell, G.H., September 1991.

UCB/EERC-91/10 "Evaluation of Seismic Performance of a Ten-Story RC Building During the Whittier Narrows Earthquake," by Miranda, E. and Bertero, V.V., October 1991.

UCB/EERC-91/11 "Seismic Performance of an Instrumented Six Story Steel Building," by Anderson, J.C. and Bertero, V.V., November 1991.

UCB/EERC-91/12 "Performance of Improved Ground During the Loma Prieta Earthquake," by Mitchell, J.K. and Wentz, Jr., F.J., October 1991.

UCB/EERC-91/13 "Shaking Table - Structure Interaction," by Rinawi, A.M. and Clough, R.W., October 1991.

UCB/EERC-91/14 "Cyclic Response of RC Beam-Column Knee Joints: Test and Retrofit," by Mazzoni, S., Moehle, J.P. and Thewalt, C.R., October 1991.

UCB/EERC-91/15 "Design Guidelines for Ductility and Drift Limits: Review of State-of-the-Practice and State-of-the-Art in Ductility and Drift-Based Earthquake-Resistant Design of Buildings," by Bertero, V.V., Anderson, J.C., Krawinkler, H., Miranda, E. and The CUREe and The Kajima Research Teams,, July 1991.

UCB/EERC-91/16 "Evaluation of the Seismic Performance of a Thirty-Story RC Building," by Anderson, J.C., Miranda, E., Bertero, V.V. and The Kajima Project Research Team,, July 1991.

UCB/EERC-91/17 "A Fiber Beam-Column Element for Seismic Response Analysis of Reinforced Concrete Structures," by Taucer, F., Spacone, E. and Filippou, F.C., December 1991.

UCB/EERC-91/18 "Investigation of the Seismic Response of a Lightly-Damped Torsionally-Coupled Building," by Boroschek, R. and Mahin, S.A., December 1991.

UCB/EERC-92/01 "Studies of a 49-Story Instrumented Steel Structure Shaken during the Loma Prieta Earthquake," by Bonowitz, D., Chen, C.-C. and Astaneh-Asl, A., February 1992.

UCB/EERC-92/02 "Response of the Dumbarton Bridge in the Loma Prieta Earthquake," by Fenves, G.L., Filippou, F.C. and Sze, D.T., January 1992.

UCB/EERC-92/03 "Models for Nonlinear Earthquake Analysis of Brick Masonry Buildings," by Mengi, Y., McNiven, H.D. and Tanrikulu, A.K., March 1992.